Behavior and modelling of concrete members for cyclic loading

- **Mechanisms of force transfer in prismatic concrete members:**
  - flexure,
  - shear,
  - bond of longitudinal bars <u>beyond the member end</u>:

  <u>in series</u> →
  - Member force capacity (resistance) = minimum of individual resistance;
  - Member deformations = sum of individual deformations.
- **If shear span ratio, M/Vh > ~2.5** →
  - flexure & shear ~independent (uncoupled) mechanisms;
- **If shear span ratio, M/Vh < ~2.5** →
  - flexure & shear coupled (merge into ~one mechanism).
- ↓ **shear span ratio, M/Vh,** → **shear effects** ↑

  (even for linear elasticity: $\dfrac{\sigma_{x,\max}}{\tau_{xy,\max}} = 4\dfrac{M}{Vh}$).

Flexure

(& bond of longitudinal bars past the member end)

Flexural behavior at the cross-section level (Moment-curvature behavior)

Physical meaning/importance of curvature in concrete members:

- Very convenient:

  normal strain ε at distance y from neutral axis: $\varepsilon = \varphi y$.
  - at extreme compression fibres: $\varepsilon_c=\varphi x$ ($x=\xi d$: neutral axis depth, $\xi=x/d$: dimensionless neutral axis depth);
  - tension reinforcement: $\varepsilon_{s1}=\varphi(d-x)=\varphi(1-\xi)d$
  - compression steel at distance d_1 from extreme compression fibres: $\varepsilon_{s2}=\varphi(x- d_1)$.
- But after cracking: curvature loses physical meaning:
  - concrete cracking,
  - cover spalling,
  - bar buckling,
  - concrete crushing:

  are all of discrete nature.
- Curvature: $\varphi=\Delta\theta/\Delta x$: relative rotation $\Delta\theta$ of two sections over their finite distance, Δx~$h/2$ to h (:distance of flexural cracks, length within which concrete spalls or crushes, bars buckle or break).

M-φ curve:

- From any geometry of cross-section, amount/ arrangement of reinforcement & material σ-ε laws:
  - For given φ, a value of x assumed, strain distribution: $\varepsilon=\varphi y$, stress distribution from σ-ε laws.
  - Force equilibrium in axial direction: $N= \int \sigma \mathrm{d}A$ checked, value of x revised, till force equilibrium.
  - $M=\int y_{cg} \sigma \mathrm{d}A$.
  - Next value of φ: start w/ trial value of x = that of previous step.

Members with continuous ribbed (deformed) bars

M-φ at yielding of section w/ rectangular compression zone (width b, effective depth d)

- Yield moment (from moment-equilibrium & elastic σ-ε laws):

$$\frac{M_y}{bd^3} = \varphi_y \left\{ E_c \frac{\xi_y^2}{2}\left(0.5(1+\delta_1) - \frac{\xi_y}{3}\right) + \frac{E_s}{2}\left[(1-\xi_y)\rho_1 + (\xi_y - \delta_1)\rho_2 + \frac{\rho_V}{6}(1-\delta_1)\right](1-\delta_1)\right\}$$

- ρ_1, ρ_2 : tension & compression reinforcement ratios, ρ_v: "web" reinforcement ratio, ~uniformly distributed between ρ_1, ρ_2 : (all normalized to bd); $\delta_1 = d_1/d$.
- Curvature at yielding of tension steel:
- from axial force-equilibrium & elastic σ-ε laws ($\alpha = E_s/E_c$):

$$\varphi_y = \frac{f_y}{E_s(1-\xi_y)d}$$

$$\xi_y = \left(\alpha^2 A^2 + 2\alpha B\right)^{1/2} - \alpha A$$

$$A = \rho_1 + \rho_2 + \rho_v + \frac{N}{bdf_y}, \qquad B = \rho_1 + \rho_2\delta_1 + 0.5\rho_v(1+\delta_1) + \frac{N}{bdf_y}$$

- Curvature at ~onset of nonlinearity of concrete:

$$\varphi_y = \frac{\varepsilon_c}{\xi_y d} \approx \frac{1.8 f_c}{E_c \xi_y d}$$

$$A = \rho_1 + \rho_2 + \rho_v - \frac{N}{\varepsilon_c E_s bd} \approx \rho_1 + \rho_2 + \rho_v - \frac{N}{1.8\alpha\, bdf_c}, \quad B = \rho_1 + \rho_2\delta_1 + 0.5\rho_v(1+\delta_1)$$

Moment & curvature at corner of bilinear envelope to experimental moment-deformation curve vs calculated values

2282 beams/columns, cov:16.9%; 326 rect. walls, cov:18.6%

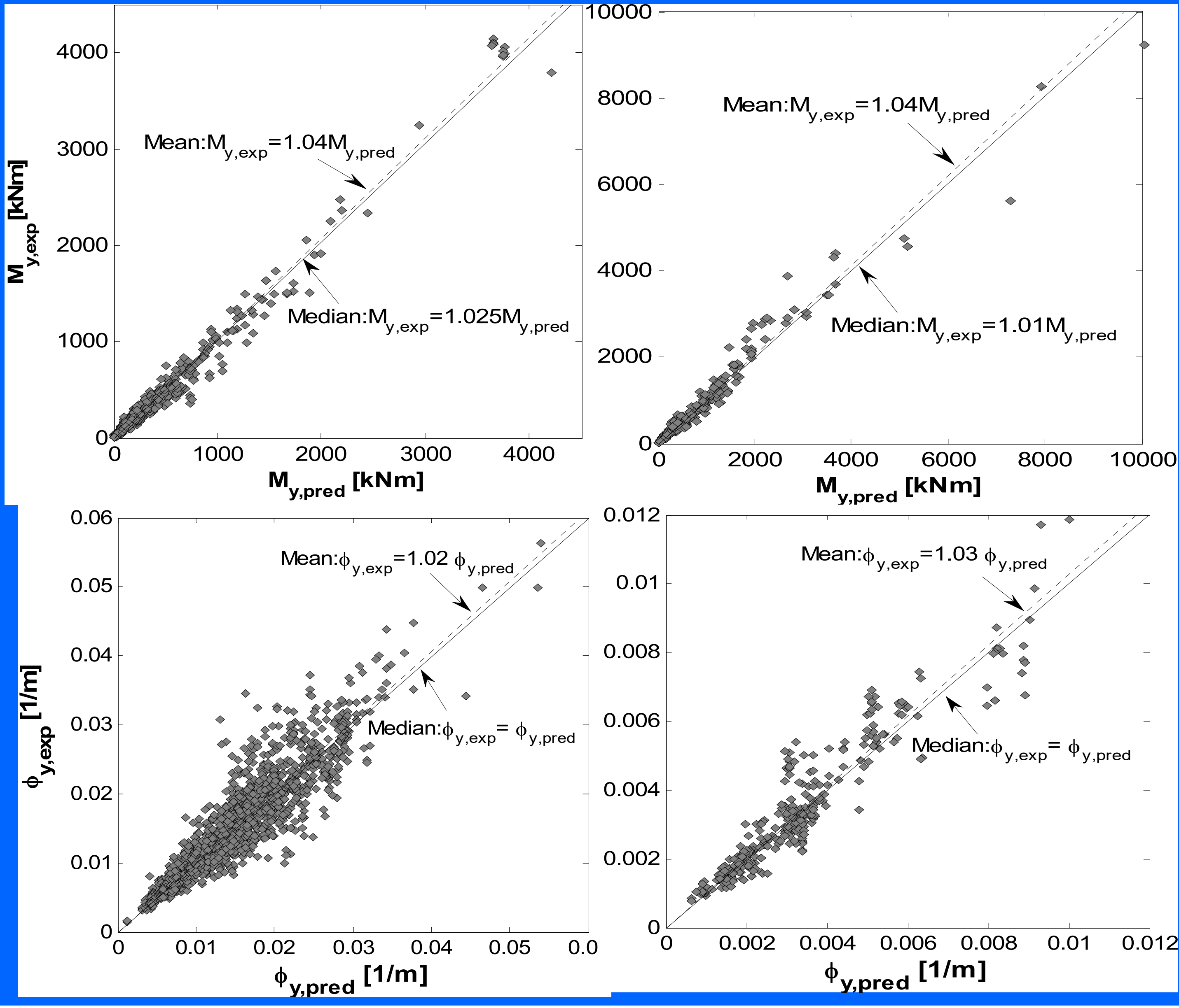

Moment & curvature at corner of bilinear (envelope to) experimental moment-deformation curve v values from analysis

392 non-rect. walls, CoV:16%

332 circular columns, CoV:13.7%

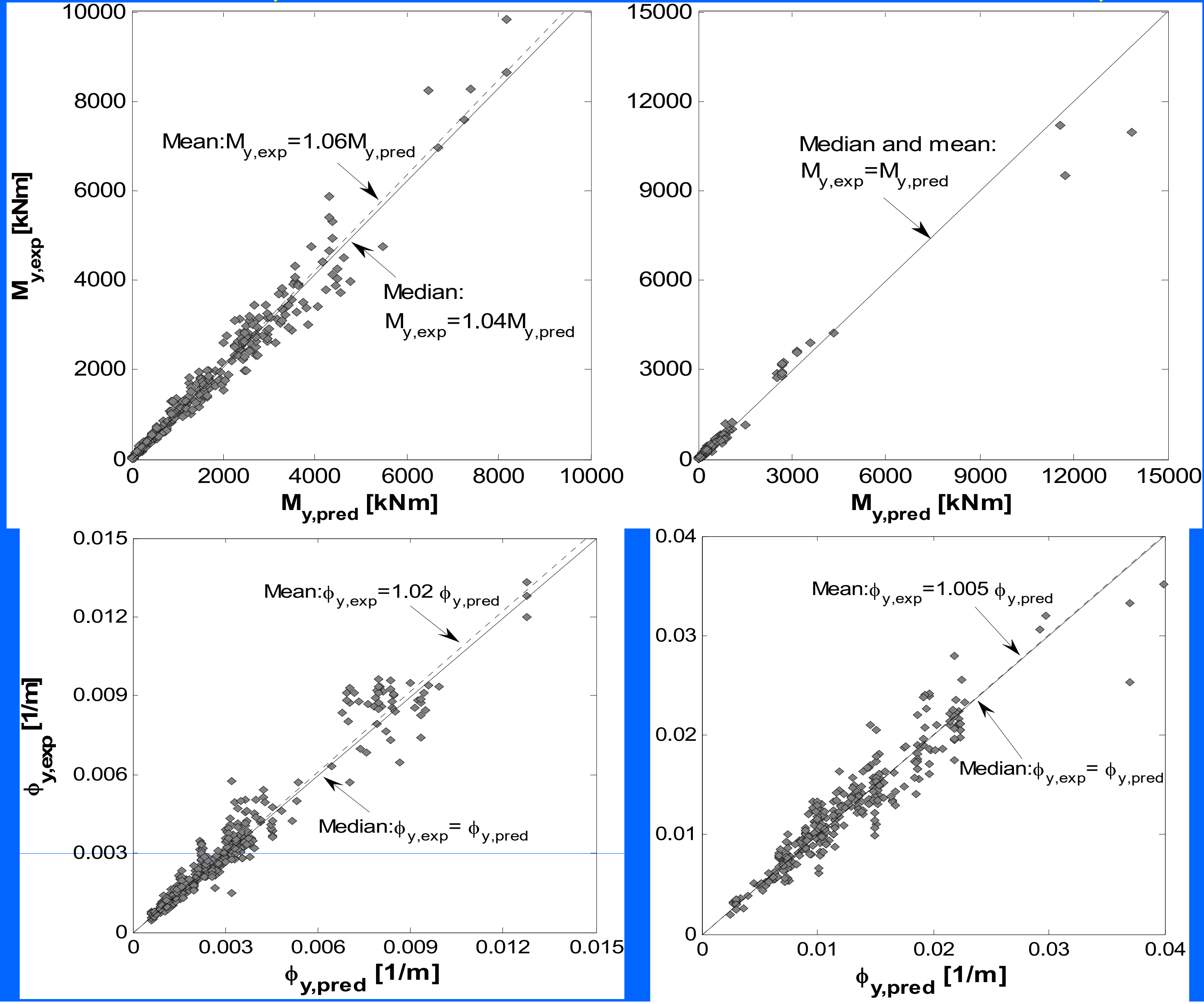

Empirical formulas for yield curvature - section w/ rectangular compression zone

for rectangular columns or beams: $\phi_y \approx \frac{1.53 f_y}{E_s d}$ $\phi_y \approx \frac{1.74 f_y}{E_s h}$

for walls, rectangular or not: $\phi_y \approx \frac{1.34 f_y}{E_s d}$ $\phi_y \approx \frac{1.43 f_y}{E_s h}$

for circular columns: $\phi_y \approx \frac{1.99 f_y}{E_s d}$ $\phi_y \approx \frac{2.1 f_y}{E_s D}$

The empirical expressions give no bias w.r.to the experimental yield moment; but the scatter greater:

In ~3000 test beams, columns or walls: cov: 16.5%

(The "theoretical" expressions underestimate the yield point by up to 4% because the corner of the bilinear envelope to the experimental curve is above the point of first yielding in a section).

Cyclic M-φ behavior

Experimental curves:
M vs. (mean) φ,
symmetrically
reinforced section

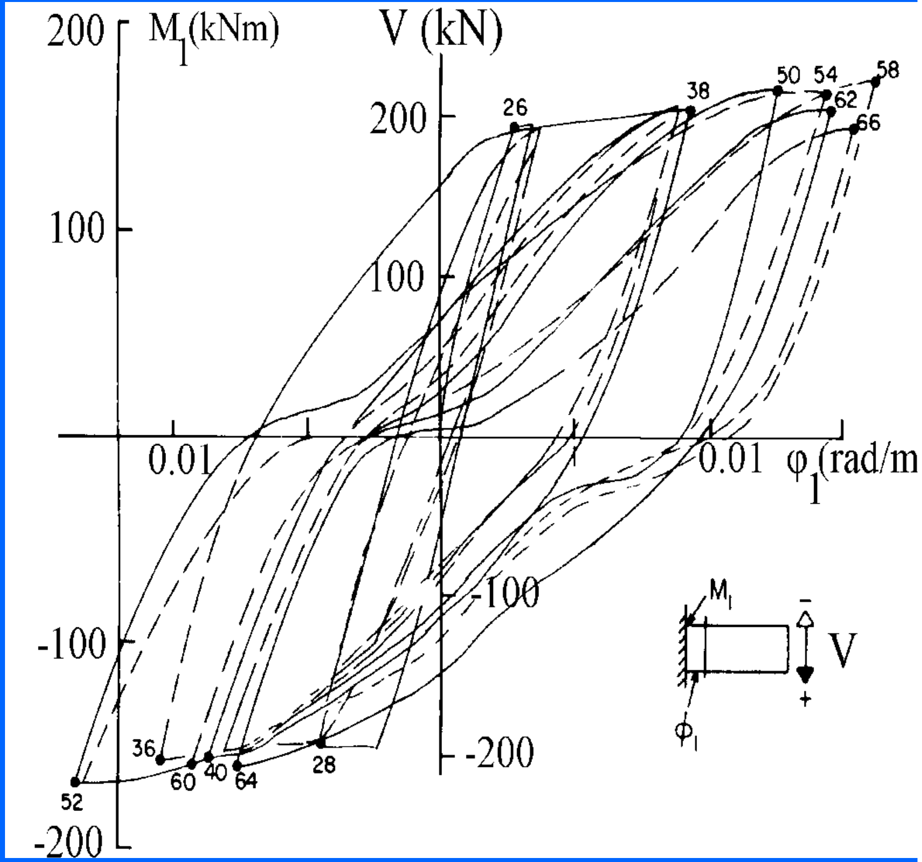

- **Unloading:**
- Unloading stiffness: initially high, ~"elastic" secant stiffness, M_y/φ_y.
- Unloading branch softens, as $M \rightarrow 0$.
- Overall, down to M=0, unloading slope < "elastic" stiffness to yielding.
- Unloading slope ↓ as curvature, φ_r (from where unloading started) ↑ ("stiffness degradation").

- **Reloading** (loading in opposite direction):
- After *M* changes sign, “stiffness” in “reloading” ↓:
  – crack is open through section depth, as compression steel previously yielded in tension & has plastic extension locked-in;
  – *M* resisted only by force couple between tension & compression steel, until crack closes ~when compression steel yields;
  – till then, slope of M-φ diagram < slope of unloading to M=0;
  – when crack closes, reloading slope ↑ again.
- Reloading towards maximum previous curvature in current direction of loading.
- Unloading-reloading curve: inverted-S shape; “pinching” of hysteresis loop.
- Axial load closes the crack, reduces pinching

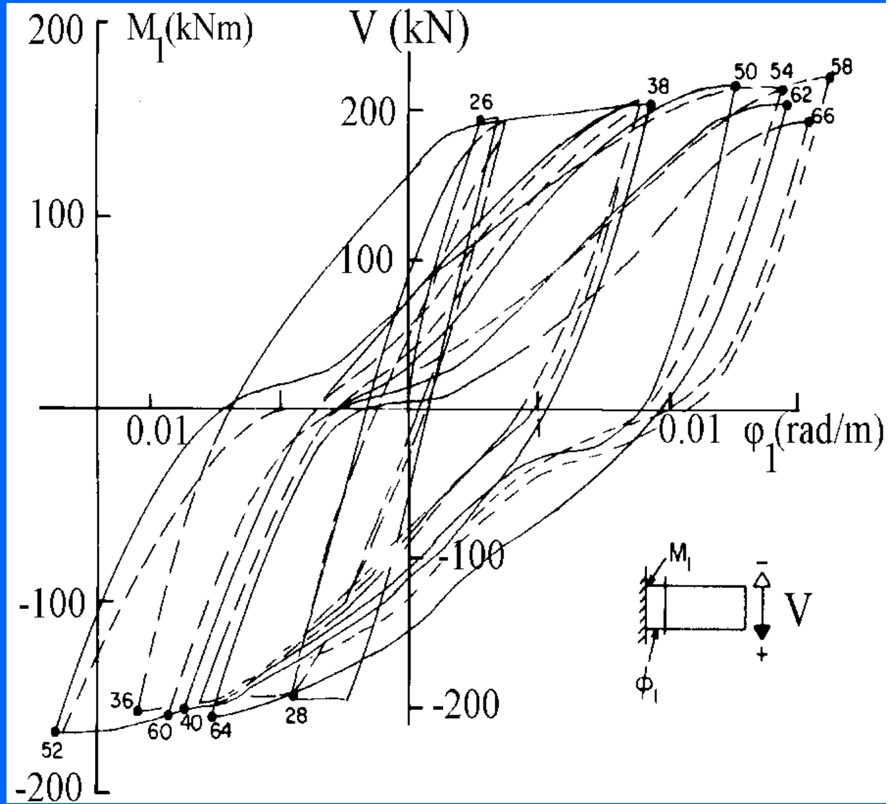

Experimental curves: M–(mean) φ, symmetrically reinforced section

Cyclic *M-φ* behavior

- **Effect of section asymmetry**
- Larger moment resistance & “elastic” stiffness in the direction that induces tension to the side w/ more reinforcement;
- Unloading-reloading curve: **inverted-S shape** only for reloading towards the direction of the larger moment resistance:
  - in the other direction, steel of tension side is too little to yield in compression the steel on the other side → The open crack may never close there.

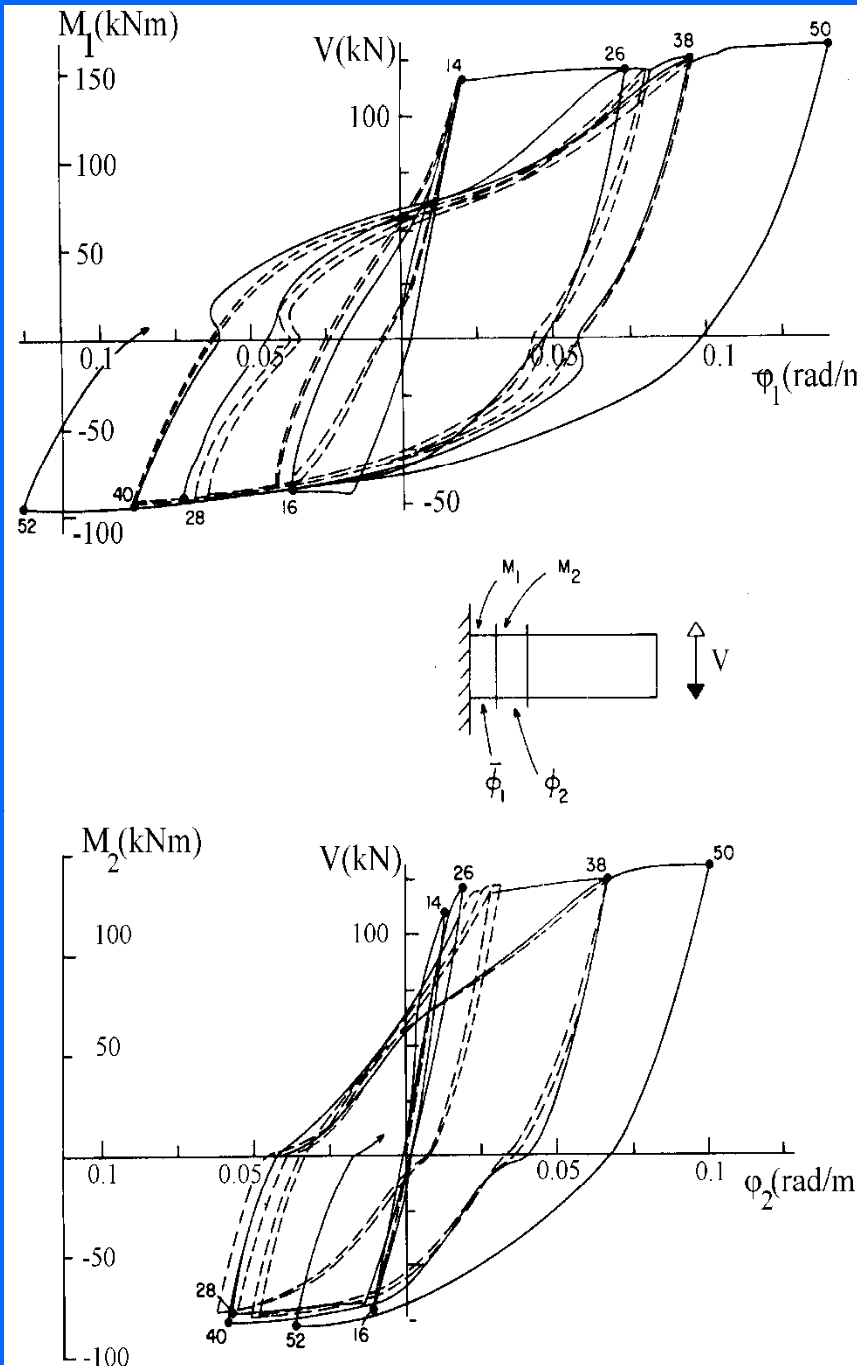

Experimental curves:
M–(mean) *φ*,
asymmetrically reinforced section

Flexural damage or failure of column tops in the field

horizontal crack, concrete spallinag at the corners, buckling of corner bars

loss of cover,
partial disintegration of concrete,
buckling of bars
in horizontal zone near column top

Flexural failure at column bottom in the lab or the field

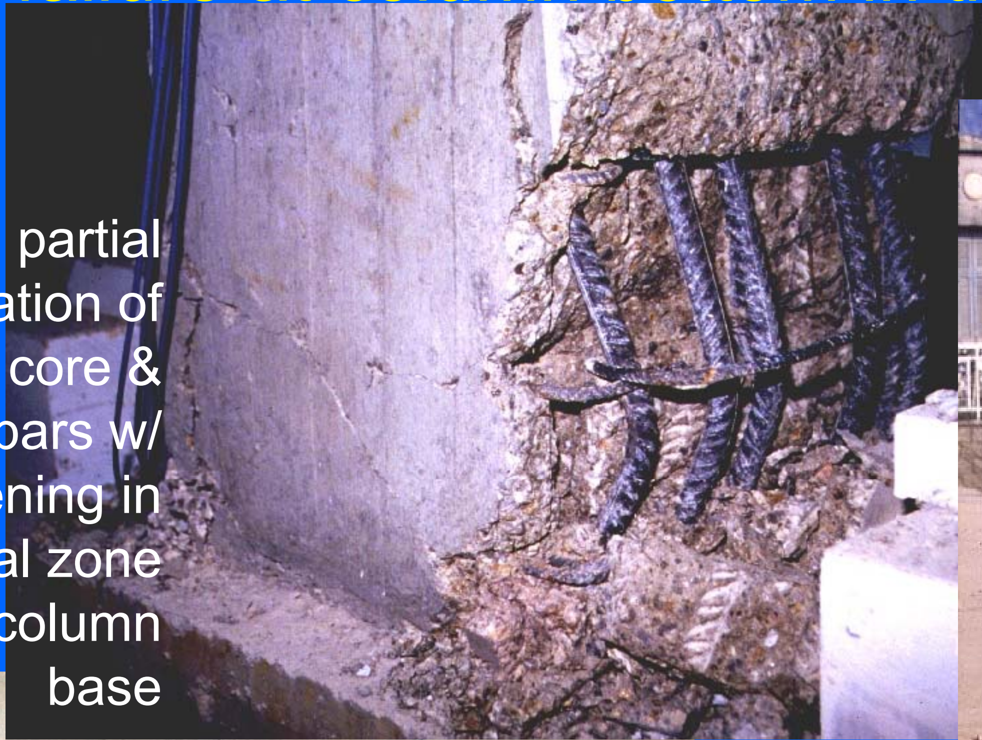

Loss of cover, partial disintegration of concrete core & buckling of bars w/ stirrups opening in horizontal zone above the column base

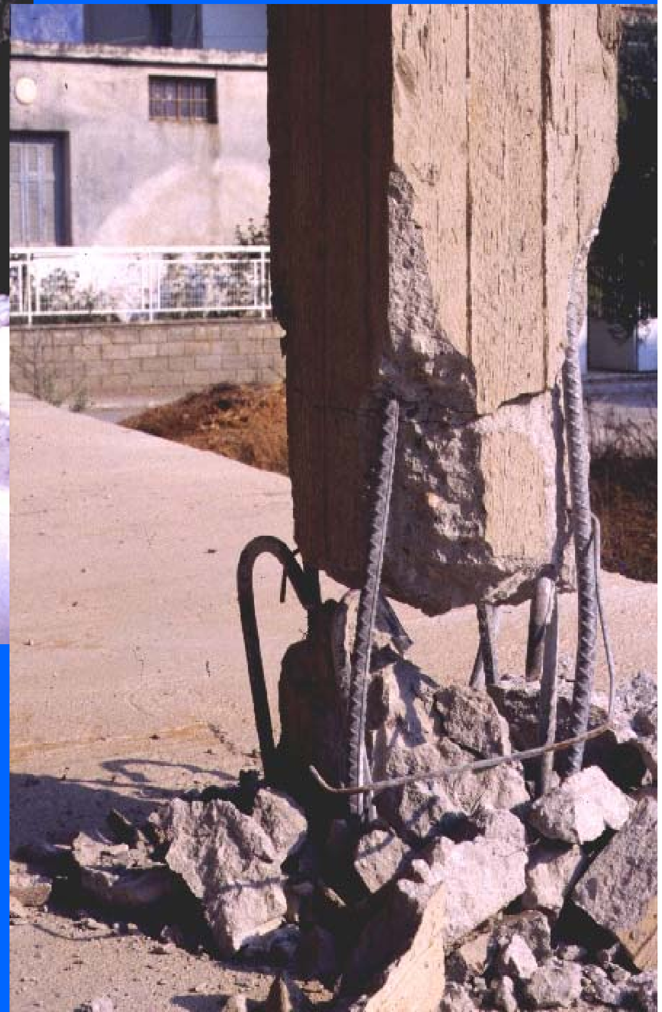

complete disintegration of concrete & buckling of bars in splice zone just above column base

Flexural damage or failure of beams in the field or the lab

through-depth cracks at support of L- or T-beams, w/ extension of cracking in slab at the top flange

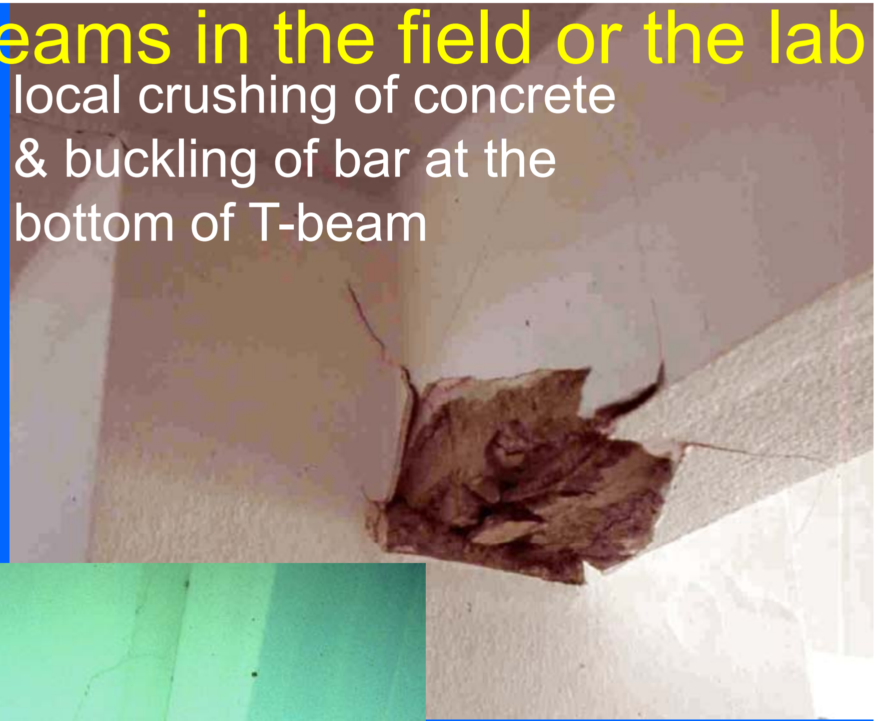

local crushing of concrete & buckling of bar at the bottom of T-beam

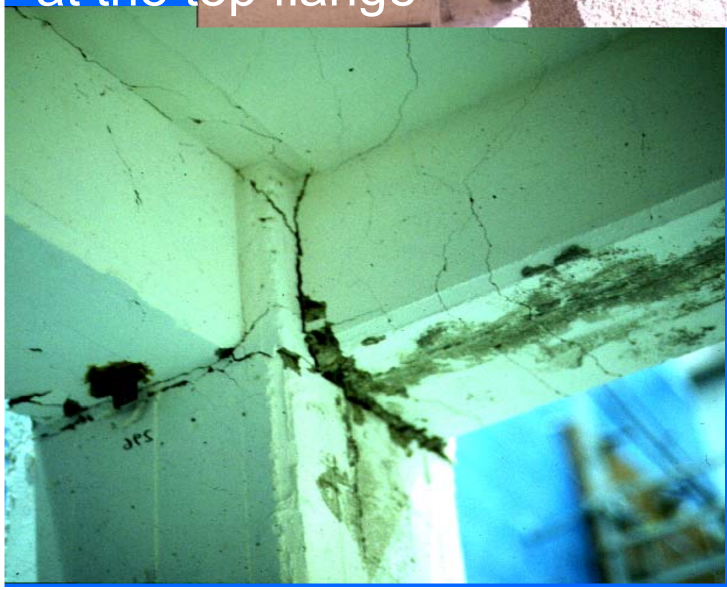

disintegration of concrete, bar buckling at bottom of L-beam, extension of through-depth flexural cracks into slab at top flange

Conventional definition of ultimate deformation

The value beyond which, any increase in deformation cannot increase the resistance above 80% of the maximum previous (ultimate) resistance.

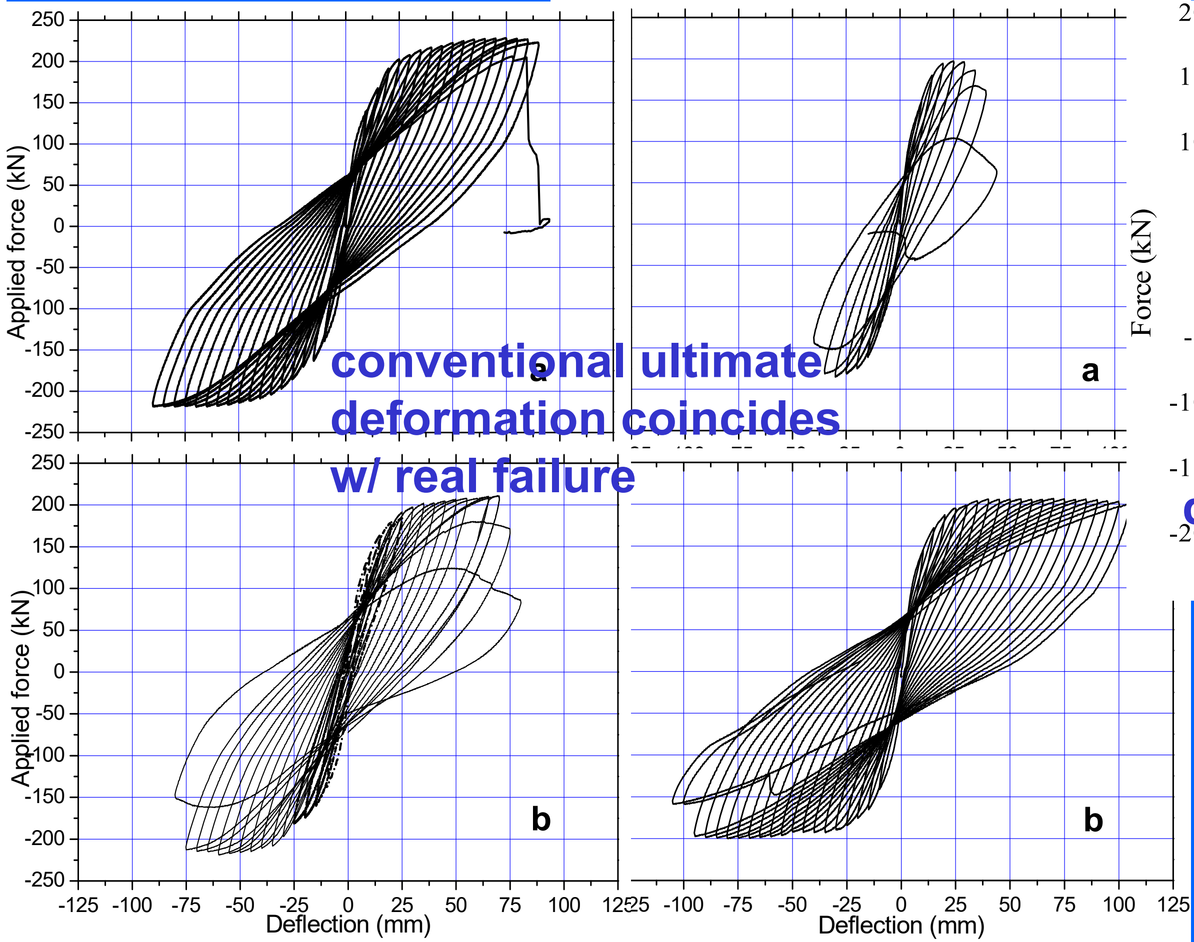

conventional ultimate deformation coincides w/ real failure

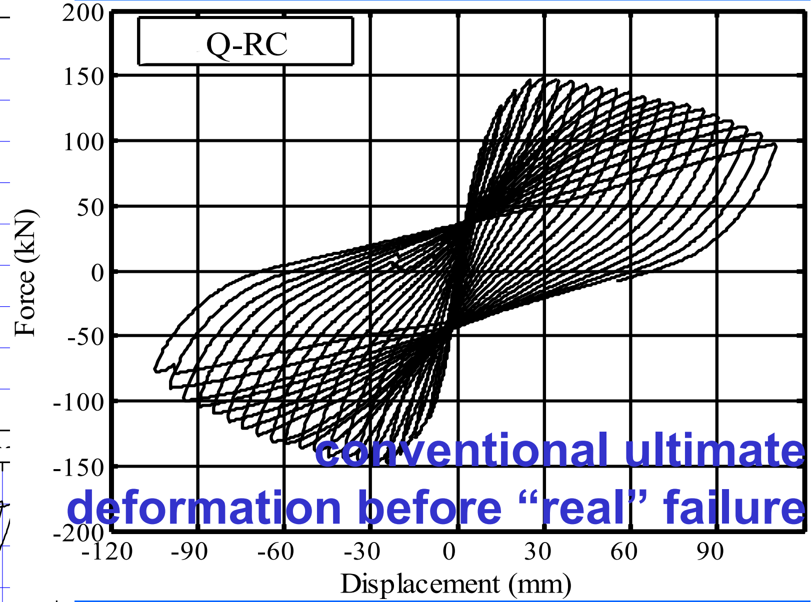

conventional ultimate deformation before “real” failure

Calculation of ultimate curvature of sections with rectangular compression zone, from 1st principles

- Concrete σ-ε law:
  - Parabolic up to a stress f_c, at a strain ε_{co},
  - constant stress (rectangular) for $\varepsilon_{co} < \varepsilon < \varepsilon_{cu}$
- Steel σ-ε law:
  - Elastic-perfectly plastic, if steel strain low and concrete fails;
  - elastic-perfectly plastic up to the strain ε_{sh}, linearly strain-hardening thereafter, until steel breaks at stress and strain f_t, ε_{su}

Notation:

Normalisation to effective depth $d=h-d_1$ and to d times compression zone width b

Indices: 1, 2, v: tension, compression & "web" reinforcement ~uniformly spread between tension & compression reinforcement.

$\delta_1=d_1/d$, $\xi=x/d$: dimensionless neutral axis depth.

$v=N/bdf_c$: dimensionless axial load; $\omega=\rho\, f_y/f_c$ mechanical reinforcement ratio.

Possibilities for ultimate curvature:

1. Section fails by rupture of tension steel, $\varepsilon_{s1} = \varepsilon_{su}$, before extreme compression fibres reach their ultimate strain (spalling), $\varepsilon_c < \varepsilon_{cu}$ →
   Ultimate curvature occurs in unspalled section, due to steel rupture:

$$\varphi_{su} = \frac{\varepsilon_{su}}{(1-\xi_{su})d} \qquad (1)$$

2. Compression fibres reach their ultimate strain (spalling): $\varepsilon_c = \varepsilon_{cu}$ →
   the confined concrete core becomes now the member section.
   Two possibilities:
   i. The moment capacity of the spalled section, M_{Ro}, never increases above 80% of the moment at spalling, M_{Rc}: $M_{Ro} < 0.8M_{Rc}$ →
      Ultimate curvature occurs in unspalled section, due to the concrete:

$$\varphi_{cu} = \frac{\varepsilon_{cu}}{\xi_{cu} d} \qquad (2)$$

   ii. Moment capacity of spalled section increases above 80% of moment at spalling: $M_{Ro} > 0.8M_{Rc}$ →
      The confined concrete core is now the member section and Cases 1 and 2(i) - <u>applied for the confined core</u> - are the two possibilities for attainment of the ultimate curvature → φ_{su}, φ_{cu} calculated as above but for the confined core; the <u>minimum</u> of the two is the ultimate curvature.

if:

Ultimate curvature by steel rupture:

$$\varphi_{su} = \frac{\varepsilon_{su}}{\left(1-\xi_{su}\right)d}$$

- If: $\delta_1 \le \dfrac{\varepsilon_{cu}-\varepsilon_{y2}}{\varepsilon_{cu}+\varepsilon_{su}}$ (3)

➢ Steel rupture occurs before concrete crushes, after compression steel yields, if:

$$\frac{\delta_1\varepsilon_{su1}+\varepsilon_{y2}-\left(1-\delta_1\right)\frac{\varepsilon_{co}}{3}}{\varepsilon_{su1}+\varepsilon_{y2}}+\omega_2-\omega_1\frac{f_{t1}}{f_{y1}}-\omega_v\left[\frac{\varepsilon_{su1}-\varepsilon_{y2}}{\varepsilon_{su1}+\varepsilon_{y2}}+\frac{1}{2}\frac{\varepsilon_{su1}-\varepsilon_{shv}}{\varepsilon_{su1}+\varepsilon_{y2}}\left(1+\frac{f_{tv}}{f_{yv}}\right)\right]\equiv\nu_{s,y2}\le\nu\le\nu_{s,c}\equiv\frac{\varepsilon_{cu}-\frac{\varepsilon_{co}}{3}}{\varepsilon_{cu}+\varepsilon_{su1}}+\omega_2-\omega_1\frac{f_{t1}}{f_{y1}}-\frac{\omega_v}{\left(1-\delta_1\right)}\left[\delta_1-\frac{\varepsilon_{su1}-\varepsilon_{cu}}{\varepsilon_{su1}+\varepsilon_{cu}}+\frac{1}{2}\frac{\varepsilon_{su1}-\varepsilon_{shv}}{\varepsilon_{su1}+\varepsilon_{cu}}\left(1+\frac{f_{tv}}{f_{yv}}\right)\right] \quad (4)$$

- ξ_{su} and ultimate moment computed from axial force and moment equilibrium:

$$\xi_{su}\approx\frac{\left(1-\delta_1\right)\left(\nu+\omega_1\frac{f_{t1}}{f_{y1}}-\omega_2+\frac{\varepsilon_{co}}{3\varepsilon_{su1}}\right)+\left(1+\delta_1+\frac{1}{2}\left(1-\frac{\varepsilon_{shv}}{\varepsilon_{su1}}\right)\left(1+\frac{f_{tv}}{f_{yv}}\right)\right)\omega_v}{\left(1-\delta_1\right)\left(1+\frac{\varepsilon_{co}}{3\varepsilon_{su1}}\right)+\left(2+\frac{1}{2}\left(1-\frac{\varepsilon_{shv}}{\varepsilon_{su1}}\right)\left(1+\frac{f_{tv}}{f_{yv}}\right)\right)\omega_v} \quad (5)$$

$$\frac{M_R}{bd^2f_c}=\left(1-\xi\right)\left[\frac{\xi}{2}-\frac{\varepsilon_{co}}{3\varepsilon_{su1}}\left(\frac{1}{2}-\xi+\frac{\varepsilon_{co}}{4\varepsilon_{su1}}\left(1-\xi\right)\right)\right]+$$
$$\frac{\left(1-\delta_1\right)}{2}\left(\omega_1\frac{f_{t1}}{f_{y1}}+\omega_2\right)+\frac{\omega_v}{1-\delta_1}\left\{(\xi-\delta_1)(1-\xi)-\frac{1}{3}\left(\frac{\left(1-\xi\right)\varepsilon_{yv}}{\varepsilon_{su1}}\right)^2+\left[\frac{\left(1-\delta_1\right)}{4}-\left(1-\frac{\varepsilon_{shv}}{\varepsilon_{su1}}\right)\frac{1-\xi}{6}\right]\left(1-\frac{\varepsilon_{shv}}{\varepsilon_{su1}}\right)\left(\frac{f_{t1}}{f_{y1}}-1\right)\left(1-\xi\right)\right\} \quad (6)$$

➢ The tension bars rupture, before the concrete crushes or the compression steel yields, if:

$$\nu\le\frac{\delta_1\varepsilon_{su1}+\varepsilon_{y2}-\left(1-\delta_1\right)\frac{\varepsilon_{co}}{3}}{\varepsilon_{su1}+\varepsilon_{y2}}+\omega_2-\omega_1\frac{f_{t1}}{f_{y1}}-\omega_v\left[\frac{\varepsilon_{su1}-\varepsilon_{y2}}{\varepsilon_{su1}+\varepsilon_{y2}}+\frac{1}{2}\frac{\varepsilon_{su1}-\varepsilon_{shv}}{\varepsilon_{su1}+\varepsilon_{y2}}\left(1+\frac{f_{tv}}{f_{yv}}\right)\right]\equiv\nu_{s,y2} \quad (7)$$

- ξ_{su} and the ultimate moment from:

$$\left[1+\frac{\varepsilon_{co}}{3\varepsilon_{su}}+\frac{\omega_v}{2(1-\delta_1)}\left(1+\frac{f_{tv}}{f_{yv}}\left(1-\frac{\varepsilon_{shv}}{\varepsilon_{su1}}\right)+\frac{\varepsilon_{shv}-3\varepsilon_{yv}}{\varepsilon_{su1}}-\frac{\varepsilon_{su1}}{\varepsilon_{yv}}\right)\right]\xi^2-$$
$$\left[1+\nu+\frac{2\varepsilon_{co}}{3\varepsilon_{su}}+\omega_1\frac{f_{t1}}{f_{y1}}+\omega_2\frac{\varepsilon_{su1}}{\varepsilon_{y2}}+\frac{\omega_v}{(1-\delta_1)}\left(1+\frac{f_{tv}}{f_{yv}}\left(1-\frac{\varepsilon_{shv}}{\varepsilon_{su1}}\right)+\frac{\varepsilon_{shv}-3\varepsilon_{yv}}{\varepsilon_{su1}}-\delta_1\frac{\varepsilon_{su1}}{\varepsilon_{yv}}\right)\right]\xi \quad (8)$$
$$+\left[\nu+\frac{\varepsilon_{co}}{3\varepsilon_{su}}+\omega_1\frac{f_{tv}}{f_{yv}}+\omega_2\delta_1\frac{\varepsilon_{su}}{\varepsilon_{y2}}+\frac{\omega_v}{2(1-\delta_1)}\left(1+\frac{f_{tv}}{f_{yv}}\left(1-\frac{\varepsilon_{shv}}{\varepsilon_{su1}}\right)+\frac{\varepsilon_{shv}-3\varepsilon_{yv}}{\varepsilon_{su1}}-\delta_1^{\,2}\frac{\varepsilon_{su1}}{\varepsilon_{yv}}\right)\right]=0$$

$$\frac{M_R}{bd^2f_c}=\left(1-\xi\right)\left[\frac{\xi}{2}-\frac{\varepsilon_{co}}{3\varepsilon_{su1}}\left(\frac{1}{2}-\xi+\frac{\varepsilon_{co}}{4\varepsilon_{su1}}\left(1-\xi\right)\right)\right]+$$
$$\frac{\left(1-\delta_1\right)}{2}\left(\omega_1\frac{f_{t1}}{f_{y1}}+\omega_2\frac{\xi-\delta_1}{1-\xi}\frac{\varepsilon_{su1}}{\varepsilon_{y2}}\right)+\frac{\omega_v}{6\left(1-\delta_1\right)}\left\{\left[1-\delta_1+\xi\left(1-\frac{\varepsilon_{yv}}{\varepsilon_{su1}}\right)\right]\left[1+\frac{\varepsilon_{su1}}{\varepsilon_{yv}}\left(\frac{\xi-\delta_1}{1-\xi}\right)\right]\left[\frac{1-\delta_1}{2}-(1-\xi)\frac{\varepsilon_{yv}}{\varepsilon_{su1}}\right]+\left[\frac{2(1-\delta_1)}{3}-\left(1-\frac{\varepsilon_{shv}}{\varepsilon_{su1}}\right)(1-\xi)\right]\left(1-\frac{\varepsilon_{shv}}{\varepsilon_{su1}}\right)\left(\frac{f_{tv}}{f_{yv}}-1\right)(1-\xi)\right\} \quad (9)$$

if:

Ultimate curvature by steel rupture – transition to concrete crushing

- If: $$\delta_1 > \frac{\varepsilon_{cu} - \varepsilon_{y2}}{\varepsilon_{cu} + \varepsilon_{su}} \qquad (3a)$$

➢ Steel rupture occurs before concrete crushes, always with compression steel elastic, if:

$$\nu \le \nu_{s,c} \equiv \frac{\varepsilon_{cu} - \frac{\varepsilon_{co}}{3}}{\varepsilon_{cu} + \varepsilon_{su1}} + \omega_2 - \omega_1 \frac{f_{t1}}{f_{y1}} - \frac{\omega_v}{(1-\delta_1)}\left[\delta_1 - \frac{\varepsilon_{su1} - \varepsilon_{cu}}{\varepsilon_{su1} + \varepsilon_{cu}} + \frac{1}{2}\frac{\varepsilon_{su1} - \varepsilon_{shv}}{\varepsilon_{su1} + \varepsilon_{cu}}\left(1 + \frac{f_{tv}}{f_{yv}}\right)\right] \qquad (4a)$$

- ξ_{su} and the ultimate moment are computed from eqs. (8), (9)

- No matter the value of $\delta_1 = d_1/d$ with respect to the limit of eqs. (3), (3a), the concrete cover spalls before the tension bars rupture if

$$\nu_{s,c} \equiv \frac{\varepsilon_{cu} - \frac{\varepsilon_{co}}{3}}{\varepsilon_{cu} + \varepsilon_{su1}} + \omega_2 - \omega_1 \frac{f_{t1}}{f_{y1}} - \frac{\omega_v}{(1-\delta_1)}\left[\delta_1 - \frac{\varepsilon_{su1} - \varepsilon_{cu}}{\varepsilon_{su1} + \varepsilon_{cu}} + \frac{1}{2}\frac{\varepsilon_{su1} - \varepsilon_{shv}}{\varepsilon_{su1} + \varepsilon_{cu}}\left(1 + \frac{f_{tv}}{f_{yv}}\right)\right] < \nu \qquad (10)$$

Ultimate curvature for concrete crushing

$$\varphi_{cu} = \frac{\varepsilon_{cu}}{\xi_{cu} d}$$

- If: $$\delta_1 \le \frac{\varepsilon_{cu} - \varepsilon_{y2}}{\varepsilon_{cu} + \varepsilon_{y1}} \qquad (11)$$

➢ The extreme concrete fibers crush with tension and compression bars past yielding if:

$$\omega_2 - \omega_1 + \frac{\omega_v}{1-\delta_1}\left(\delta_1 \frac{\varepsilon_{cu} + \varepsilon_{y2}}{\varepsilon_{cu} - \varepsilon_{y2}} - 1\right) + \delta_1 \frac{\varepsilon_{cu} - \frac{\varepsilon_{co}}{3}}{\varepsilon_{cu} - \varepsilon_{y2}} \equiv \nu_{c,y2} \le \nu < \nu_{c,y1} \equiv \omega_2 - \omega_1 + \frac{\omega_v}{1-\delta_1}\left(\frac{\varepsilon_{cu} - \varepsilon_{y1}}{\varepsilon_{cu} + \varepsilon_{y1}} - \delta_1\right) + \frac{\varepsilon_{cu} - \frac{\varepsilon_{co}}{3}}{\varepsilon_{cu} + \varepsilon_{y1}} \qquad (12)$$

- ξ_{cu} and the ultimate moment are computed as:

$$\xi_{cu} = \frac{(1-\delta_1)(\nu + \omega_1 - \omega_2) + (1+\delta_1)\omega_v}{(1-\delta_1)\left(1 - \frac{\varepsilon_{co}}{3\varepsilon_{cu}}\right) + 2\omega_v} \qquad (13)$$

$$\frac{M_{Rc}}{bd^2 f_c} = \xi\left[\frac{1-\xi}{2} - \frac{\varepsilon_{co}}{3\varepsilon_{cu}}\left(\frac{1}{2} - \xi + \frac{\varepsilon_{co}}{4\varepsilon_{cu}}\xi\right)\right] + \frac{(1-\delta_1)(\omega_1 + \omega_2)}{2} + \frac{\omega_v}{1-\delta_1}\left[(\xi - \delta_1)(1-\xi) - \frac{1}{3}\left(\frac{\xi\varepsilon_{yv}}{\varepsilon_{cu}}\right)^2\right] \qquad (14)$$

➢ Tension bars are elastic & compression bars yield if:

$$\nu_{c,y1} \equiv \omega_2 - \omega_1 + \frac{\omega_v}{1-\delta_1}\left(\frac{\varepsilon_{cu} - \varepsilon_{y1}}{\varepsilon_{cu} + \varepsilon_{y1}} - \delta_1\right) + \frac{\varepsilon_{cu} - \frac{\varepsilon_{co}}{3}}{\varepsilon_{cu} + \varepsilon_{y1}} < \nu$$

- ξ_{cu} and the ultimate moment are computed from:

$$\left[1 - \frac{\varepsilon_{co}}{3\varepsilon_{cu}} - \frac{\omega_v}{2(1-\delta_1)}\frac{(\varepsilon_{cu} - \varepsilon_{yv})^2}{\varepsilon_{cu}\varepsilon_{yv}}\right]\xi^2 + \left[\omega_2 + \omega_1\frac{\varepsilon_{cu}}{\varepsilon_{y1}} - \nu + \frac{\omega_v}{1-\delta_1}\left(\frac{\varepsilon_{cu}}{\varepsilon_{yv}} - \delta_1\right)\right]\xi - \left[\frac{\omega_1}{\varepsilon_{y1}} + \frac{\omega_v}{2(1-\delta_1)\varepsilon_{yv}}\right]\varepsilon_{cu} = 0 \qquad (15)$$

$$\frac{M_R}{bd^2 f_c} = \xi\left[\frac{1-\xi}{2} - \frac{\varepsilon_{co}}{3\varepsilon_{cu}}\left(\frac{1}{2} - \xi + \frac{\varepsilon_{co}}{4\varepsilon_{cu}}\xi\right)\right] + \frac{(1-\delta_1)}{2}\left(\omega_1\frac{1-\xi}{\xi}\frac{\varepsilon_{cu}}{\varepsilon_{y1}} + \omega_2\right) + \frac{\omega_v}{4(1-\delta_1)}\left[1 - \xi\left(1 - \frac{\varepsilon_{yv}}{\varepsilon_{cu}}\right)\right]\left[1 + \frac{\varepsilon_{cu}}{\varepsilon_{yv}}\left(\frac{1-\xi}{\xi}\right)\right]\left[\frac{1}{3} - \delta_1 + \frac{2}{3}\xi\left(1 - \frac{\varepsilon_{yv}}{\varepsilon_{cu}}\right)\right] \qquad (16)$$

➢ Tension bars yield & compression bars are elastic if:

$$\nu < \omega_2 - \omega_1 + \frac{\omega_v}{1-\delta_1}\left(\delta_1\frac{\varepsilon_{cu} + \varepsilon_{y2}}{\varepsilon_{cu} - \varepsilon_{y2}} - 1\right) + \delta_1\frac{\varepsilon_{cu} - \frac{\varepsilon_{co}}{3}}{\varepsilon_{cu} - \varepsilon_{y2}} \equiv \nu_{c,y2}$$

- ξ_{cu} and the ultimate moment are computed from:

$$\left[1 - \frac{\varepsilon_{co}}{3\varepsilon_{cu}} + \frac{\omega_v}{2(1-\delta_1)}\frac{(\varepsilon_{cu} + \varepsilon_{yv})^2}{\varepsilon_{cu}\varepsilon_{yv}}\right]\xi^2 - \left[\nu + \omega_1 - \omega_2\frac{\varepsilon_{cu}}{\varepsilon_{y2}} + \frac{\omega_v}{1-\delta_1}\left(1 + \frac{\varepsilon_{cu}\delta_1}{\varepsilon_{yv}}\right)\right]\xi - \left[\frac{\omega_2}{\varepsilon_{y2}} - \frac{\omega_v\delta_1}{2(1-\delta_1)\varepsilon_{yv}}\right]\varepsilon_{cu}\delta_1 = 0 \qquad (17)$$

$$\frac{M_R}{bd^2 f_c} = \xi\left[\frac{1-\xi}{2} - \frac{\varepsilon_{co}}{3\varepsilon_{cu}}\left(\frac{1}{2} - \xi + \frac{\varepsilon_{co}}{4\varepsilon_{cu}}\xi\right)\right] + \frac{(1-\delta_1)}{2}\left(\omega_1 + \omega_2\frac{\xi - \delta_1}{\xi}\frac{\varepsilon_{cu}}{\varepsilon_{y2}}\right) + \frac{\omega_v}{4(1-\delta_1)}\left[\xi\left(1 + \frac{\varepsilon_{yv}}{\varepsilon_{cu}}\right) - \delta_1\right]\left[1 + \frac{\varepsilon_{cu}}{\varepsilon_{yv}}\left(\frac{\xi - \delta_1}{\xi}\right)\right]\left[1 - \frac{\delta_1}{3} - \frac{2}{3}\xi\left(1 + \frac{\varepsilon_{yv}}{\varepsilon_{cu}}\right)\right] \qquad (18)$$

Ultimate curvature by concrete crushing (cont'd)

- If: $\delta_1 > \dfrac{\varepsilon_{cu} - \varepsilon_{y2}}{\varepsilon_{cu} + \varepsilon_{y1}}$ (11a)

➤ When the extreme compression fibers crush, tension and compression bars are elastic, if:

$$\frac{\omega_2}{\varepsilon_{y2}}\left((1-\delta_1)\varepsilon_{cu} - \delta_1\varepsilon_{y1}\right) - \omega_1 + \frac{\omega_v}{2\varepsilon_{yv}}\left(\varepsilon_{cu} - \frac{1+\delta_1}{1-\delta_1}\varepsilon_{y1}\right) + \frac{\varepsilon_{cu} - \frac{\varepsilon_{co}}{3}}{\varepsilon_{cu} + \varepsilon_{y1}} \equiv \bar{\nu}_{c,y1} \le \nu < \bar{\nu}_{c,y2}$$
$$\equiv \omega_2 - \frac{\omega_1}{\varepsilon_{y1}}\frac{(1-\delta_1)\varepsilon_{cu} - \varepsilon_{y2}}{\delta_1} + \frac{\omega_v}{\delta_1\varepsilon_{yv}}\left(\frac{1+\delta_1}{1-\delta_1}\varepsilon_{y2} - \varepsilon_{cu}\right) + \delta_1\frac{\varepsilon_{cu} - \frac{\varepsilon_{co}}{3}}{\varepsilon_{cu} - \varepsilon_{y2}} \quad (19)$$

- ξ_{cu} and the ultimate moment are computed from:

$$\left[1 - \frac{\varepsilon_{co}}{3\varepsilon_{cu}}\right]\xi^2 - \left[\nu - \left(\frac{\omega_1}{\varepsilon_{y1}} + \frac{\omega_2}{\varepsilon_{y2}} + \frac{\omega_v}{(1-\delta_1)\varepsilon_{yv}}\right)\varepsilon_{cu}\right]\xi - \left(\frac{\omega_1}{\varepsilon_{y1}} + \frac{\delta_1\omega_2}{\varepsilon_{y2}} + \frac{\omega_v(1+\delta_1)}{2(1-\delta_1)\varepsilon_{yv}}\right)\varepsilon_{cu} = 0 \quad (20)$$

$$\frac{M_R}{bd^2 f_c} = \xi\left[\frac{1-\xi}{2} - \frac{\varepsilon_{co}}{3\varepsilon_{cu}}\left(\frac{1}{2} - \xi + \frac{\varepsilon_{co}}{4\varepsilon_{cu}}\xi\right)\right] + \frac{(1-\delta_1)\varepsilon_{cu}}{2\xi}\left((1-\xi)\frac{\omega_1}{\varepsilon_{y1}} + (\xi - \delta_1)\frac{\omega_2}{\varepsilon_{y2}}\right) + \frac{\omega_v(1-\delta_1)^2}{12\xi}\frac{\varepsilon_{cu}}{\varepsilon_{yv}} \quad (21)$$

➤ When the extreme compression fibers crush, tension bars have yielded but compression bars are elastic, if:

$$\nu < \frac{\omega_2}{\varepsilon_{y2}}\left((1-\delta_1)\varepsilon_{cu} - \delta_1\varepsilon_{y1}\right) - \omega_1 + \frac{\omega_v}{2\varepsilon_{yv}}\left(\varepsilon_{cu} - \frac{1+\delta_1}{1-\delta_1}\varepsilon_{y1}\right) + \frac{\varepsilon_{cu} - \frac{\varepsilon_{co}}{3}}{\varepsilon_{cu} + \varepsilon_{y1}} \equiv \bar{\nu}_{c,y1}$$

- ξ_{cu} and the ultimate moment are computed from eqs. (17), (18):

➤ When the extreme compression fibers crush, tension bars are elastic but compression bars have yielded, if:

$$\bar{\nu}_{c,y2} \equiv \omega_2 - \frac{\omega_1}{\varepsilon_{y1}}\frac{(1-\delta_1)\varepsilon_{cu} - \varepsilon_{y2}}{\delta_1} + \frac{\omega_v}{\delta_1\varepsilon_{yv}}\left(\frac{1+\delta_1}{1-\delta_1}\varepsilon_{y2} - \varepsilon_{cu}\right) + \delta_1\frac{\varepsilon_{cu} - \frac{\varepsilon_{co}}{3}}{\varepsilon_{cu} - \varepsilon_{y2}} < \nu$$

- ξ_{cu} and the ultimate moment are computed from eqs. (15), (16).

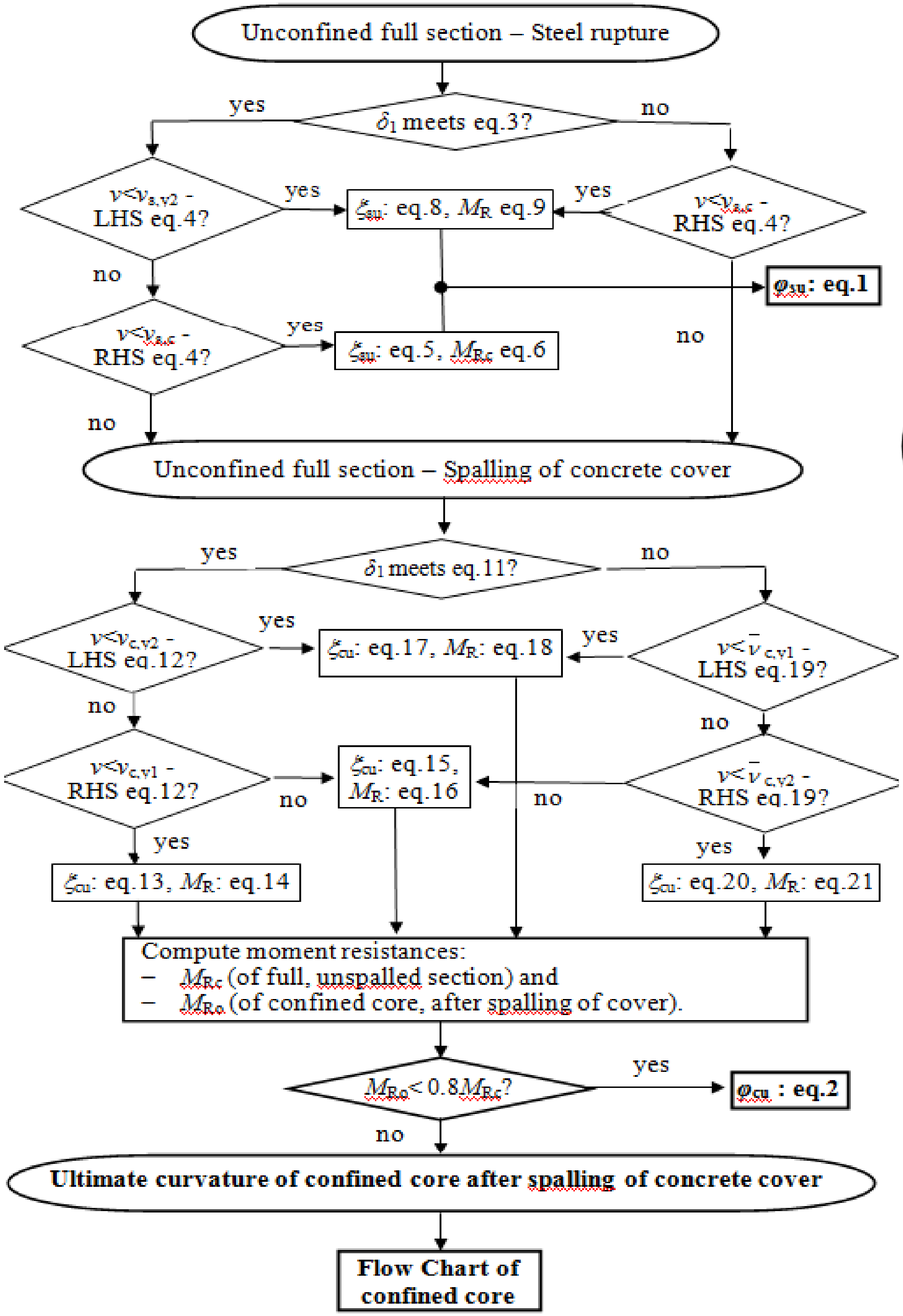

Confined core after spalling of concrete cover.

Parameters are denoted by an asterisk and computed with:

- σ-ε parameters of confined concrete, f_c^*, ε_{c1}^*, ε_{cu}^*, used instead of f_c, ε_{c1}, ε_{cu}
- b, d, d_1 are replaced by geometric parameters of the core: b_c, d_c, d_{c1};
- N, ρ_1, ρ_2, ρ_v are normalized to $b_c d_c$, instead of bd.

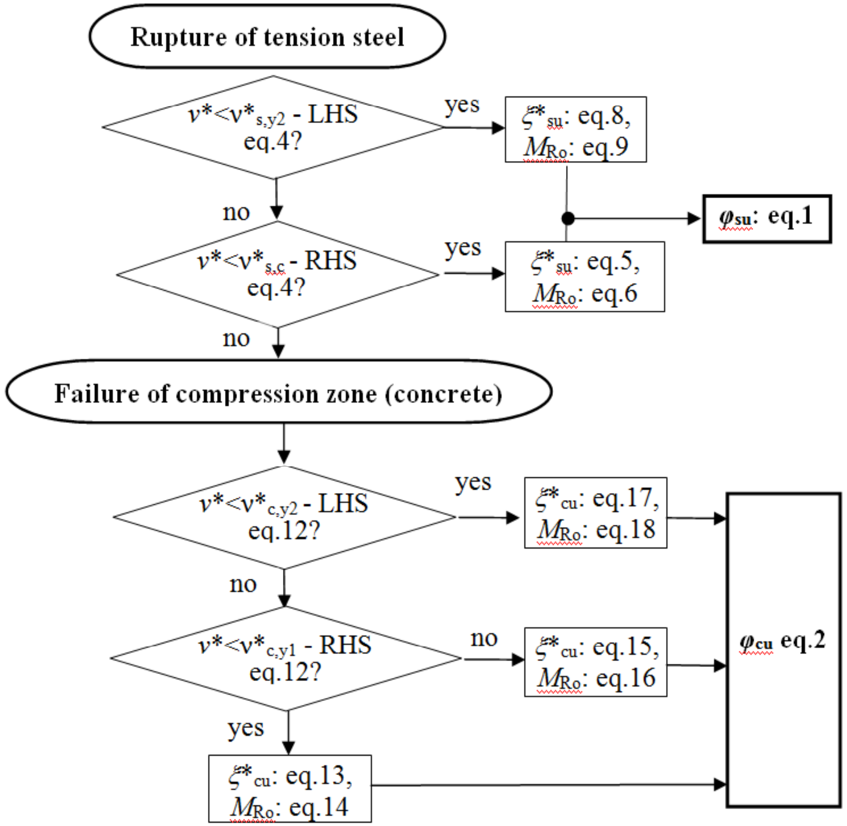

Ultimate strains inferred from experimental curvatures by back-analysis

- ***Before spalling*: Steel -** Monotonic: $$\varepsilon_{su,mon} = \left(1 - 0.3\sqrt{\ln N_{bars,tens}}\right)\varepsilon_{su,nom}$$
  Steel - Cyclic: $$\varepsilon_{su,cy} = 0.4\varepsilon_{su,nom}$$
  Concrete: $$0.0035 \le \varepsilon_{cu} = \left(18.5/h(mm)\right)^2 \le 0.01$$
- ***After spalling*: Steel -** Cyclic: $$\varepsilon_{su,cy} = \frac{4}{15}\left(1 + 3\frac{d_b}{s_h}\right)\left(1 - 0.75e^{-0.4N_{bars.compr}}\right)\varepsilon_{su,nom}$$
  Confined concrete: *fib* MC2010: $$f_{cc}/f_c = 1 + 3.5\left(\alpha\rho_w f_{yw}/f_c\right)^{3/4}$$
  - rect. compression zone: $$\varepsilon_{cu,c} = \varepsilon_{cu} + 0.04\sqrt{a\rho_s f_{yw}/f_c}$$
  - in circular sections: $$\varepsilon_{cu,c} = \varepsilon_{cu} + 0.07\sqrt{a\rho_s f_{yw}/f_c}$$
  - triangular compression zone: $$\varepsilon_{cu,c} = \varepsilon_{cu} + 0.12\sqrt{a\rho_s f_{yw}/f_c}$$
    - ρ_s: tie steel ratio in direction of bending;
    - f_{yw}: tie yield stress,
    - α: confinement effectiveness factor

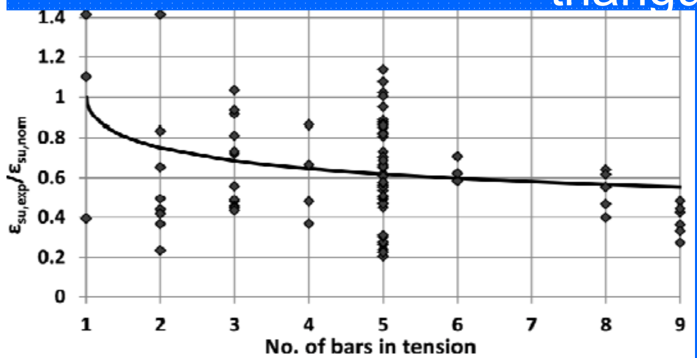

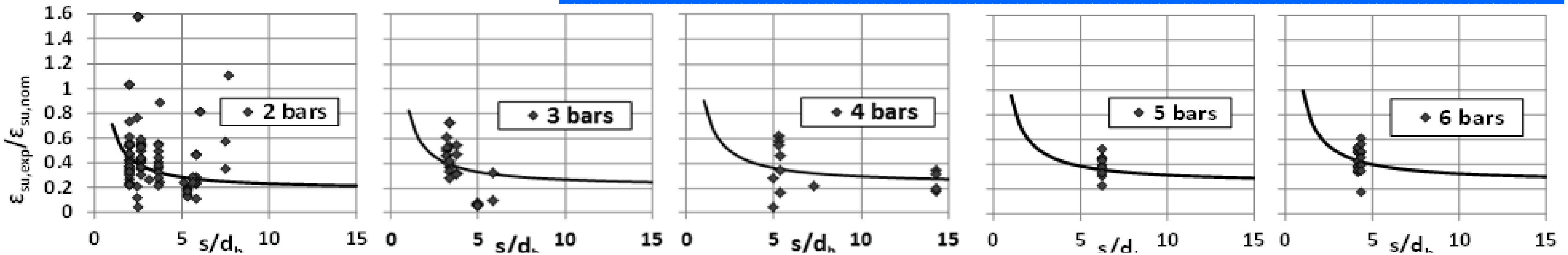

(374) measured ultimate curvatures from (184) cyclic tests vs values calculated using ultimate strains from current seismic codes

(a) Eurocode 8 (2005) for existing buildings, with confinement model of MC1990 or Eurocode 2 (2004) – CoV:59.5%;

(b) Eurocode 8 (2005) for existing buildings but with its own confinement model – CoV:54.5%;

(c) Caltrans (2006) for bridges – CoV:72%;

(d) Eurocode 8 (2005) for bridges – CoV:64%.

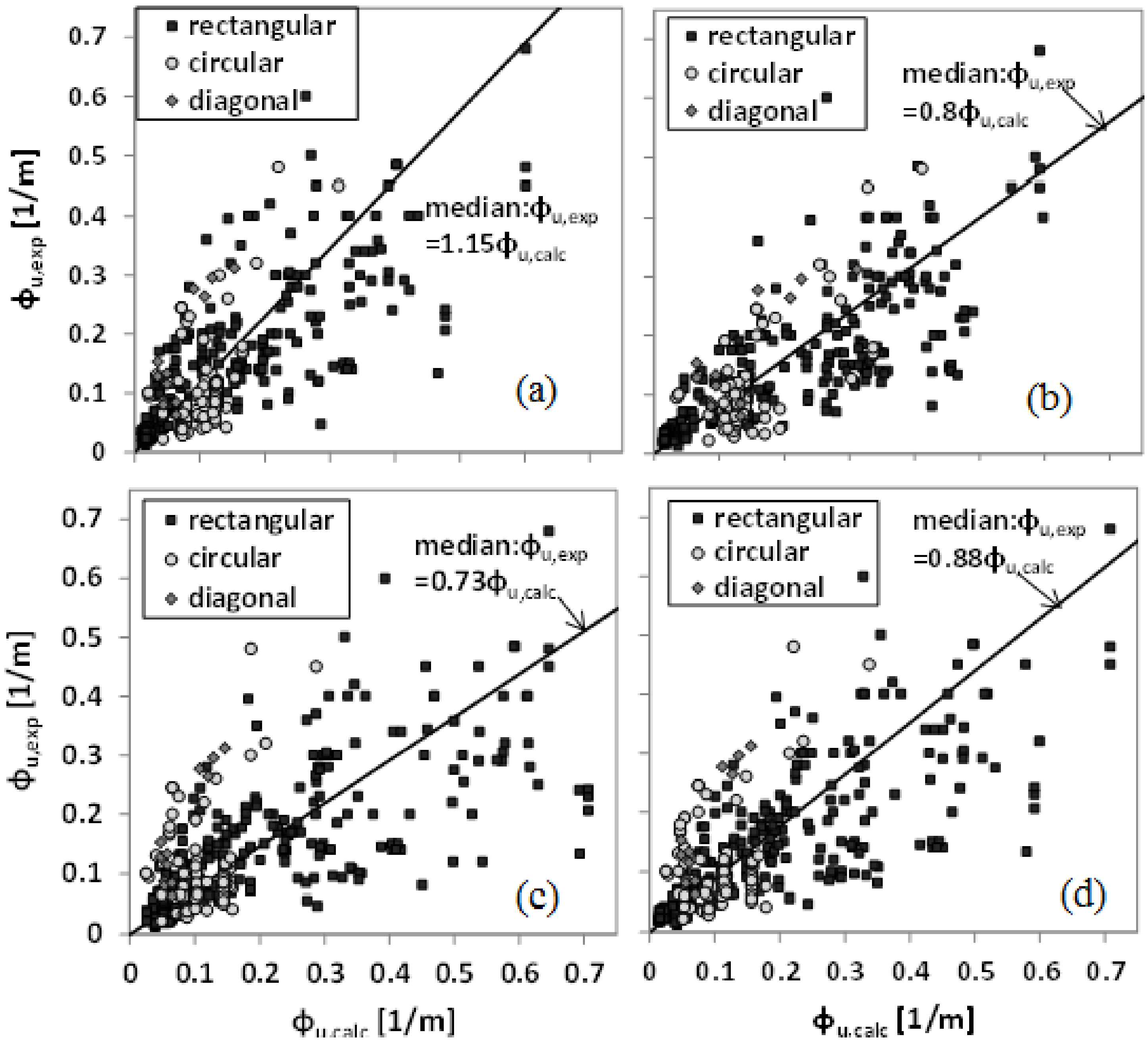

(645) measured ultimate curvatures in (410) tests vs values calculated using ultimate strains from Grammatikou et al 2016

monotonic & cyclic data, CoV:46%

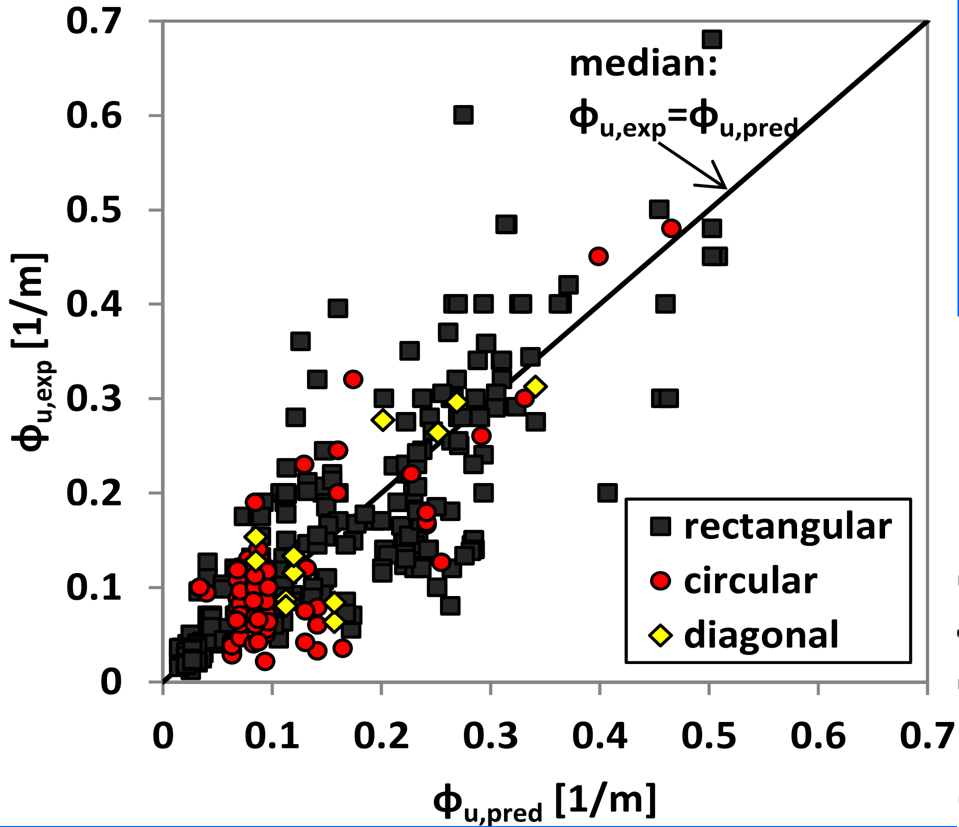

cyclic data, CoV:46%

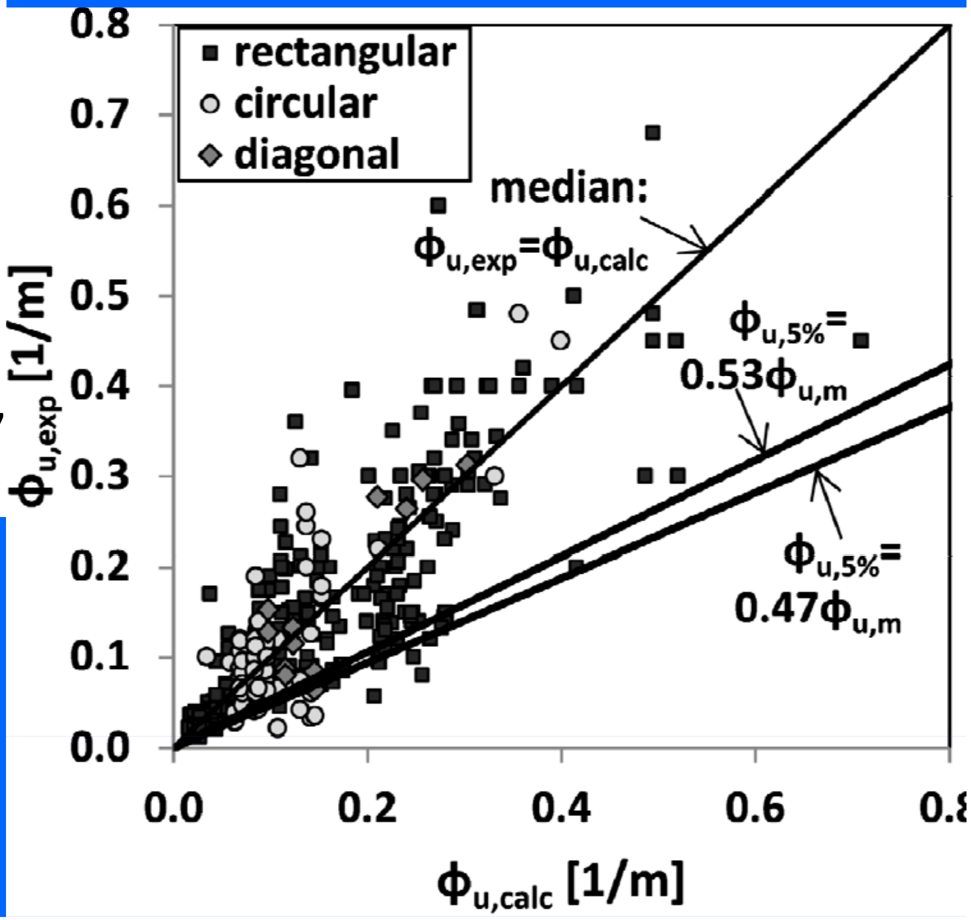

Fixed-end rotation of member end due to pull-out of straight ribbed bars from the zone beyond member’s end

- Slippage (pull-out) of tension bars from region beyond end section (e.g. from joint or footing) →

  rigid-body rotation of entire shear span = fixed-end rotation, θ_{slip}

  (included in measured chord-rotations of test specimen w.r. to base or joint; doesn’t affect measured relative rotations between any two member sections).
- If s = slippage of tension bars from anchorage → $\theta_{slip} = s/(1-\xi)d$
- If bond stress uniform over straight length l_b of ribbed bar past section of maximum moment → bar stress decreases along l_b from σ_s (=f_{yL} at yielding) at section of maximum M to zero at end of l_b → $s=\sigma_s l_b/(2E_s)$
- l_b= bond force demand per unit length (=$A_s\sigma_s/(\pi d_{bL})=d_{bL}\sigma_s/4$), divided by ~bond strength (assume =$\sqrt{f_c}$)
- $\varepsilon_s(=\sigma_s/E_s)/(1-\xi)d = \varphi$
- At yielding of member end section

$$\theta_{y,slip} = \frac{\varphi_y d_{bL} f_y}{8\sqrt{f_c}} \quad (f_{yL},\ f_c \text{ in MPa })$$

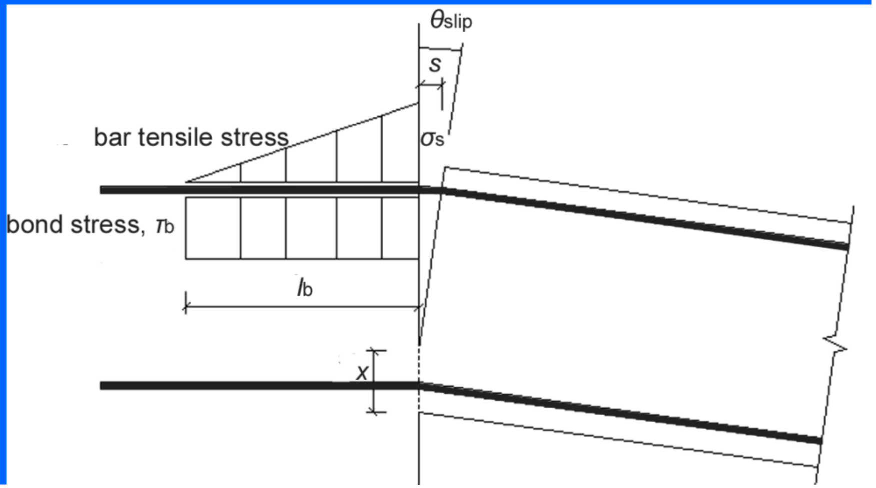

Fixed-end rotation of member end due to ribbed bar pull-out from zone beyond member end, at member yielding

$\varphi_{y,measured}/(\varphi_{y,predicted}+\theta_{y,slip,}/l_{gauge})$ no.160 measurements w/ slip: median = 1.0, C.o.V = 34%

Ratio: experimental-to-predicted yield curvature (w/ correction for fixed-end-rotation): independent of gauge length

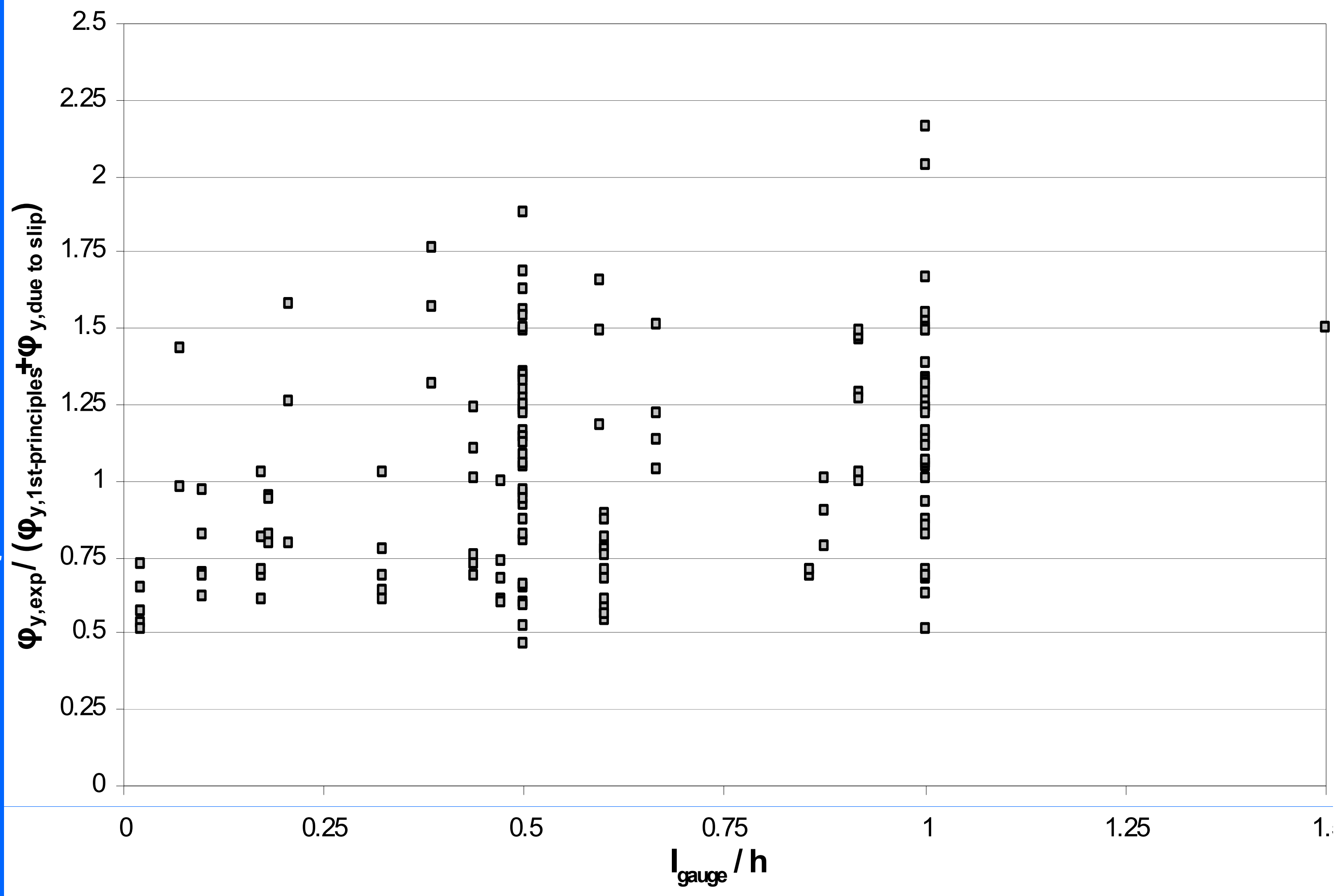

Fixed-end rotation of member end due to ribbed bar pull-out from yield penetration length in zone beyond the member end, at member **ultimate curvature**

- Monotonic flexure: $\Delta\theta_{u,slip} = 9d_b\left(\phi_u + \phi_y\right), -or- \Delta\theta_{u,slip} = 10d_b\phi_u$
- Cyclic flexure: $\Delta\theta_{u,slip} = 4.25d_b\left(\phi_u + \phi_y\right), -or- \Delta\theta_{u,slip} = 4.5d_b\phi_u$

Complete pull-out of beam bars, due to short anchorage in corner joint

← →

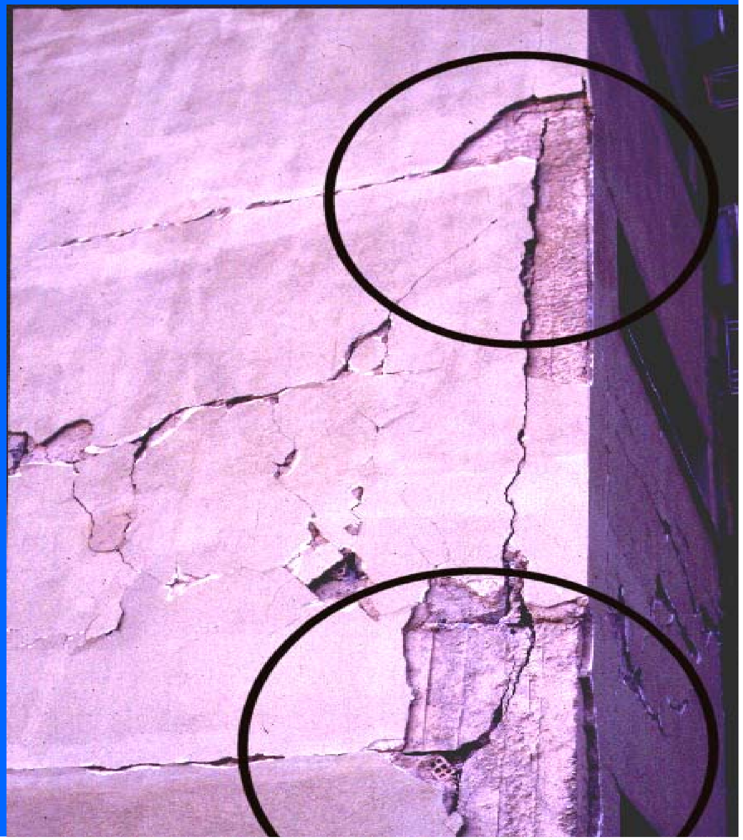

Mean axial deformations due to flexural response

- Over entire member length:
  - Additional mean axial strain (at section centroid): $\Delta\varepsilon_o = |\varphi|(0.5-\xi)d$
  - Member axial elongation between ends A, B, due to flexural deformation:

$$\Delta\delta_x = \int_l \Delta\varepsilon_o \, dx = (0.5-\xi)d \int_l |\varphi| \, dx = (0.5-\xi)\theta_{AB} d$$

- Only in region that yielded - plastic hinge:
  - Mean axial strain at φ = 0, ε_o= mean permanent strain in bars of both sides ≠ 0
  - ε_o ↑ w/ cycling of flexural deformations.
  - ε_o = tensile, if N = 0 or low.
  - In columns, after loss of cover & partial disintegration of concrete core or bar buckling, ε_o turns from extension to shortening when cyclic failure approaches
  - In columns w/ intermediate to high values of v=A_c/f_c (e.g., v >0.15-0.2), ε_o is shortening from the beginning of cyclic flexure.

Evolution of mean axial strain, ε_o, in plastic hinge w/ lateral deflection cycling

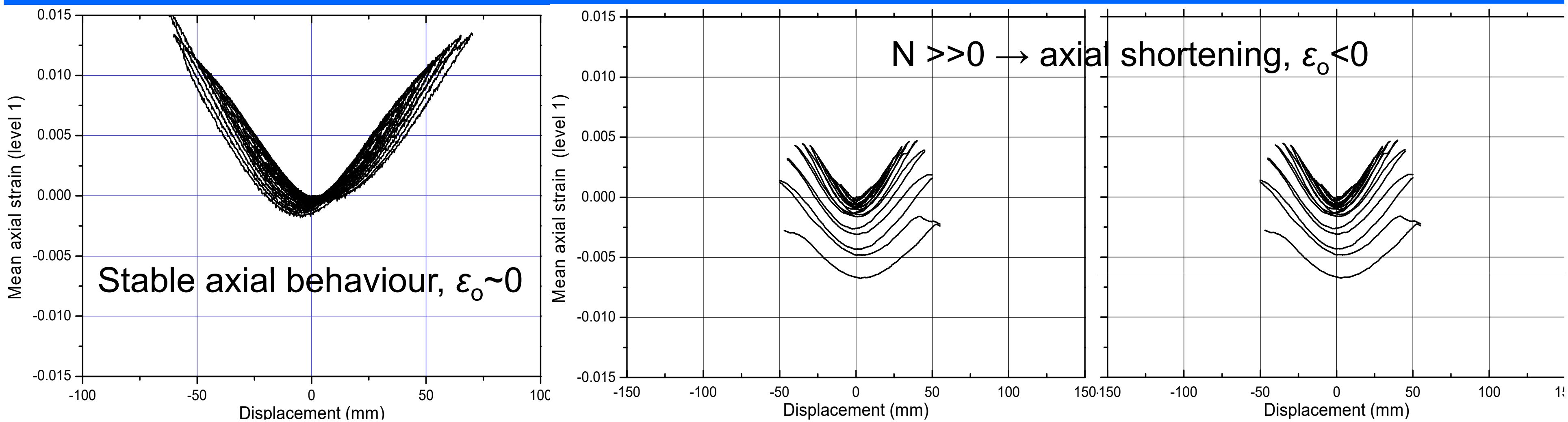

Effect of axial load variation w/ cyclic flexure (exterior columns due to overturning moment)

- Yield moment, M-resistance, stiffness in virgin loading & unloading/reloading:
  - All ↑, when compressive N ↑,
  - All ↓, when compressive N ↓.
- If N varies w.r.to mean value ~in proportion to M:
  - effect of N gradual: it accelerates softening when N ↓; reduces it (even to stiffening) when N ↑ *(deflection may even ↓ w/ ↑ transverse force if stiffening due to N↑ governs)*
  - N ~constant after yielding in virgin loading or reloading.
- If N varies w.r.to mean ~in proportion to deflection:
  - when N ↑
    - yield moment & resistance, post yield stiffness: ↑ ;
    - after yielding: large strength decay for cycling at ~same peak deflection (failure w/ cycling sooner).
  - when N ↓
    - after yielding: M ↓;
    - cyclic failure delayed.

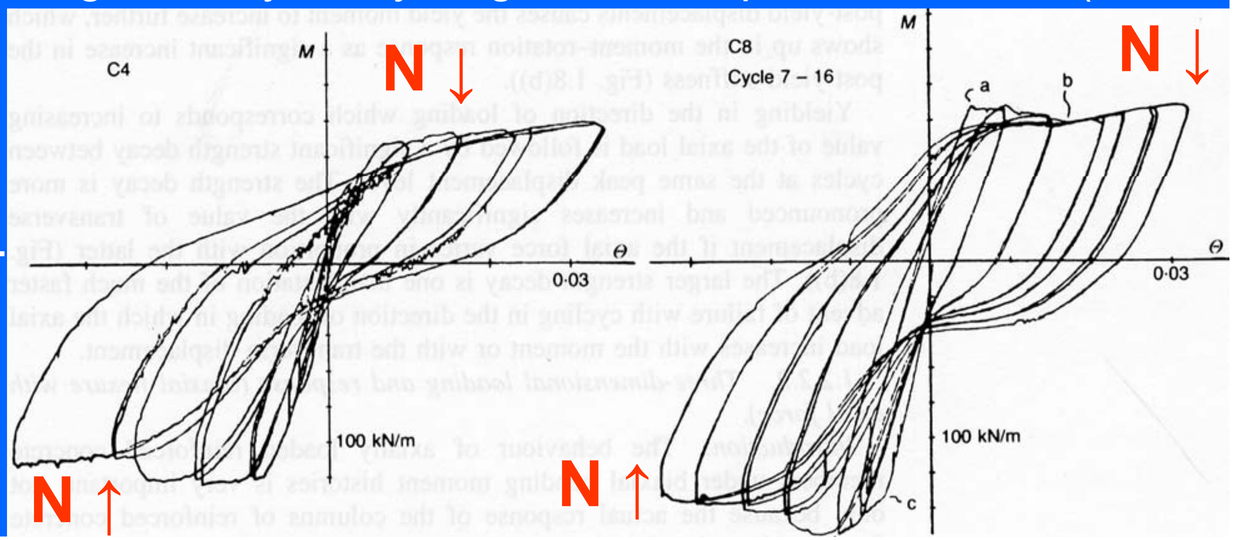

Cyclic biaxial flexure w/ axial force

- Biaxial flexure:
  - M-resistance ↓,
  - deterioration of stiffness & strength w/ cycling ↑.

→ Against strong-column/weak-beam behaviour, even when columns capacity-designed separately in 2 orthogonal horizontal directions.

- After flexural yielding under M_x-M_y → strong coupling between behaviour in the two orthogonal transverse directions →

  In each individual direction:
  - apparent resistance & stiffness ↓;

    (ratcheting flexural deformations in direction where M = constant due to cycling of flexural deformation in the other direction).
  - deformation capacity ↓

    (individual deformation components, normalized by the corresponding ultimate deformation under uniaxial loading: ~circular interaction diagram).

- Strong coupling of behavior in the two orthogonal transverse directions → ↑ apparent hysteretic energy dissipation (wider hysteresis loops)
  - φ_x-φ_y vector trails M_x-M_y vector by "phase lag", ψ;
  - sinψ = viscous damping ratio, equivalent to additional hysteretic energy dissipation due to coupling;
  - ψ ↑ when inelasticity ↑.

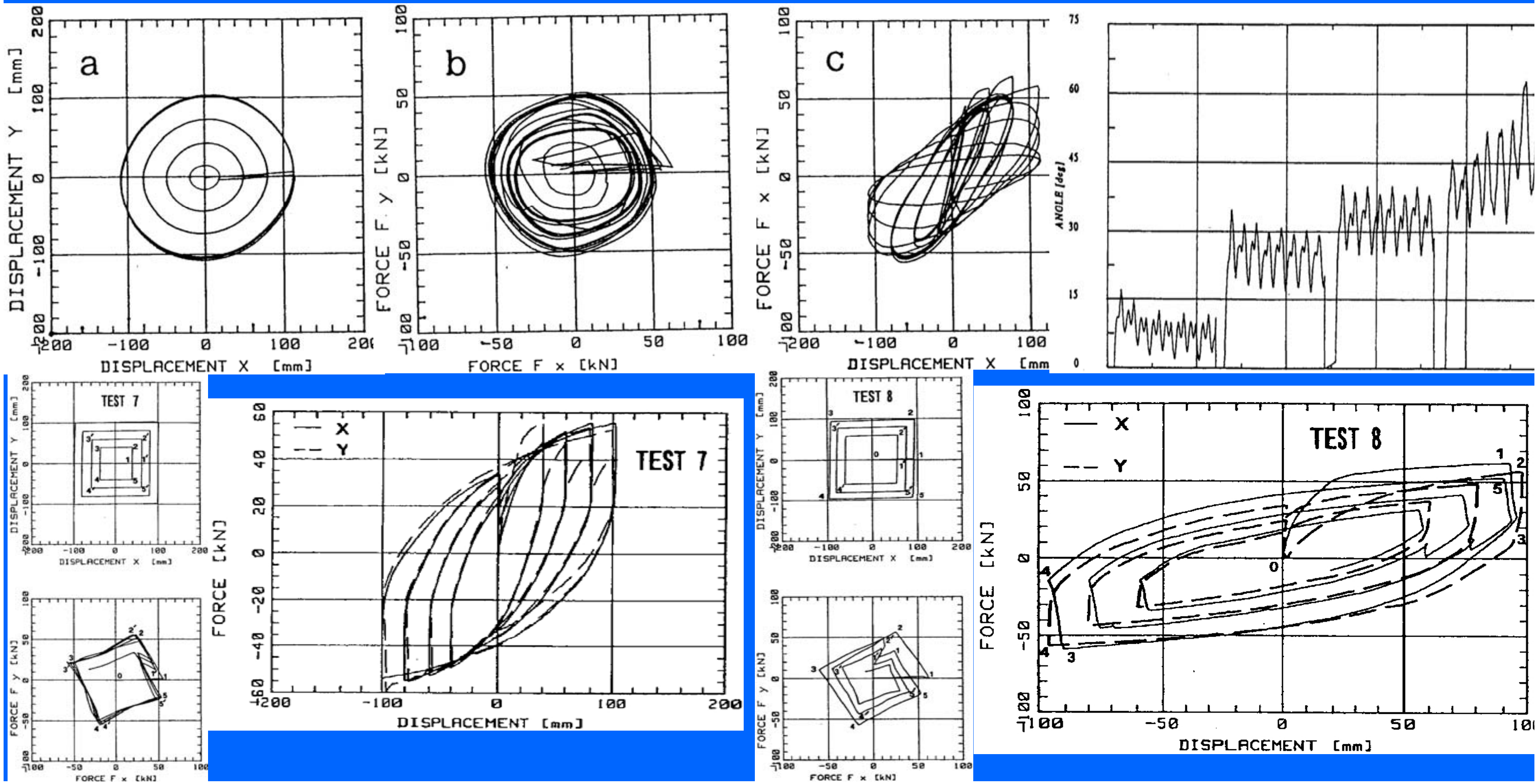

Flexure of member (Moment-chord rotation behavior)

Chord rotation at the end of a member, θ:

angle between normal to end section and chord connecting member ends at displaced position).

$$\theta_A = \frac{1}{x_B - x_A} \int_{x_A}^{x_B} \varphi(x)\left(x_B - x\right)dx$$

$$\theta_B = \frac{1}{x_B - x_A} \int_{x_A}^{x_B} \varphi(x)\left(x_A - x\right)dx$$

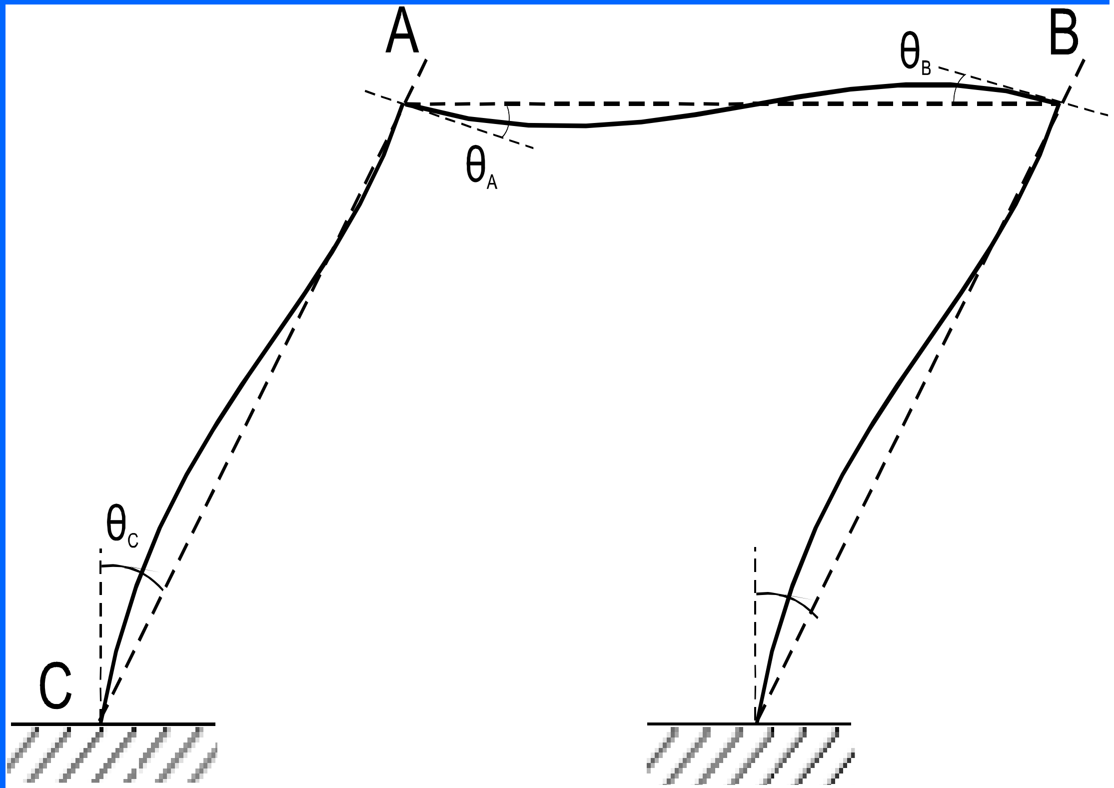

Relative rotation between ends A, B:

$$\theta_{AB} = \int_{x_A}^{x_B} \varphi(x)dx = \theta_A - \theta_B$$

Elastic moments at ends A, B from chord rotations at A, B:

- $M_A = (2EI/L)(2\theta_A + \theta_B)$,
- $M_B = (2EI/L)(2\theta_B + \theta_A)$

Chord rotation of shear span at yielding of end section

Rectangular beams or columns:

$$\theta_y = \varphi_y \frac{L_s + a_V z}{3} + 0.0019\left(1 + \frac{h}{1.6L_s}\right) + a_{sl}\theta_{y,slip}$$

Walls & hollow piers:

$$\theta_y = \varphi_y \frac{L_s + a_V z}{3} + 0.0011\left(1 + \frac{h}{3L_s}\right) + a_{sl}\theta_{y,slip}$$

Circular columns:

$$\theta_y = \varphi_y \frac{L_s + a_V z}{3} + 0.0025\max\left(0;1 - \frac{L_s}{8D}\right) + a_{sl}\theta_{y,slip}$$

"shift rule" (in ULS dimensioning in bending):

Diagonal cracking shifts value of force in tension reinforcement to a section at a distance from member end equal to *z*: internal lever arm

- $z = d - d_1$ in beams, columns, or walls of barbelled or T-section,
- $z = 0.8h$ in rectangular walls.

– $a_v = 0$, if $V_{Rc} > M_y/L_s$;

– $a_v = 1$, if $V_{Rc} \leq M_y/L_s$.

V_{Rc} = force at diagonal cracking, according to Eurocode 2 (in kN, dimensions in m, f_c in MPa):

$$V_{R,c} = \left\{\max\left[180(100\rho_1)^{1/3},\ 35\sqrt{1+\sqrt{\frac{0.2}{d}}}\ f_c^{1/6}\right]\left(1+\sqrt{\frac{0.2}{d}}\right)f_c^{1/3} + 0.15\frac{N}{A_c}\right\}b_w d$$

– $a_{sl} = 0$, if no slip from zone beyond the end section;

– $a_{sl} = 1$, if there is slip from the zone past the end section.

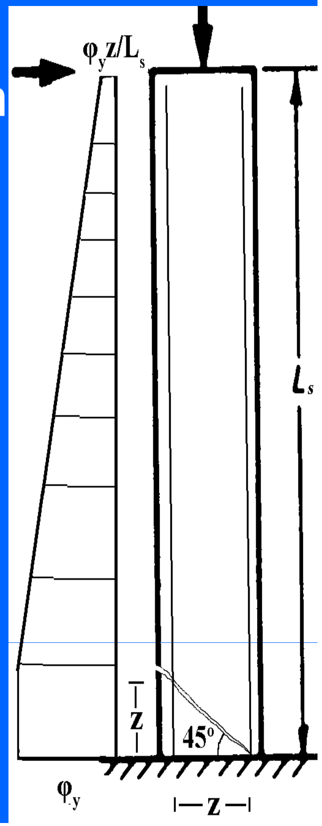

Effective elastic stiffness, EI_{eff} (for analysis, linear or nonlinear)

- Part 1of EC8 (force-based design of new buildings):
  - EI_{eff} : secant stiffness at yielding =50% of uncracked gross-section stiffness.
  - Safe-sided for forces in force-based design of new buildings;
  - Unsafe in displacement-based design or assessment (underestimates displacement demands).
- More realistic:

$$EI_{eff} = \frac{M_y L_s}{3\theta_y}$$

  - secant stiffness at yielding of end of shear span L_s=M/V
  - on average, ~25% of un-cracked, gross-section stiffness

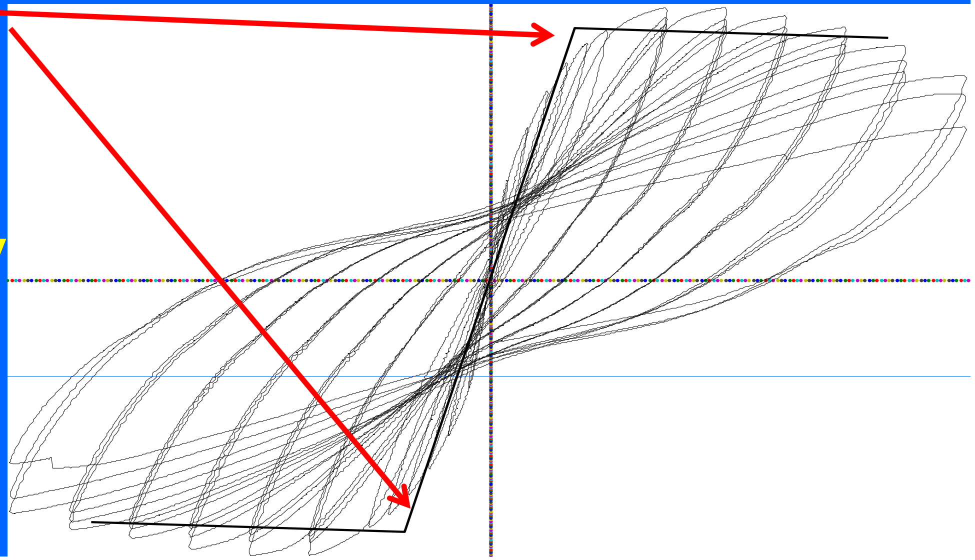

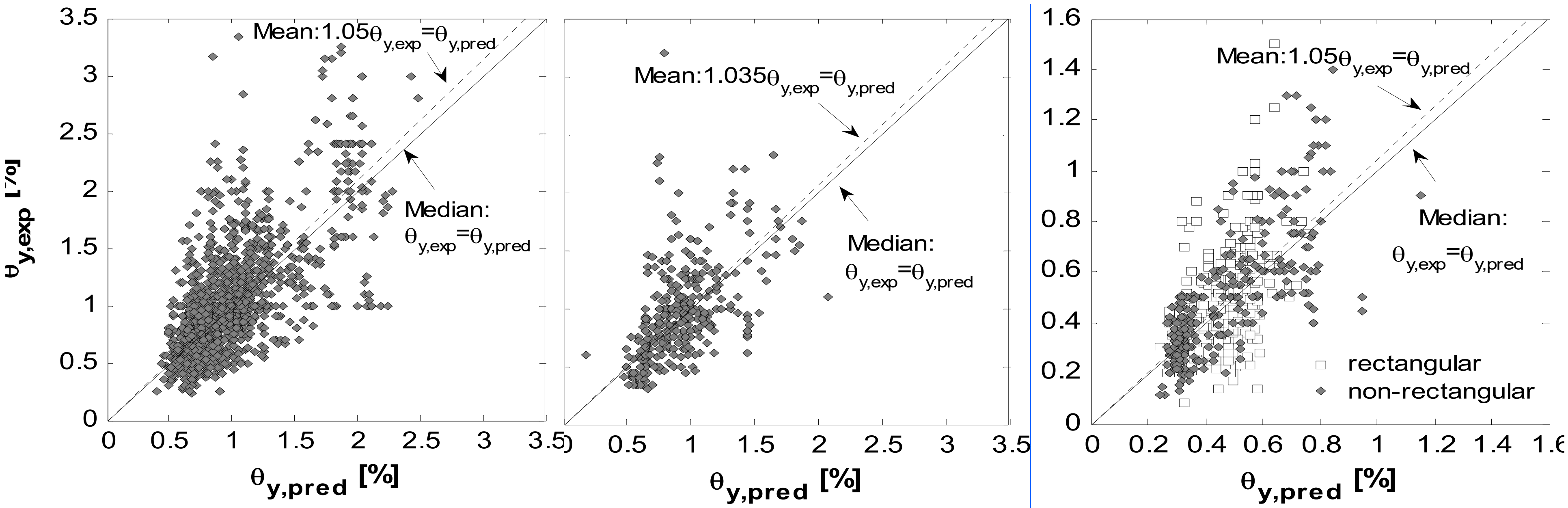

1841 **Rect. beam/columns CoV 33%** 316 **Circ. columns CoV 31%** 596 **Walls, box piers CoV 32%**

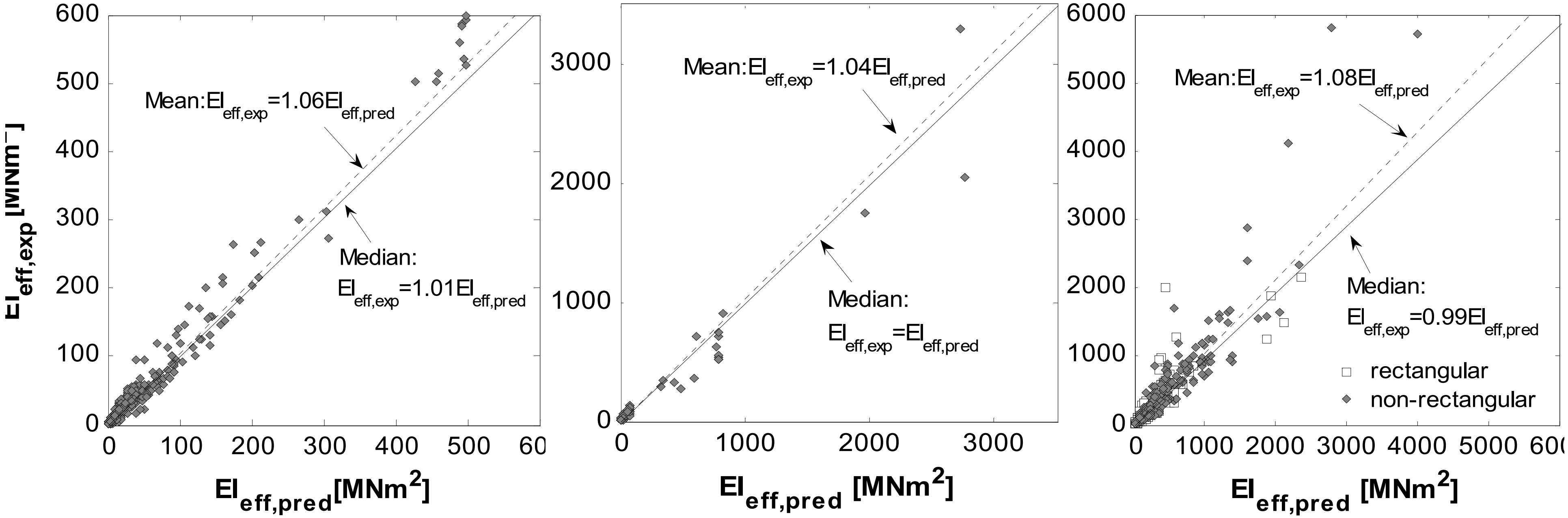

1804 **Rect. beam/columns CoV 37%** 298 **Circ. columns CoV 31%** 596 **Walls, box piers CoV 40%**

Member ultimate deformations

- For seismic loading, material failure at the local level (even loss of a bar) is not by itself member failure. A plastic hinge fails by accumulating local material failures during cycling of deformations, until it loses a good part (~20%) of its moment resistance.

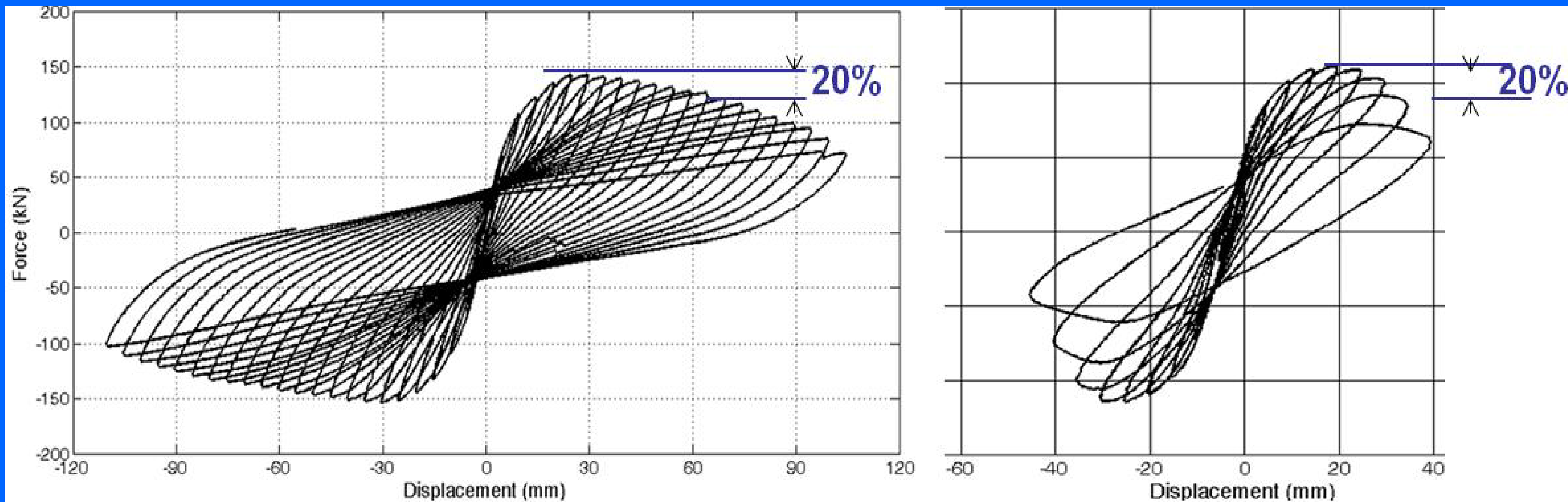

- Deformation measures used in the verifications should reflect the behavior of the plastic hinge as a whole.
- Appropriate deformation measure for plastic hinge:

plastic part of chord rotation at a member end, θ_{pl} (= plastic hinge rotation at member end, plus post-yield part of fixed-end-rotation, θ_{slip}, due to slippage of longitudinal bars from zone past the member end).

Flexure-controlled ultimate chord rotation from curvatures & plastic hinge length

Assume: entire deformation due to flexure; plastic φ=const. in "pl. hinge length"

$$\theta = \varphi_y \frac{L_s}{3} + (\varphi - \varphi_y) L_{pl}\left(1 - \frac{L_{pl}}{2L_s}\right) \qquad \theta_u = \varphi_y \frac{L_s}{3} + (\varphi_u - \varphi_y) L_{pl}\left(1 - \frac{L_{pl}}{2L_s}\right)$$

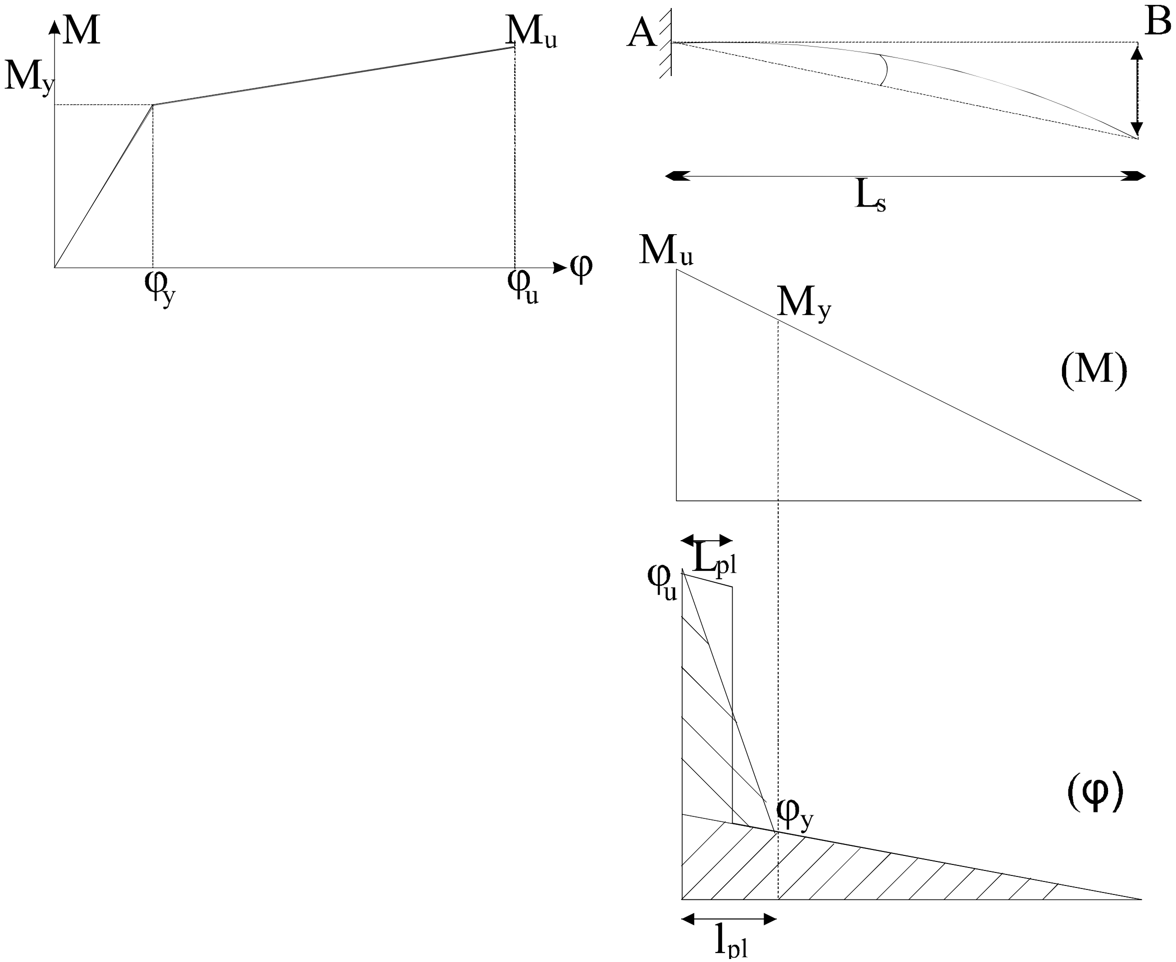

- Plastic hinge length empirically fitted to test data, in terms of member geometry.
- Fitting depends on model used for φ_y & (mainly) for φ_u (confinement, strain, limits, etc.).
- Empirical model for plastic hinge length which were developed in conjunction to specific model for φ_u, ultimate strains, etc., should not be used with other φ_u , etc., models.

Plastic hinge length, empirically fitted to data

Modified expression accounting for slip from anchorage zone & shear effects on chord rotation at yielding:

$$\theta_u = \theta_y + a_{sl}\Delta\theta_{u,slip} + (\varphi_u - \varphi_y)L_{pl}\left(1 - \frac{L_{pl}}{2L_s}\right)$$

- Using the models for θ_y, φ_y, φ_u:
- From ~300 <u>monotonic</u> tests of members with <u>non-circular</u> section:

$$L_{pl} = 0.34h\left(1 + 1.1\min\left(9; \frac{L_s}{h}\right)\right)\left(1 - 0.5\sqrt{\min\left(2.5; \max\left(0.05; \frac{b_w}{h}\right)\right)}\right)\left(1 - 0.5\min(0.7; \nu)\right)$$

- From ~1200 <u>cyclic</u> tests of members with <u>non-circular</u> section (beams, columns, walls) with detailing conforming to recent seismic codes:

$$L_{pl} = 0.3h\left[1 + 0.4\min\left(9; \frac{L_s}{h}\right)\right]\left(1 - \frac{1}{3}\sqrt{\min\left(2.5; \max\left(0.05; \frac{b_w}{h}\right)\right)}\right)\left(1 - 0.45\min(0.7; \nu)\right)$$

- From ~150 <u>cyclic</u> tests on columns with <u>circular</u> section:

$$L_{pl} = 0.7D\left[1 + \frac{1}{7}\min\left(9; \frac{L_s}{D}\right)\right]\left(1 - 0.7\min(0.7; \nu)\right)$$

- From ~50 <u>cyclic</u> tests on members <u>not conforming</u> to seismic codes:

$$L_{pl,\text{non-conforming}} = 1.3 L_{pl,\text{conforming}}$$

Non-circular columns beams, walls

301 monotonic tests: CoV 71%

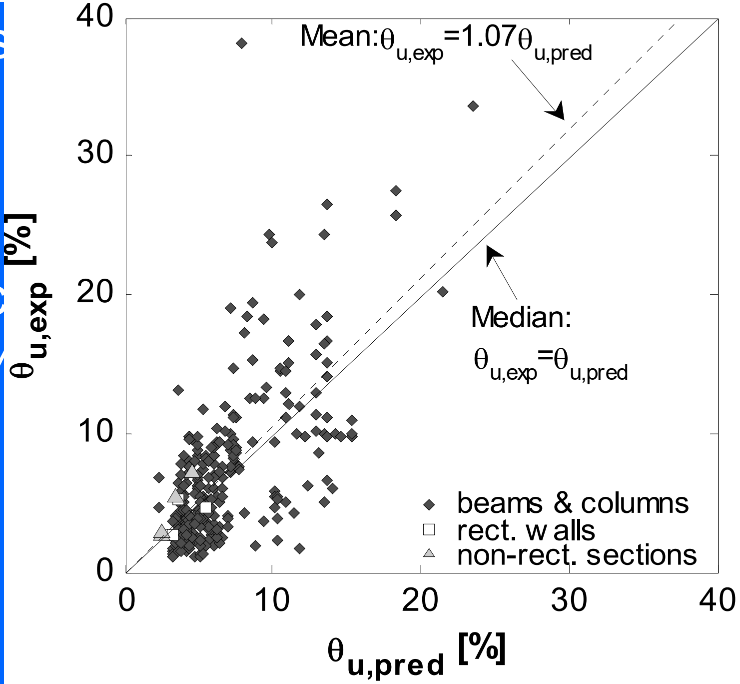

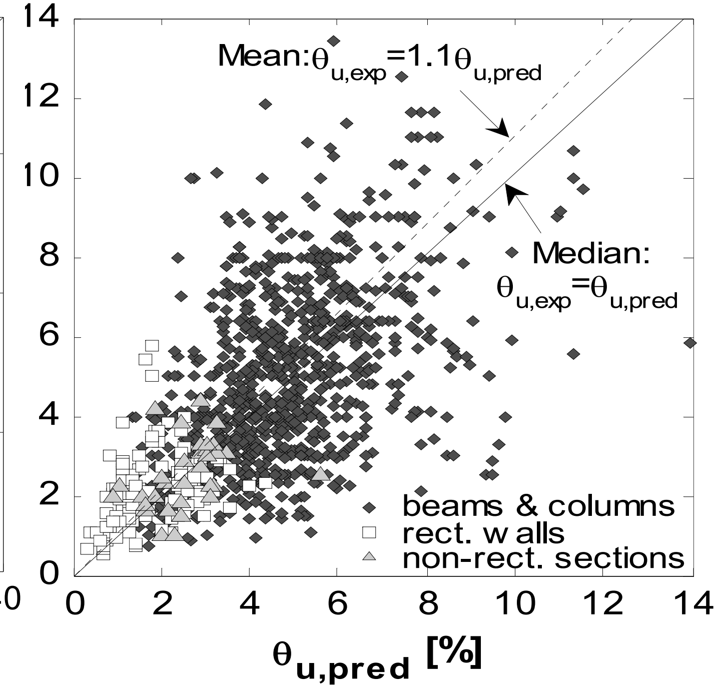

47 cyclic tests, non-conforming: CoV 34.5%

1198 cyclic tests, conforming: CoV 45%

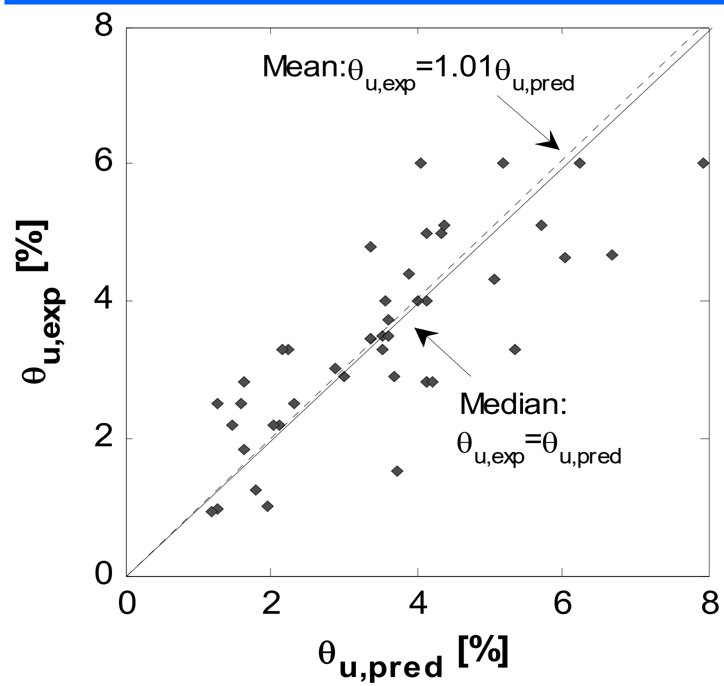

147 cyclic tests, circular columns CoV 35%

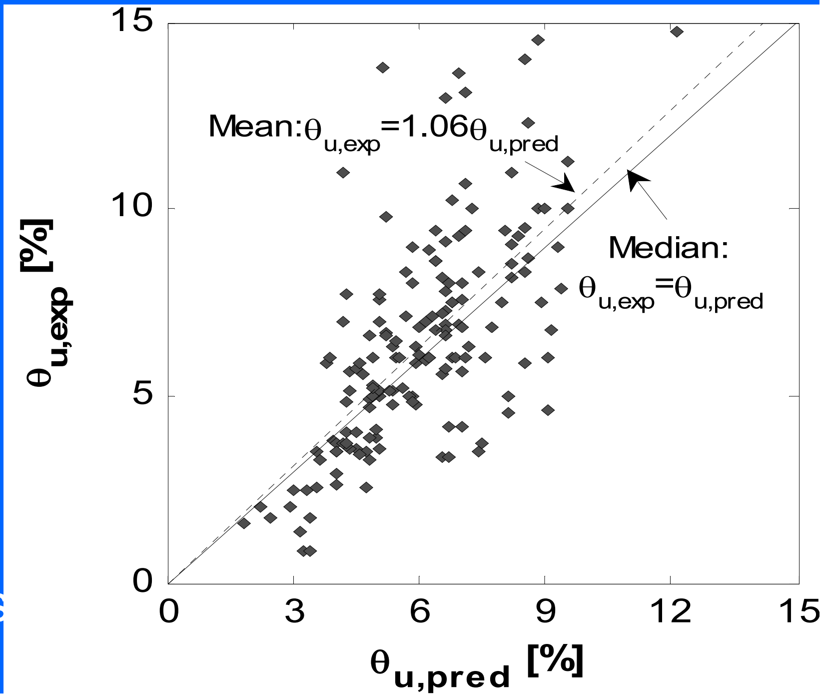

Empirical ultimate chord rotation – rect. compression zone

Option 1: the simplest

$$\theta_u = 0.0231(1-0.36a_{st})(1-0.2a_{cy}a_{nc})(1-0.42a_{cy})(1+0.58a_{sl})0.325^{\min(0.7;\nu)}\left(\min(50; f_c(MPa))\right)^{0.15}$$
$$(1-0.4a_{w,r})(1-0.33a_{w,nr})\left[\frac{\max(0.01;\omega_2)}{\max(0.01;\omega_{tot}-\omega_2)}\right]^{0.2}\left(\min\left(9;\frac{L_s}{h}\right)\right)^{0.35} 12.5^{\left(\frac{\alpha\rho_s f_{yw}}{f_c}\right)} 1.3^{100\rho_d}$$

Option 2: elastic part separate

$$\theta_u = \theta_y + 0.0242(1-0.45a_{st})(1+0.7a_{sl})(1-0.22a_{cy}a_{nc})(1-0.5a_{cy})0.2^{\min(0.7;\nu)}\left(\min(50; f_c(MPa))\right)^{0.1}$$
$$(1-0.41a_{w,r})(1-0.31a_{w,nr})\left[\frac{\max(0.01;\omega_2)}{\max(0.01;\omega_{tot}-\omega_2)}\right]^{0.25}\left[\min\left(9;\frac{L_s}{h}\right)\right]^{0.35} 24^{(\alpha\rho_s f_{yw}/f_c)} 1.225^{100\rho_d}$$

Option 3: elastic & fixed-end-rotation separate; unified approach for walls.

$$\theta_u = \theta_y + a_{sl}\Delta\theta_{u,slip} + 0.0183(1-0.45a_{st})(1-0.08a_{cy}a_{nc})(1-0.42a_{cy})0.225^{\min(0.7;\nu)}\left[\min(50; f_c(MPa))\right]^{0.2}$$
$$\left(1-0.048\max\left(4;\min\left(8,\frac{h}{b_w}\right)\right)\right)\left[\frac{\max(0.01;\omega_2)}{\max(0.01;\omega_{tot}-\omega_2)}\right]^{0.175}\left[\min\left(9;\frac{L_s}{h}\right)\right]^{0.4} 8.5^{\left(\frac{\alpha\rho_s f_{yw}}{f_c}\right)} 1.565^{100\rho_d}$$

a_{st} = 0 for hot-rolled or heat-treated tempcore steel; a_{st} = 1 for brittle cold-worked steel;
a_{cy} = 1 for cyclic loading, a_{cy} = 0 for monotonic loading;
a_{nc} = 1 for members non-conforming to seismic codes, a_{nc} = 0 otherwise;
a_{sl} = 1, if slip of long. bars from anchorage zone possible, a_{sl} = 0 otherwise
$a_{w,r}$ = 1 for rectangular walls; $a_{w,r}$ = 0 otherwise;
$a_{w,nr}$ = 1 for non-rectangular walls; $a_{w,nr}$ = 0 otherwise;
ω_{tot}, ω_2: mechanical ratio of longitudinal steel, total or compression bars only;
$\nu = N/bhf_c$ (b: width of compression zone; N>0 for compression);
$L_s/h = M/Vh$: shear-span-to-depth ratio;
α : confinement effectiveness factor = $\alpha_n\alpha_s$
$\rho_s = A_{sh}/b_w s_h$: transverse steel ratio in direction of loading;
ρ_d: ratio of diagonal reinforcement (each direction);
b_w: width of (one) web.

301 monotonic, CoV=53.5%c 1198 conforming cyclic, CoV=38% 47 non-conform. cyclic, CoV=32.5%

Option 2

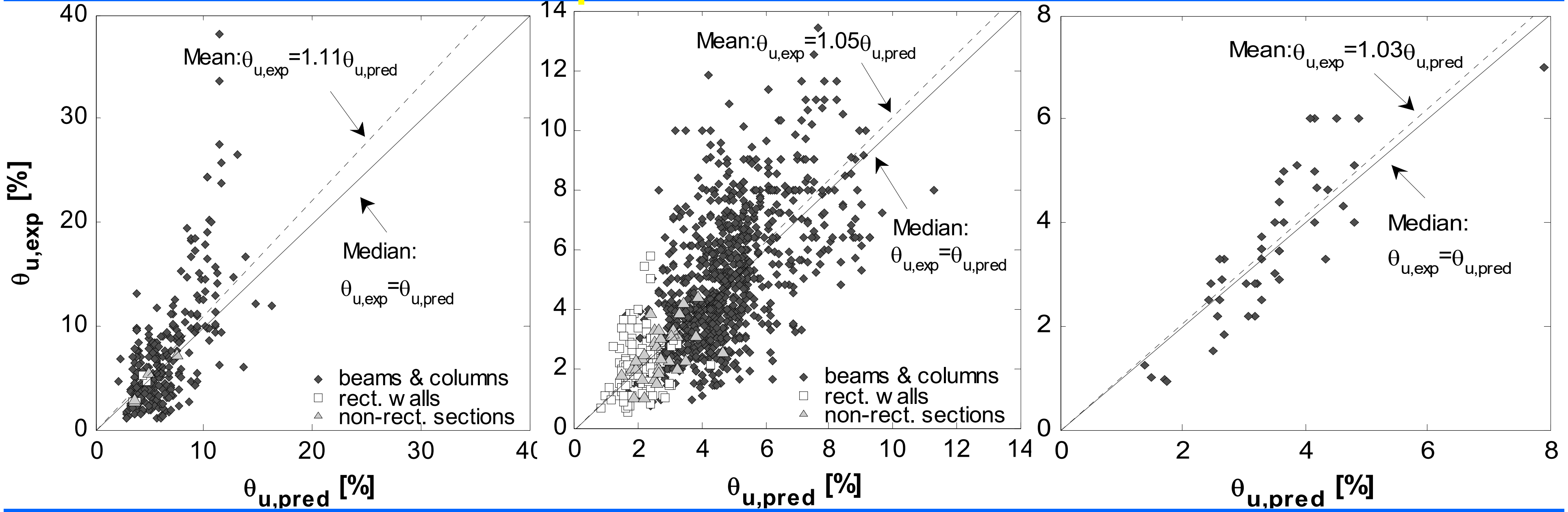

CoV=55.5%c **Option 3** CoV=37.5% CoV=28.5%

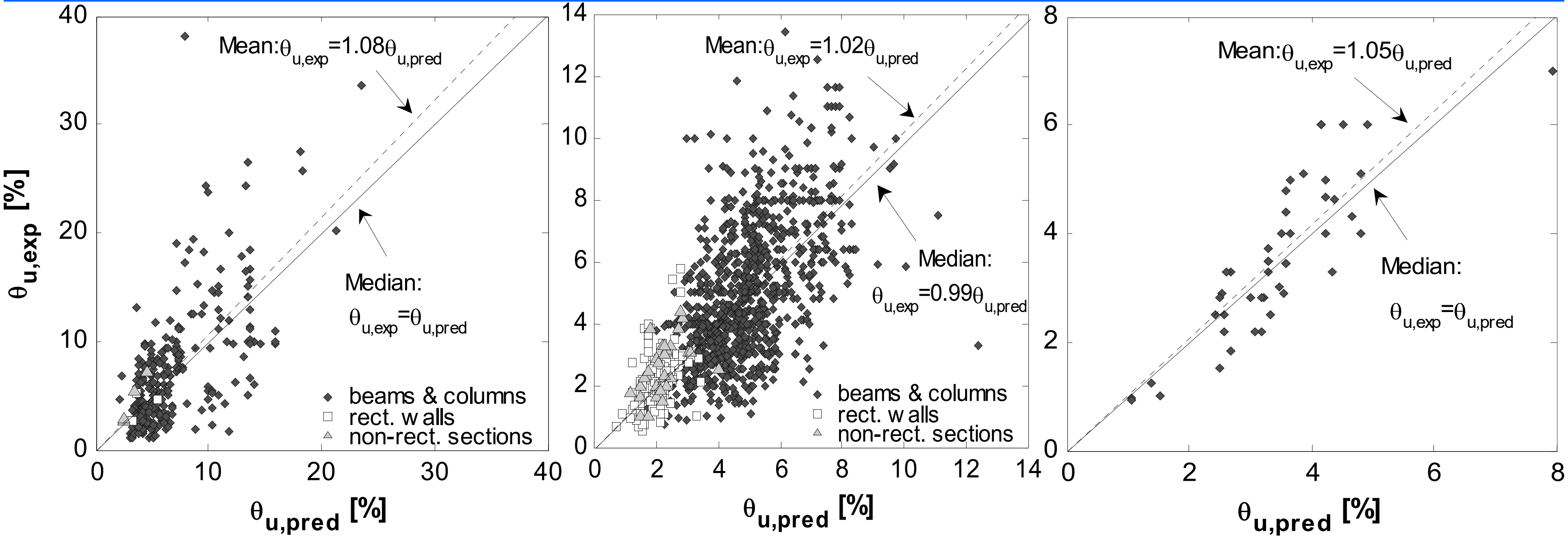

Members with continuous ribbed (deformed) bars and FRP wrapping of plastic hinge region

- **Yield moment M_y:** Enhanced by FRP jacket (tests: +9% w.r.to value w/o confinement)

- Compute M_y using Modulus from strength of FRP-confined concrete: $E_c=10000(f_{cc}(\mathrm{MPa}))^{1/3}$.

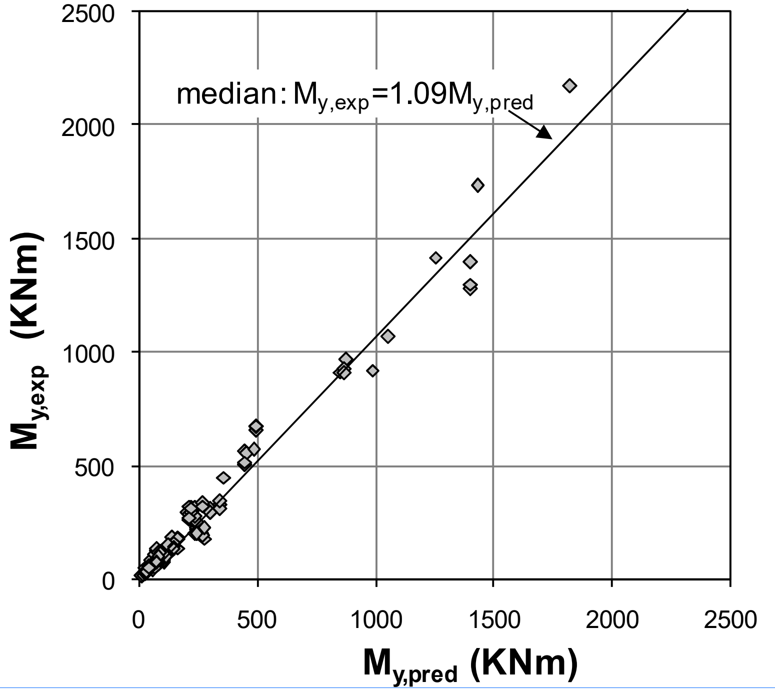

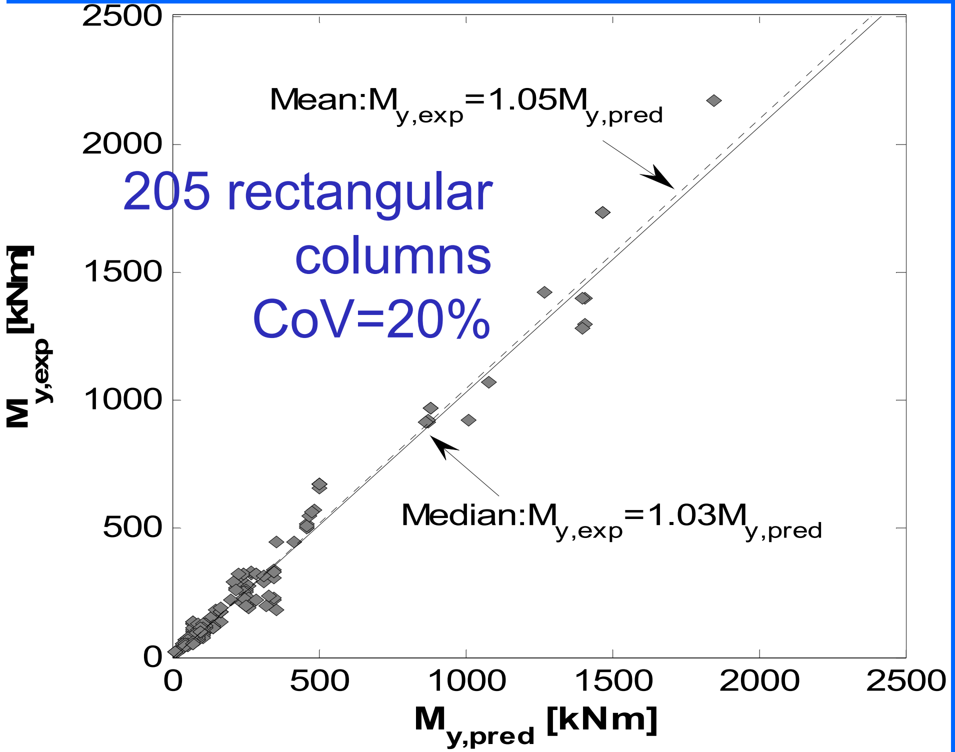

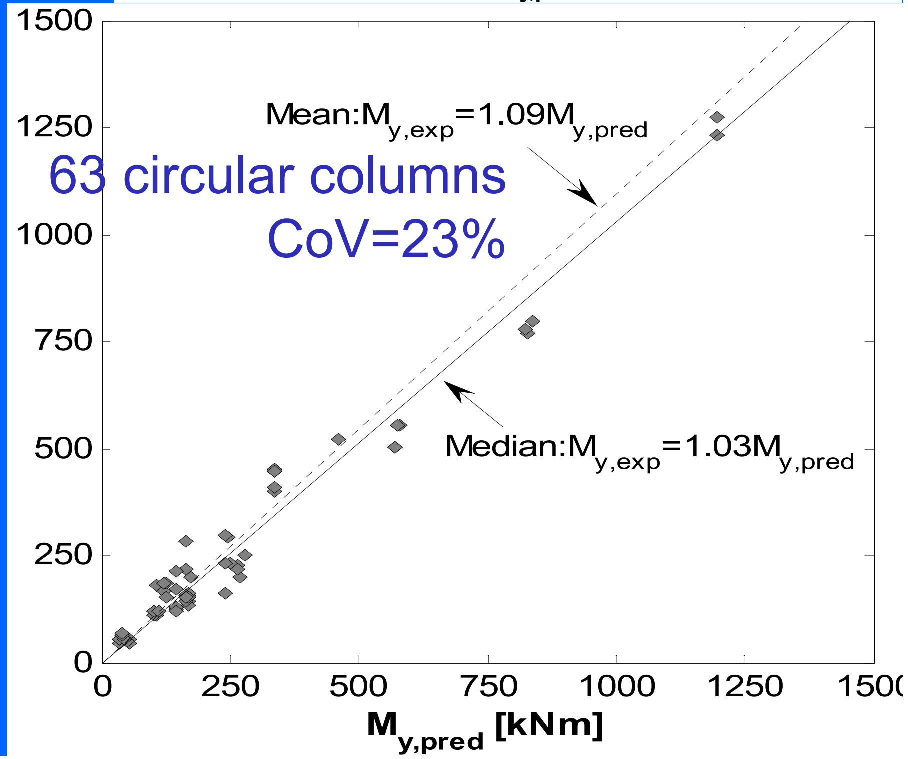

Effective (elastic) stiffness EI_{eff}

Enhanced by FRP jacket (pre-damaged columns: EI drops despite jacket)

Modulus from strength of confined concrete

159 undamaged rect. columns
median=0.99, CoV=29.4%
(22 pre-damaged columns
median=0.68, mean=0.71, CoV=25.4%)

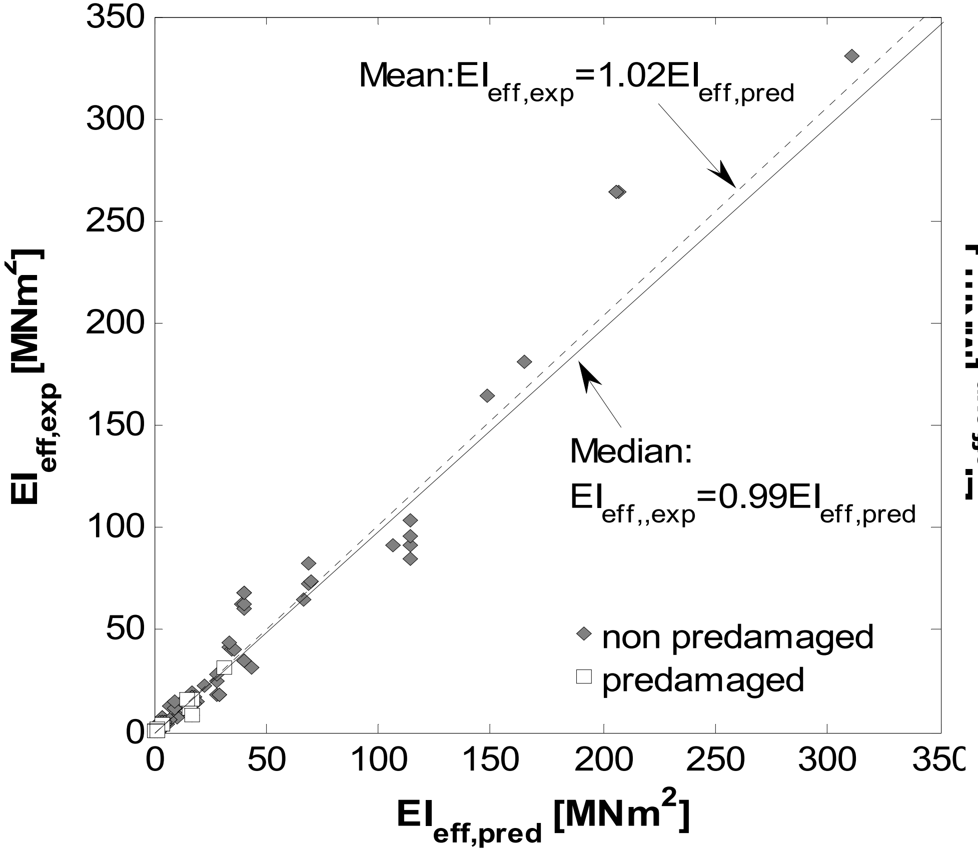

52 undamaged circular columns
median=1.15, CoV=22.4%
(5 pre-damaged columns:
mean=1.06, CoV=25.5%)

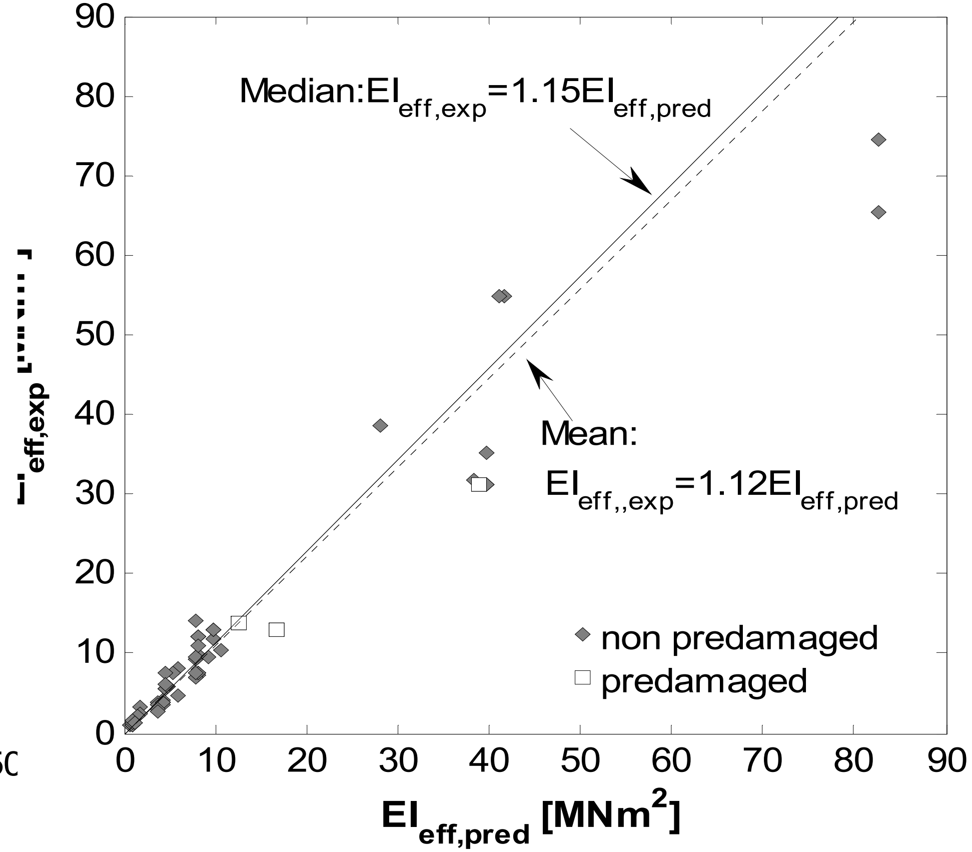

Cyclic plastic chord rotation capacity: Physical model

Only the ultimate strains in the calculation of the ultimate curvature, φ_u change:

- Steel: $\varepsilon_{su} = 0.6\varepsilon_{su,\mathrm{nom}}\sqrt{1-0.15\ln\left(N_{\mathrm{bar,tension}}\right)}$
- (Confined by FRP) concrete:

$$\varepsilon_{cu,c} = \varepsilon_{cu} + a\beta_f \min\left(0.5;\ \rho_f f_{u,f} / f_c\right)\left(1-\min\left(0.5;\ \rho_f f_{u,f} / f_c\right)\right)$$

– FRP-confinement effectiveness:

$$\alpha = 1 - \frac{(h-2R)^2 + (b-2R)^2}{3bh}$$

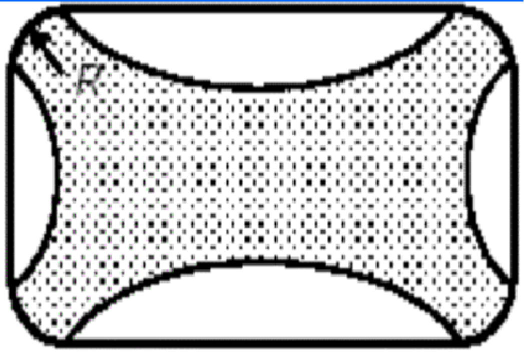

b, h: sides of circumscribed rect. section;
R: corner radius

– β_f=0.115 for CFRP/GFRP; β_f=0.1 for AFRP.

– $\rho_f=2t_f/b_w$: FRP ratio parallel to direction of loading;

– $f_{u,f}=0.6E_f\varepsilon_{u,f}$

E_f : FRP Modulus;

$\varepsilon_{u,f}$: FRP limit strain. CFRP/AFRP: $\varepsilon_{u,f}$=1.5%; GFRP: $\varepsilon_{u,f}$=2%

Empirical cyclic ultimate chord rotation

$$\theta_u^{pl} = \theta_u - \theta_y = 0.0206(1-0.41a_{w,r})(1-0.31a_{w,nr})(1-0.22a_{nc}) \cdot 24^{\max\left(\frac{\alpha\rho_s f_{yw}}{f_c};\left(\frac{\alpha\rho f_u}{f_c}\right)_f\right)}$$

$$\cdot 0.2^{\nu} \cdot \left(\min(50; f_c(MPa))\right)^{0.1} \left[\frac{\max(0.01;\omega_2)}{\max(0.01;\omega_1)}\right]^{0.25} \left[\min\left(9; \frac{L_s}{h}\right)\right]^{0.35} \cdot 1.225^{100\rho_d}$$

$$\left(\frac{a\rho f_u}{f_c}\right)_f = ac_f \min\left[0.4; \frac{0.6\varepsilon_{u,f} E_f \rho_f}{f_c}\right]\left(1 - 0.5\min\left[0.4; \frac{0.6\varepsilon_{u,f} E_f \rho_f}{f_c}\right]\right)$$

- c_f=2.8 for CFRP,
- c_f=1.15 for GFRP;
- c_f=0.95 for AFRP.
- $\rho_f=2t_f/b_w$: FRP ratio in direction of loading;

  E_f : FRP Modulus;

  $\varepsilon_{u,f}$: FRP limit strain.

  CFRP/AFRP: $\varepsilon_{u,f}$=1.5%;

  GFRP: $\varepsilon_{u,f}$=2%

Physical model

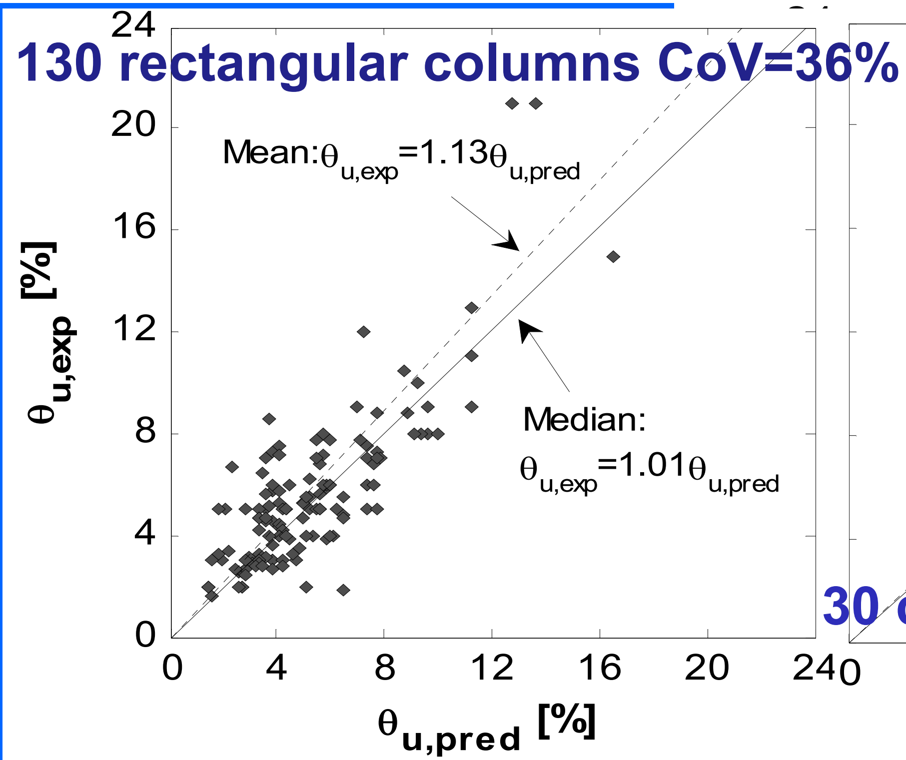

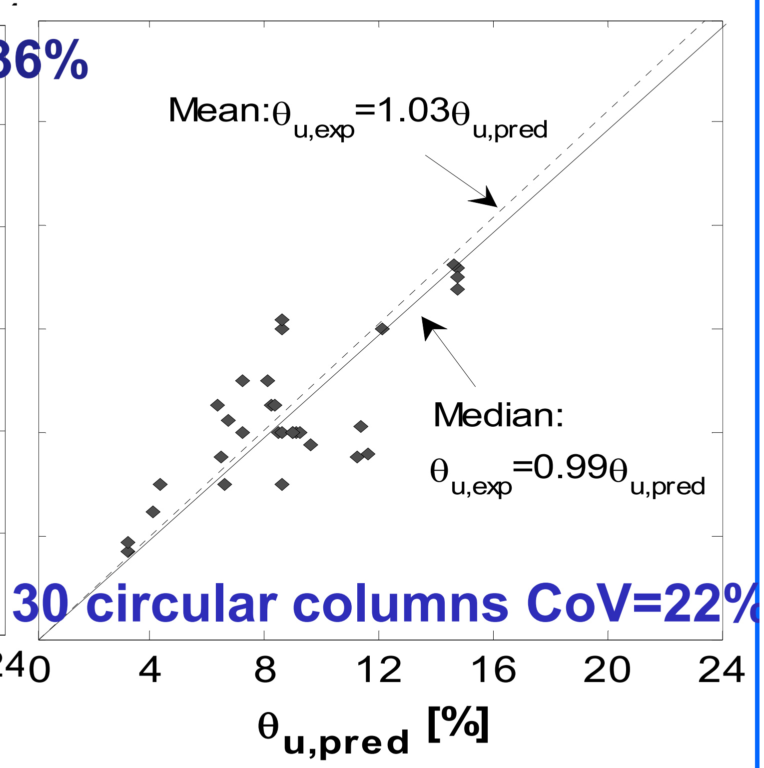

Empirical model – Option 2

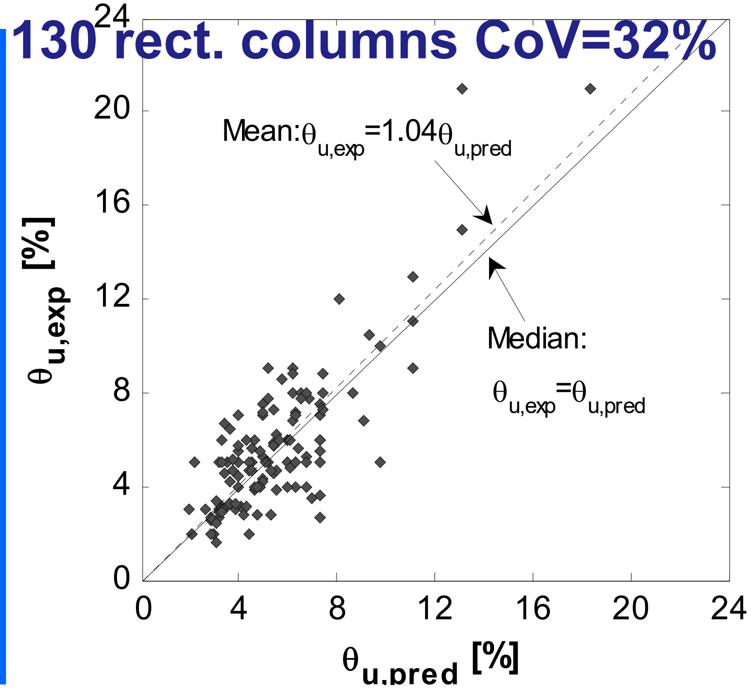

Model vs FRP bending radius

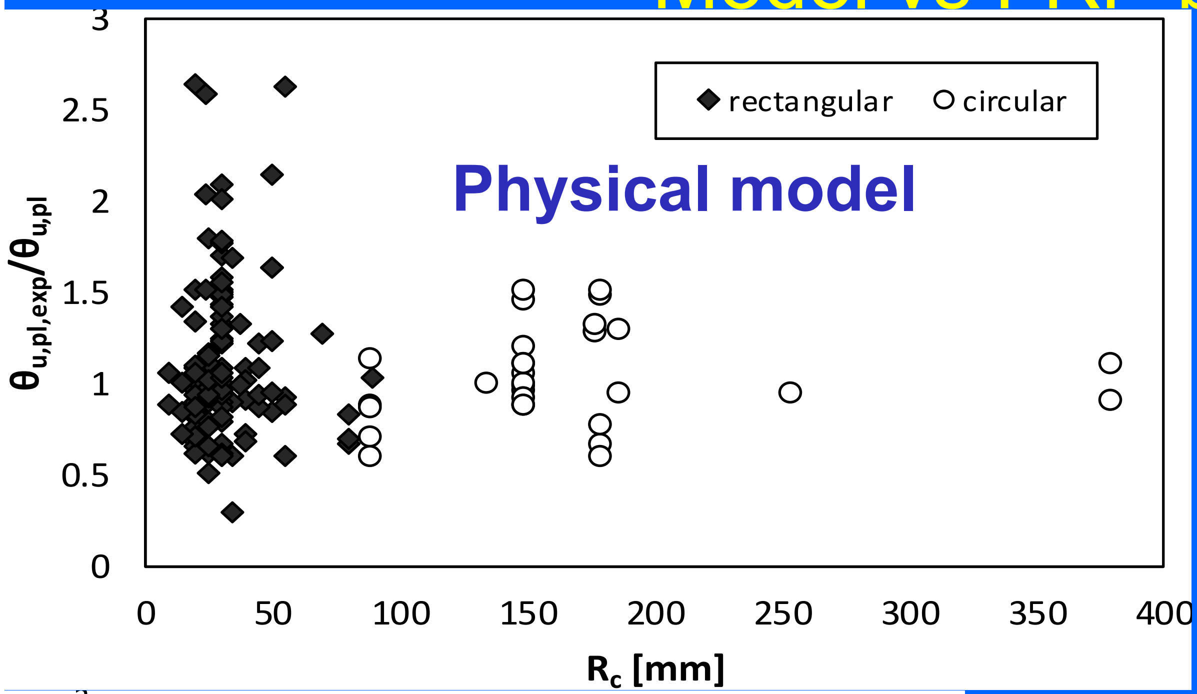

No apparent need for a lower limit more than ~15 mm on the FRP corner radius, as far as its effect on column failure is concerned.

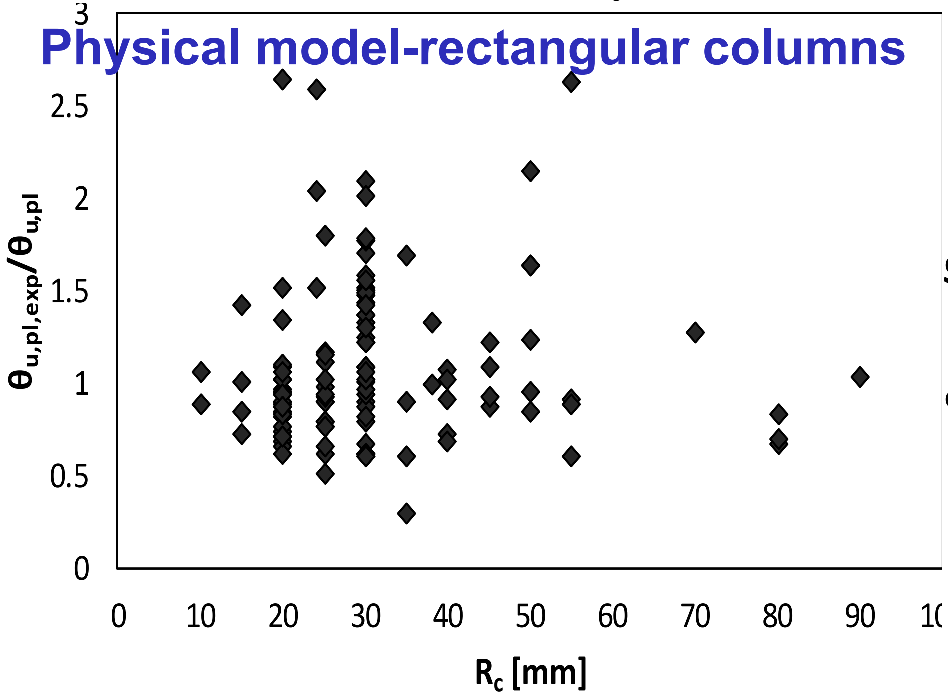

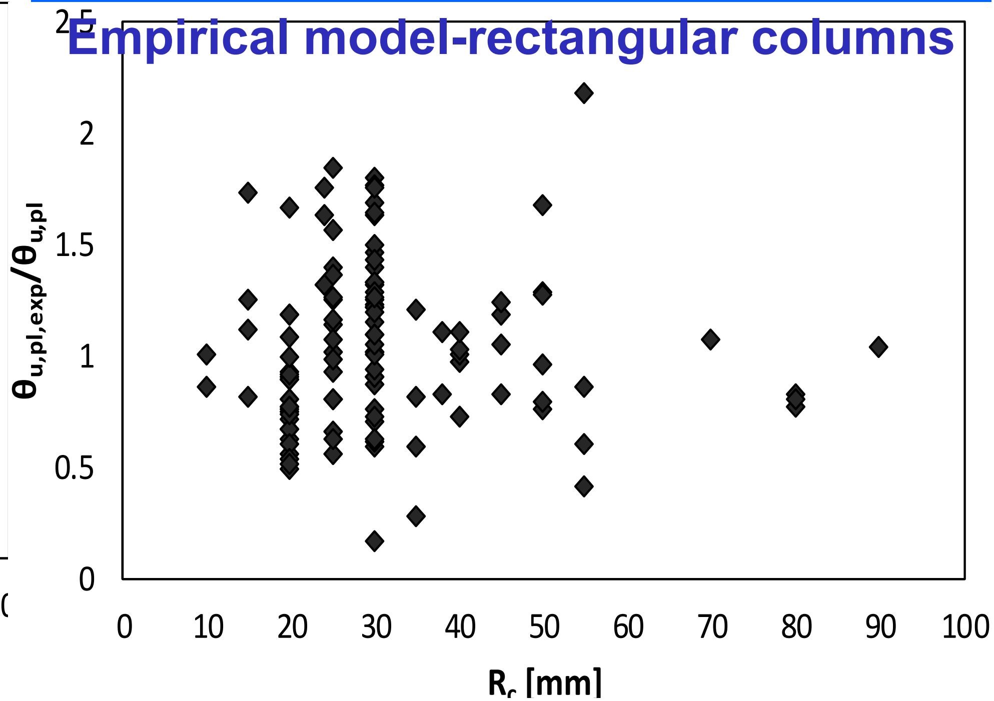

Members with ribbed (deformed) bars, lap-spliced in the plastic hinge region, starting at the member's yielding end section (without or with FRP wrapping of lap-splice region)

Ribbed bars <u>lap-spliced</u> over length l_o in plastic hinge (case without FRP wrapping: zero FRP thickness)

1. Both bars in pair of lapped compression bars count in compression steel
2. For yield properties (M_y, ϕ_y, θ_y, EI_{eff}), stress f_s of tension bars:

$$f_{sm} = \min\left(\sqrt{\frac{l_o}{l_{oy,\min}}};\quad 1\right) f_y$$

$$l_{oy,\min} = \frac{0.25 d_b f_y / f_{ct}}{\max\left(\frac{c_{\min}}{d_b}; 0.7\right)\left(1 + 4\frac{t_f}{R_c}\frac{E_f}{E_c}\right)^2}$$

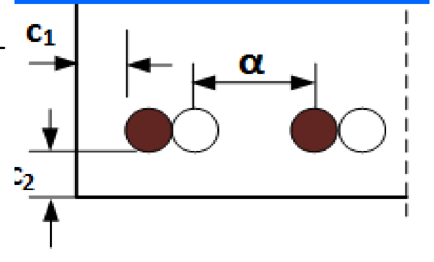

$c_{min} = \min(\alpha/2, c_1, c_2)$

- f_{ct}: concrete tensile strength
- E_f: FRP Modulus; E_c: concrete Modulus
- t_f: FRP thickness; R_c: FRP radius (chamfered corner of rect. section or around circular section);

Test-to-prediction ratio of M_y

no FRP wraps **with FRP wraps**

123 rect. columns cov=13% 42 circ. columns cov=14% 49 rect. columns cov=14% 38 circ. columns cov=12%

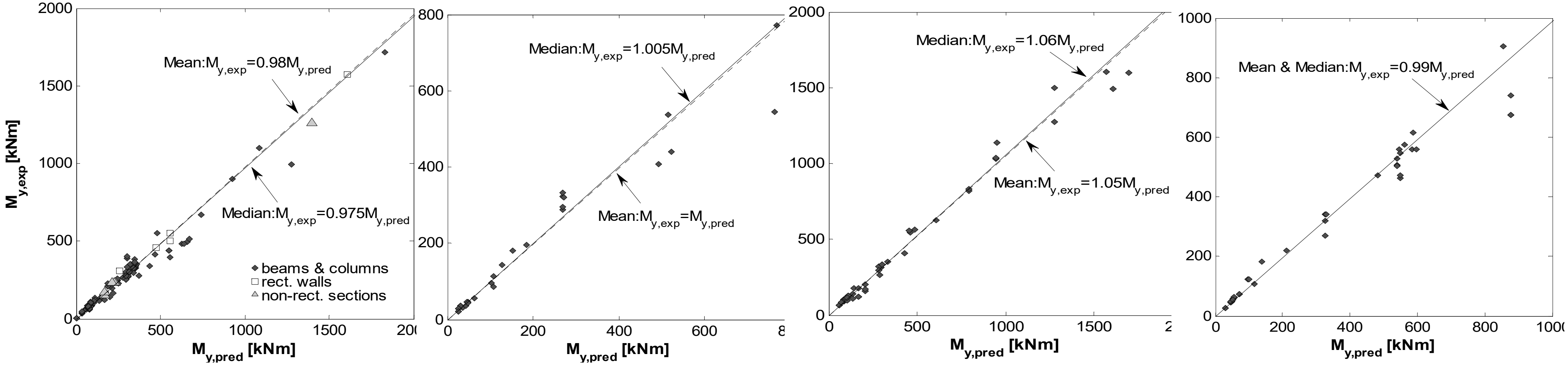

Test-to-prediction ratio of chord rotation at yielding θ_y

no FRP wraps with FRP wraps

101 rect. columns cov=22% 42 circ. columns cov=21% 49 rect. columns cov=19% 36 circ. columns cov=23%

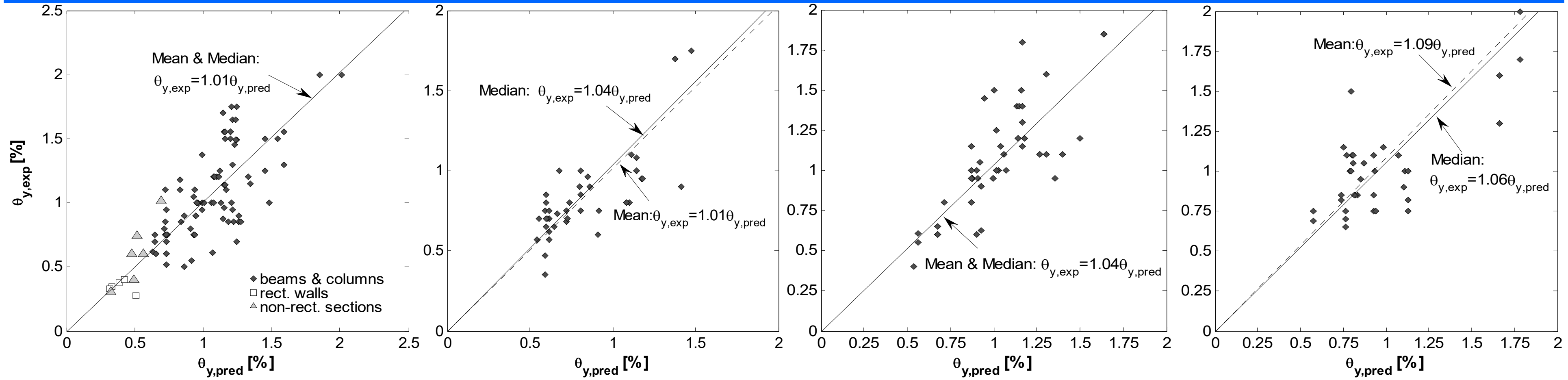

Test-to-prediction ratio of secant-to-yield-point stiffness EI_{eff}

no FRP wraps with FRP wraps

101s rect. columns cov=24% 42 circ. columns cov=23% 49 rect. columns cov=23% 36circ. columns

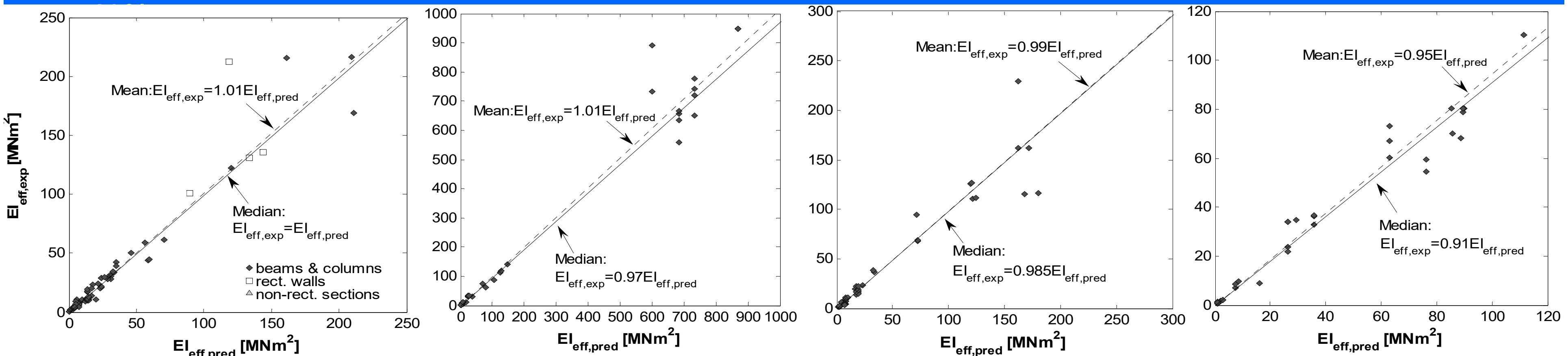

Effect of FRP bending radius, thickness & stiffness

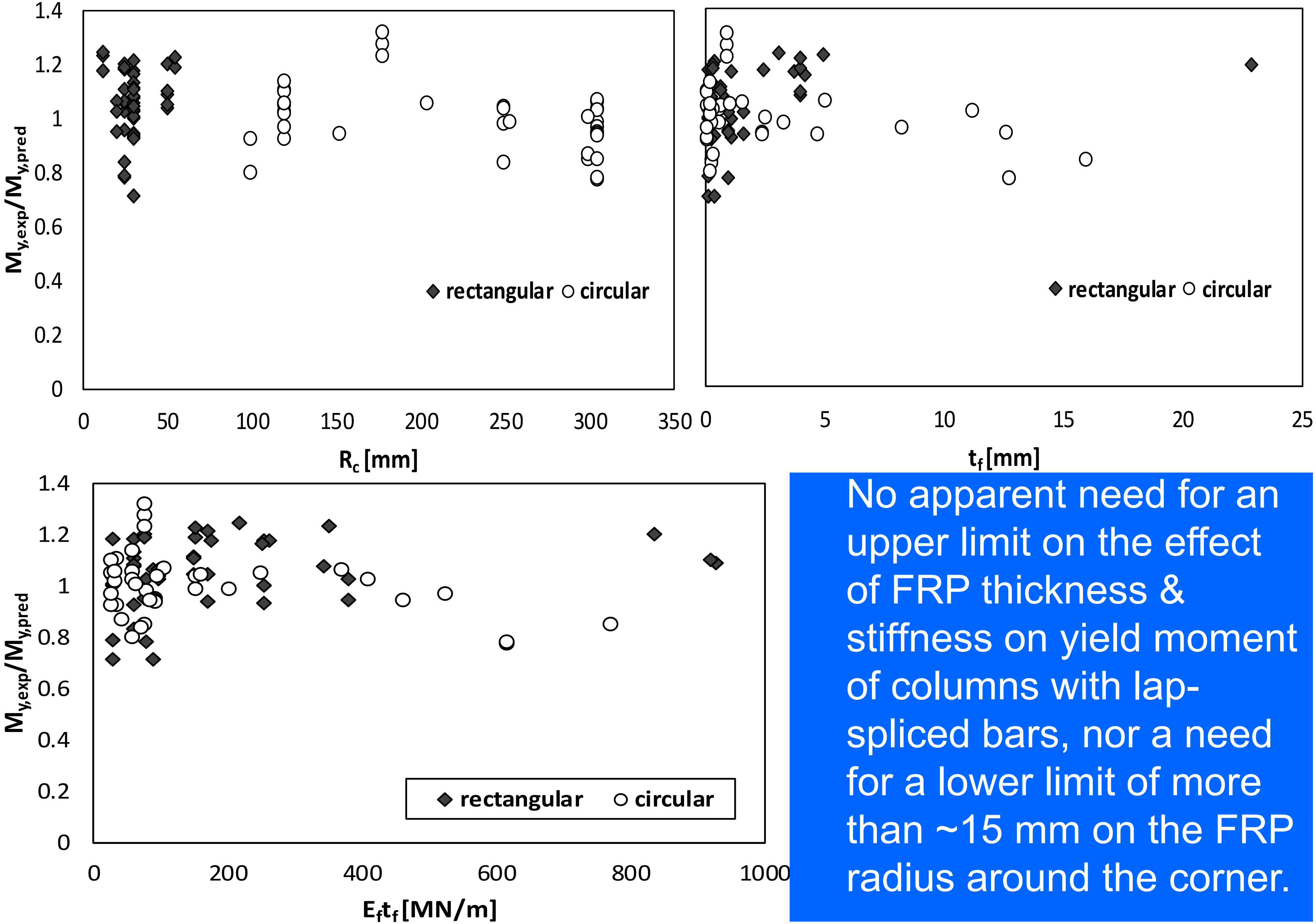

No apparent need for an upper limit on the effect of FRP thickness & stiffness on yield moment of columns with lap-spliced bars, nor a need for a lower limit of more than ~15 mm on the FRP radius around the corner.

3. **Ultimate chord rotation drops**, if lapping $l_o < l_{ou,min}$

$$l_{ou,\min} = \frac{d_b f_y / f_{ct}}{1 + a_c a_n a_s \sqrt{\frac{d_b}{2R_c}} \min\left(3; \frac{p_c}{f_{ct}}\right)\left(1 - \frac{1}{6}\min\left(3; \frac{p_c}{f_{ct}}\right)\right)}$$

- a_n: confinement effectiveness within section,
  - a_n=1 in circular section, a
  - $a_n = n_{restr}/n_{tot}$ in rect. section with n_{restr} lapped bar pairs at corners or hooks of ties or at chamfered corners of FRP jacket, out of a total of n_{tot} bar pairs;
- a_s: confinement effectiveness along member:
  - a_s=1 for FRP;
  - for steel ties $\alpha_s = \left(1 - \frac{s_h}{2b_o}\right)\left(1 - \frac{s_h}{2h_o}\right)$, w/ D_o replacing b_o, h_o in circ. columns
- a_c: confining medium factor:
  - a_c=7.5 for steel ties,
  - a_c=9.5 for CFRP, a_c=10.5 for GFRP, a_c=12 for AFRP;
- R_c: confining medium radius, = bending radius of steel tie or FRP jacket;
- p_c: confining pressure on lap splice,
  - $p_c = A_{sh} f_{yw}/(s_h R_c)$ for steel ties,
  - $p_c = t_f f_{u,f}/R_c = 0.6 E_f \varepsilon_{u,f} t_f/R_c$ for FRP with failure strain $\varepsilon_{u,f}$ & eff. strength $f_{u,f}$.

4. **The minimum value of $l_{ou,min}$ for steel or FRP confinement applies**

Physical model for ultimate plastic chord rotation (w/ curvatures & plastic hinge length)

L_{pl}, f_{cc}, ε_{cu} as in members (FRP-wraps or no) w/ continuous bars

Steel strain at ult. member deformation w/ lapping *l*o:

$$\varepsilon_{su,lap} = \min\left(1; l_o / l_{ou,\min}\right)\varepsilon_{su} \geq \left(l_o / l_{oy,\min}\right) f_y / E_s$$

Empirical ultimate plastic chord rotation for rect. columns

$$\theta_{u,laps}^{pl} = \min\left(1.4\sqrt{\frac{l_o}{l_{ou,\min}}} - 0.4; 1\right)\theta_{u,continuousbars}^{pl}$$

Ultimate chord-rotation, without FRP wrapping

Physical model / Empirical model

100 rect. columns CoV 42% | **40 circ. columns CoV 30%** | **50 rect. columns CoV 46%**

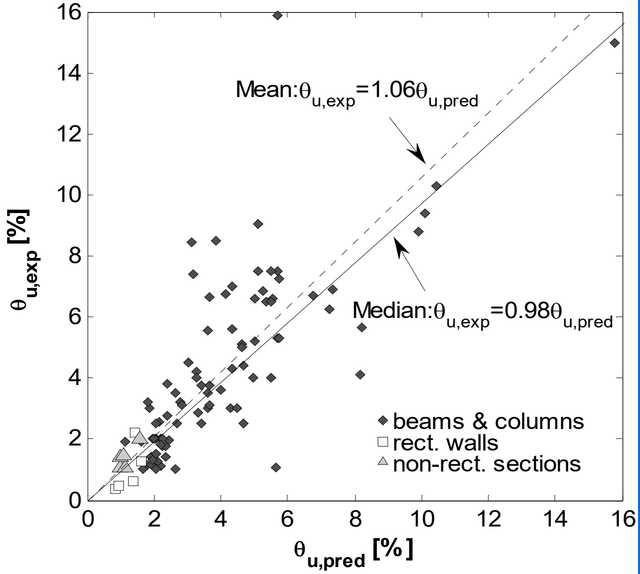

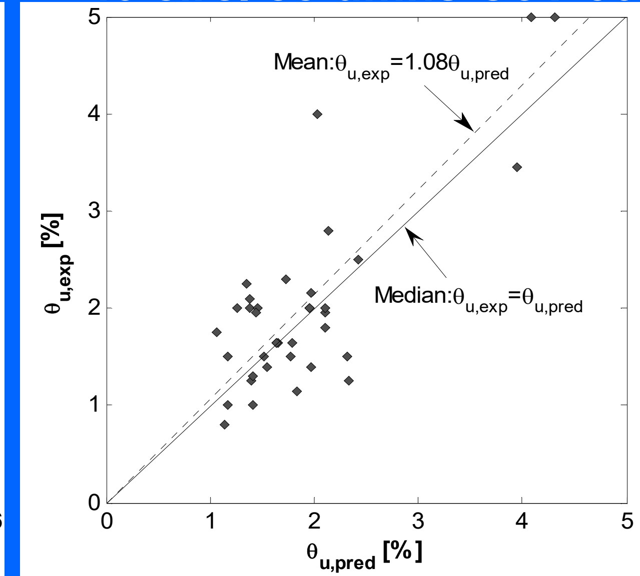

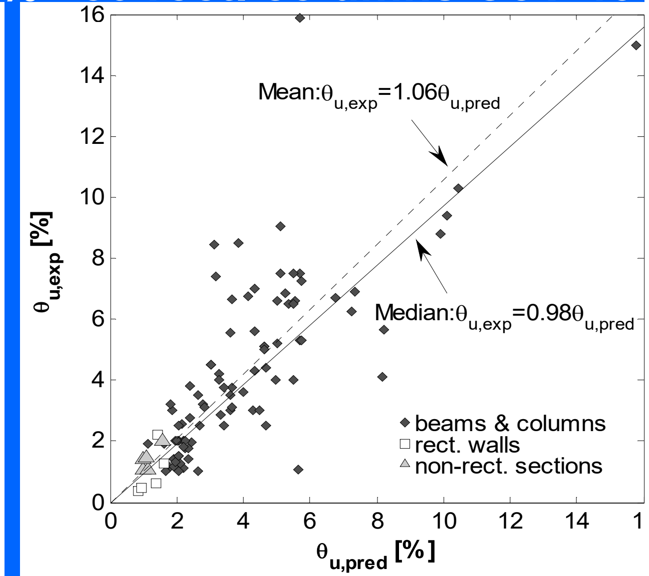

With FRP-wrapping

Physical model / Empirical model

50 rect. columns CoV 35% | **35 circ. columns CoV 31%** | **50 rect. columns CoV 30%**

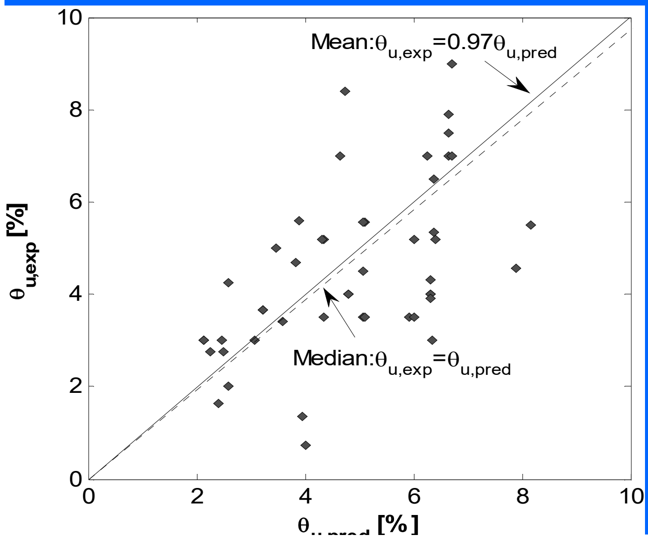

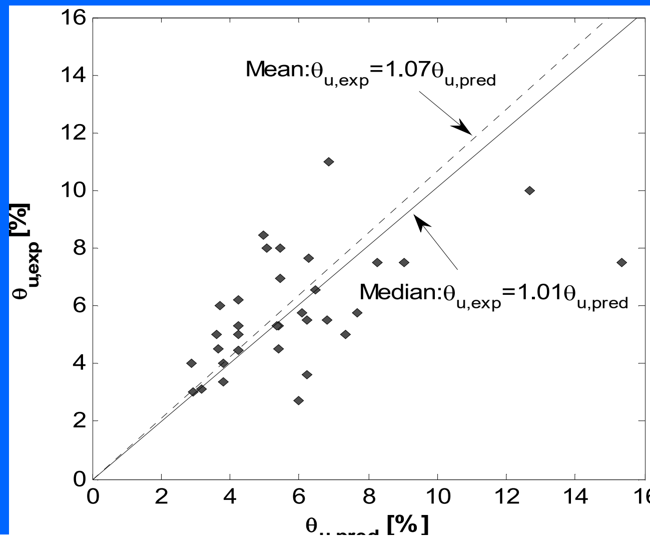

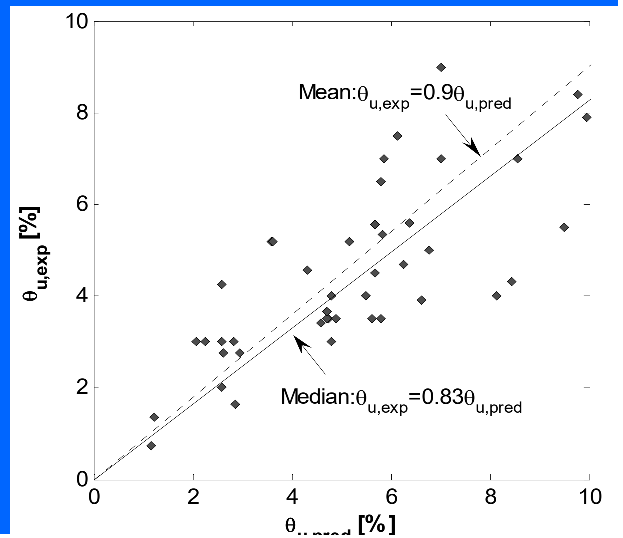

Model vs FRP bending radius

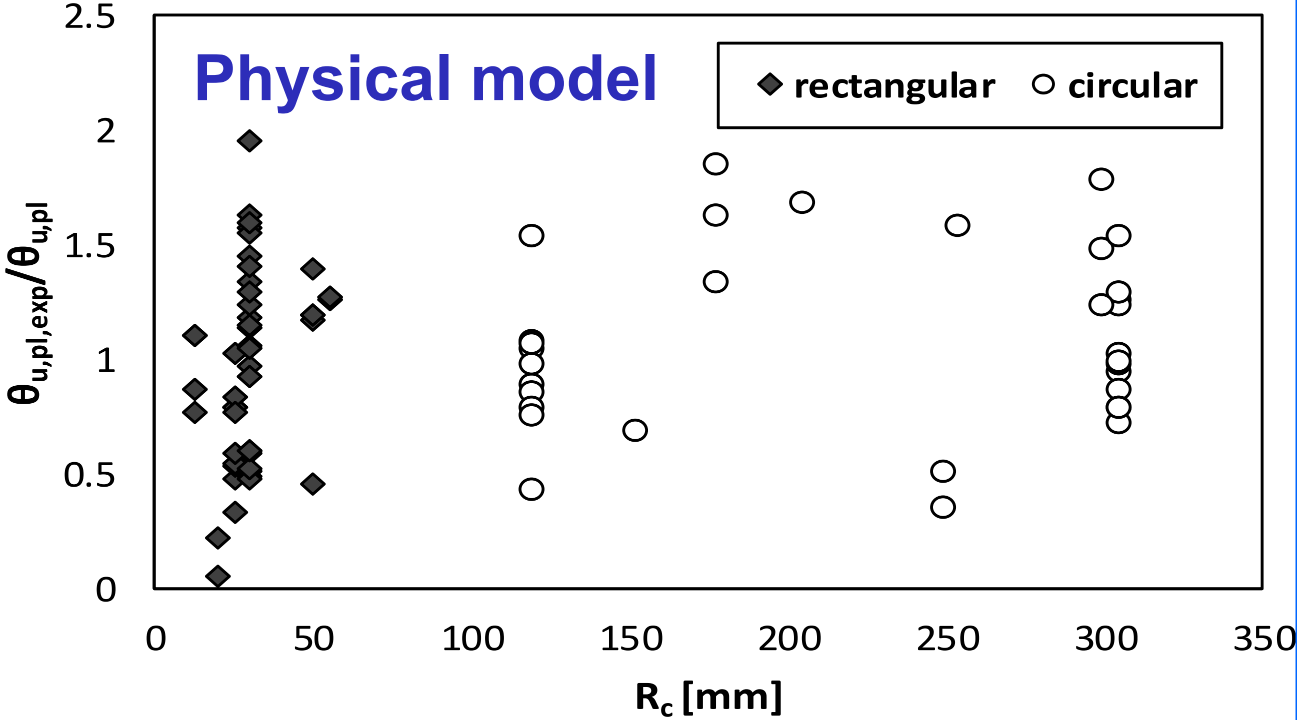

No apparent need for a lower limit of more than ~15 mm on FRP radius as far as its effect on failure of columns with lap-spliced bars is concerned.

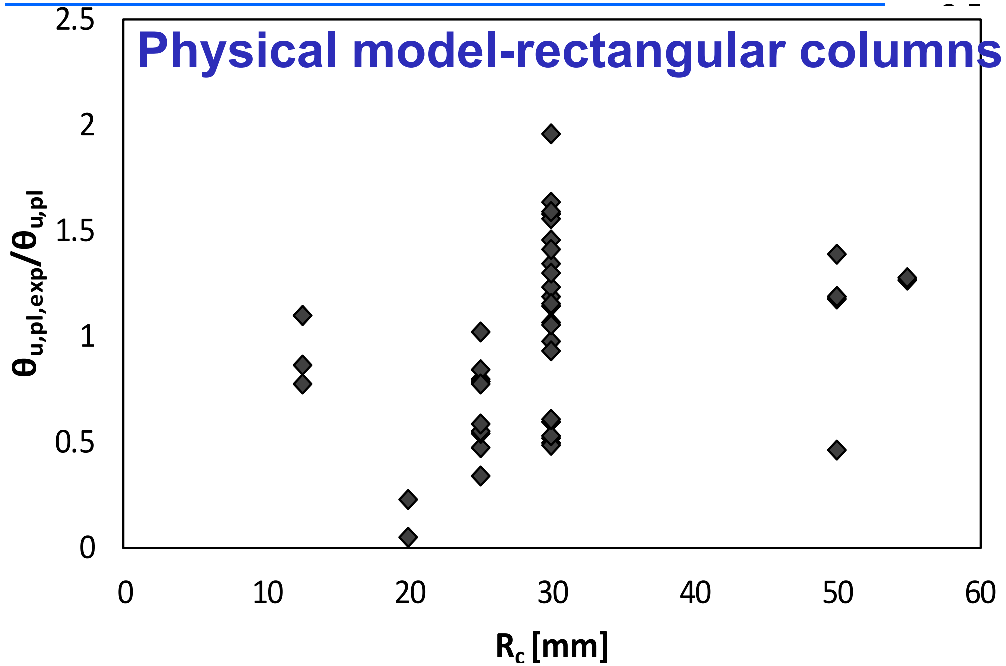

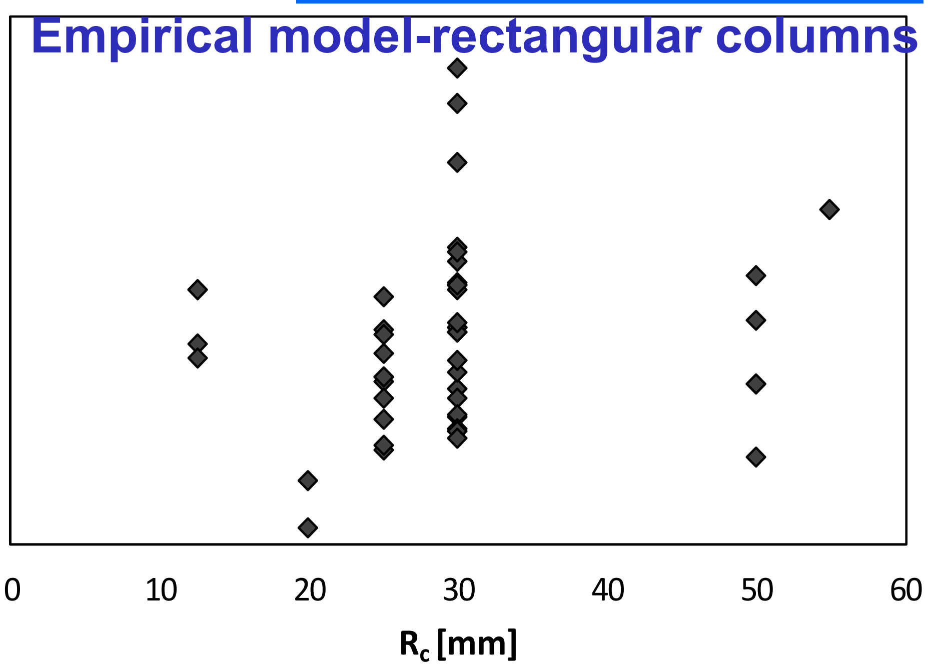

Members with smooth (plain) bars, continuous or lap-spliced (with hooks or straight ends), without or with FRP wrapping

Chord rotation at yielding, θ_y - Smooth (plain) bars

θ_y = sum of:

1. flexural component in uncracked member:

– $M_y L_s/3(EI)_g$ $(EI)_g$: uncracked, gross-section stiffness

2. shear deformation (as in members with ribbed bars)

3. fixed-end-rotation due to slippage of tension bars from their length outside & inside the member, towards the end section that yielded

$\phi_y l_{oy,min}(\min[1;(1+f_{o,1}/f_y)l_1/l_{oy,min}]+\min[1;(1+f_{o,2}/f_y)l_2/l_{oy,min}])/2$

l_1, l_2: distance of hook or bend from end section on either side of it;

$l_{oy,min}=0.5d_b f_y(\mathrm{MPa})/\sqrt{f_c}(\mathrm{MPa})$: straight anchorage length of plain bar

max. stress bar can develop ahead of hook or bend (***fib*** Bull. 72)

$$f_o(MPa) = 60\sqrt{\frac{f_c(MPa)}{25}}\left(\frac{20}{d_b(mm)}\right)^{0.2}$$

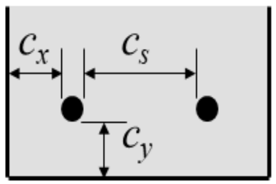

$c_{min}=\min(c_x; c_y, c_s/2)$

$c_{max}=\max(c_x; c_y, c_s/2)$

$$\left(\min\left(2;\left(\left(\min\left(3.5;\frac{c_{\min}}{d_b}\right)^{0.25}\min\left(5;\frac{c_{\max}}{c_{\min}}\right)^{0.1}+k_{conf}\min\left(0.05;\frac{\frac{A_{sw}}{s}+\frac{E_f t_f}{E_s}}{d_b n_b}\right)\right)\right)\right)\right)$$

Yield moment for plane-sections ($>15d_b$ hooked laps: $f_{eff}=f_y$; straight ends: $f_{eff} = \min(1; l_o/l_{oy,min})f_y$, $l_{oy,min}=0.5d_b f_y(\text{MPa})/\sqrt{f_c(\text{MPa})}$)

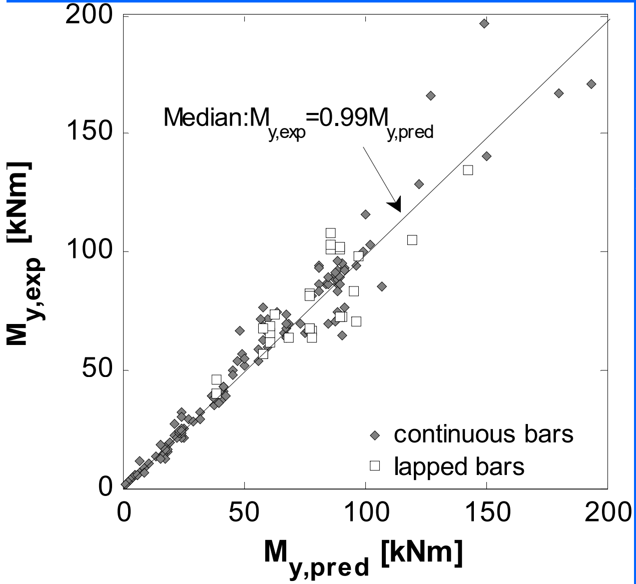

104 cantilevers/double cantilevers with continuous bars
28 with hooked lapped bars;
CoV: 15%

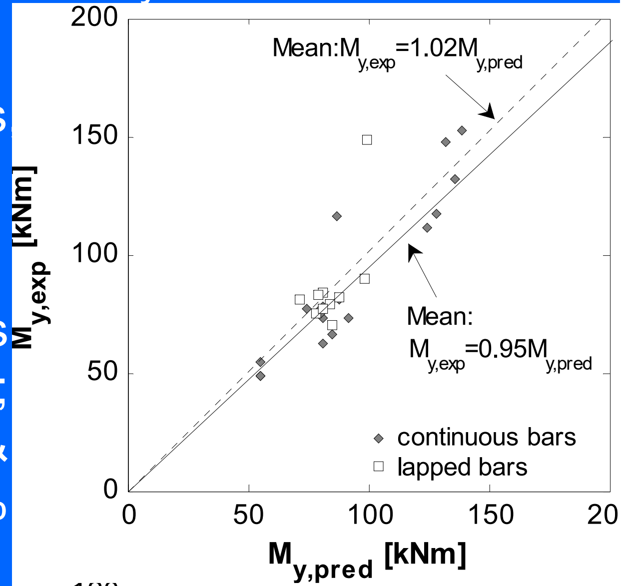

18 cantilevers with continuous bars & FRPs, Cov: 14%;
10 with hooked lapped bars & FRPs (broken line) CoV: 18%

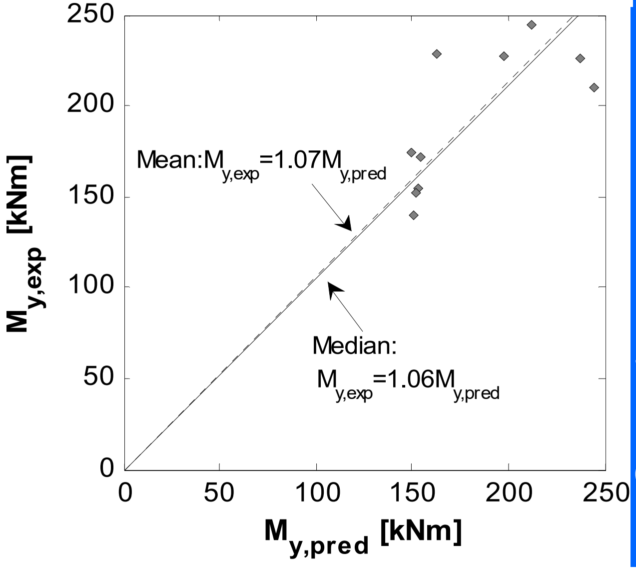

20 cantilever/double cantilevers laps & straight ends CoV: 41%;
4 with FRPs (broken line) CoV: 13%.

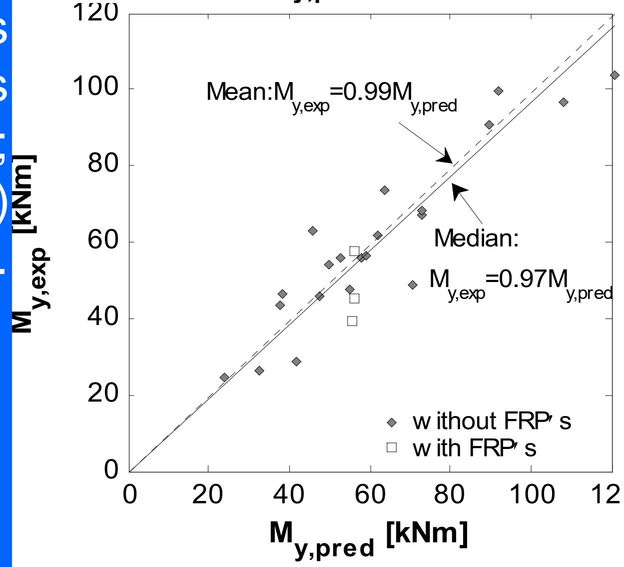

Strut-and-Tie model
10 double fixity columns, continuous bars, Cov: 14.5%
(plane sections: mean=0.74)

$$\frac{M_y}{bd^2 f_c}=\frac{M_R}{bd^2 f_c}=\omega_{tot}\left(1-\frac{f_{c,b}+f_{c,t_o}}{2f_y}\right)\frac{H}{H+l_b}\frac{z}{4d}+\frac{(1-\xi)\xi}{2\left(1+(z/H)^2\right)}$$

$$\xi=\left(\nu+\omega_{tot}\frac{H\left(1+(f_{c,b}+f_{c,t})/2f_y\right)/2+l_b}{H+l_b}\right)\left(1+\left(\frac{z}{H}\right)^2\right)$$

Test-to-prediction ratio, secant-to-yield-point stiffness

(~95 rect. columns w/ continuous or lap-spliced smooth bars

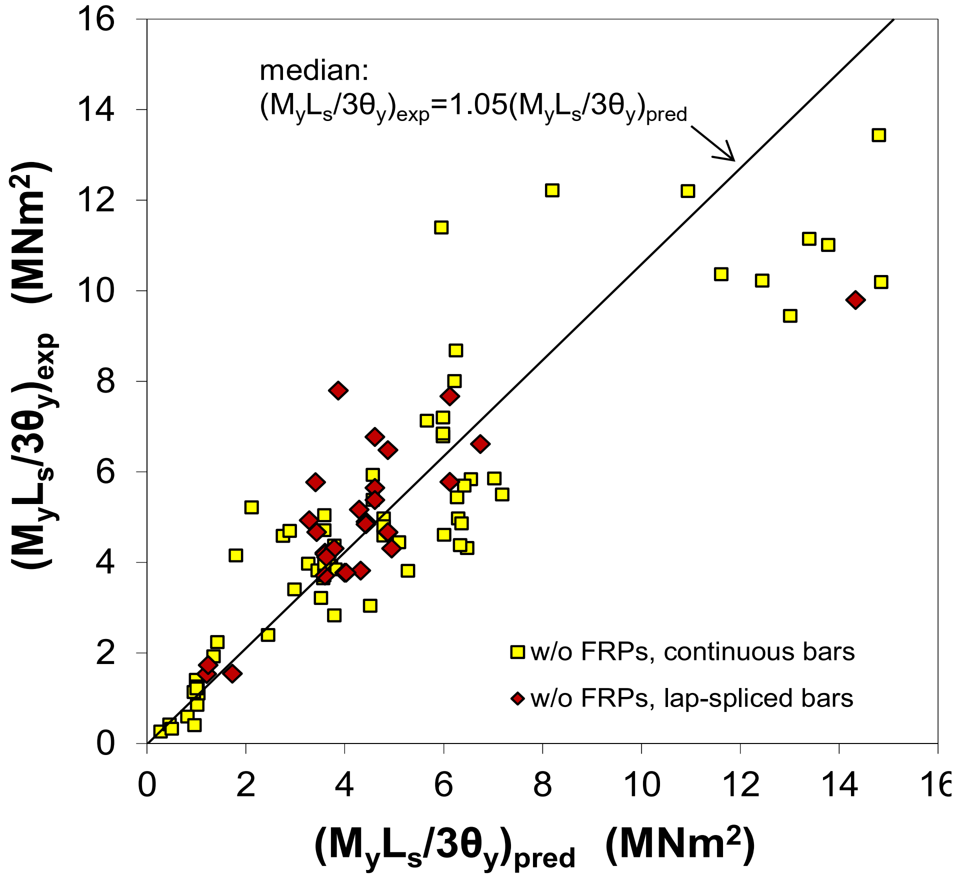

~55 cantilevers w/ cont. bars
~30 cantilevers w/ hooked laps
10 doubly fixed w/ cont. bars
Overall CoV 15.5%

18 cantilevers w/ FRP & cont. bars
10 cantilevers w/ FRPs & hooked laps
Overall CoV 20%

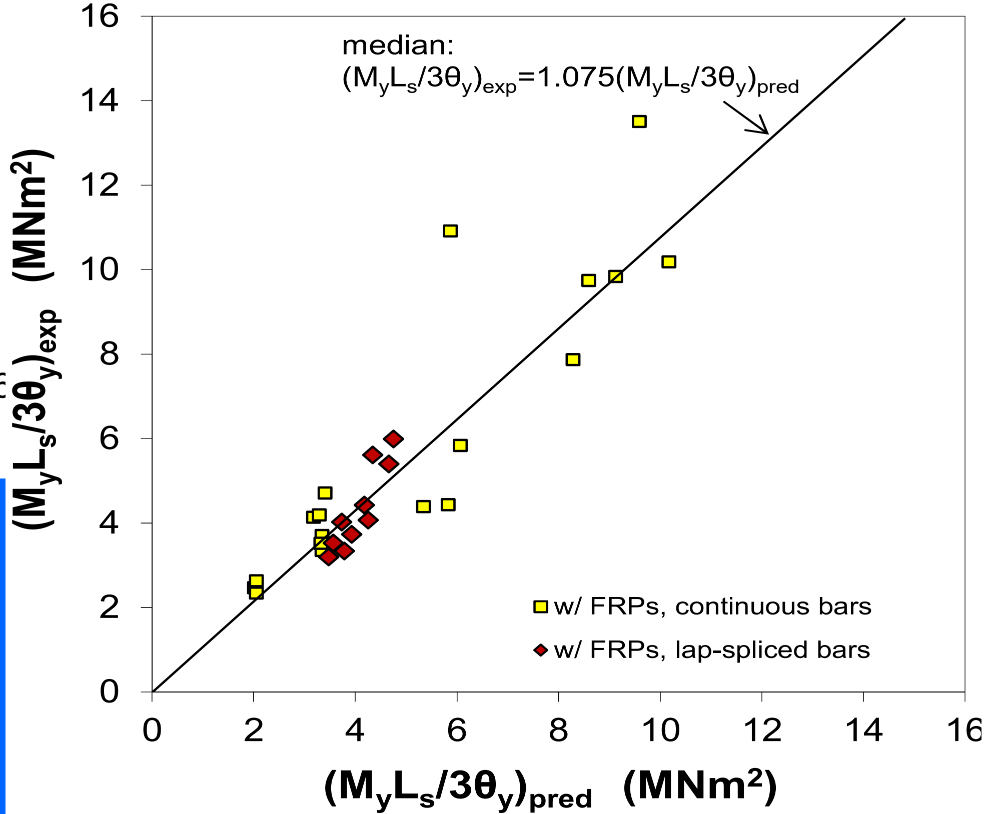

~30 FRP-wrapped rect. columns; continuous or lapped hooked bars

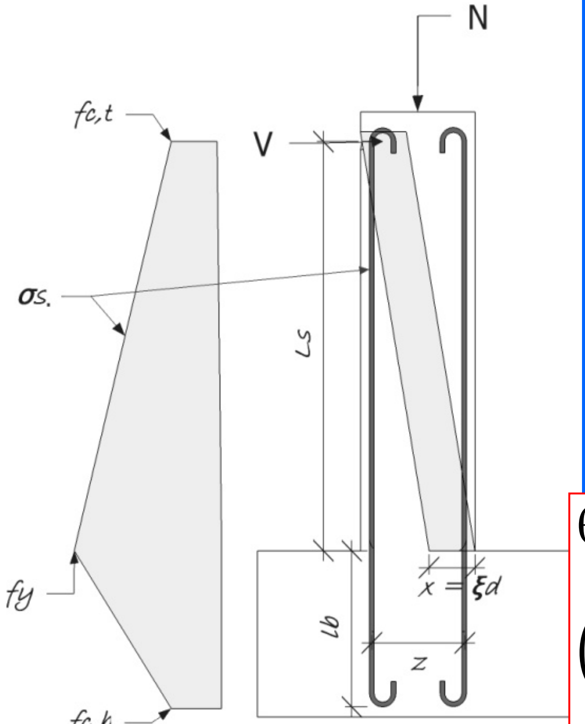

Ultimate chord rotation of members with <u>continuous</u> smooth bars

<u>Physical</u>, Strut-and-Tie model

$$\theta_{u,\text{continuous, cantilever}} = \theta_{y,\text{continuous, cantilever}} + \left(\phi_u - \phi_y\right)\left(a_{\max}\max(L_s;l_b) + a_{\min}\min(L_s;l_b)\right) + \frac{\phi_u \xi_u d}{2}\left(\frac{L_s}{z} + \frac{z}{L_s}\right)$$

a_{max}=0.08 a_{min} = 0.6

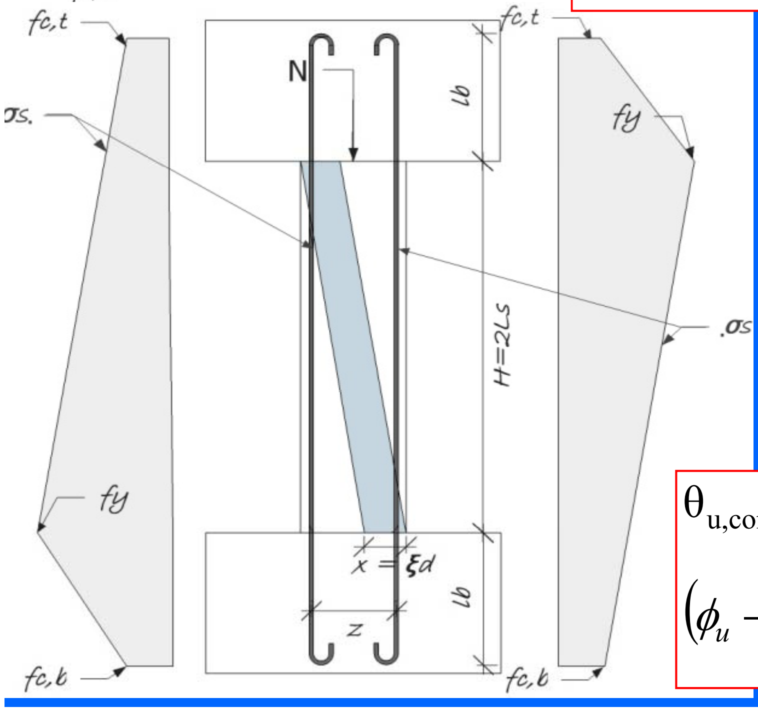

$$\theta_{u,\text{continuous, double fixity}} = \theta_{y,\text{continuous, double fixity}} + \left(\phi_u - \phi_y\right)\left(a_{\max}\max\left(\frac{H}{2};l_b\right) + a_{\min}\min\left(\frac{H}{2};l_b\right)\right) + \frac{\phi_u \xi_u d}{2}\left(\frac{H}{z} + \frac{z}{H}\right)$$

Ultimate chord rotation of members with continuous smooth bars & FRP wraps

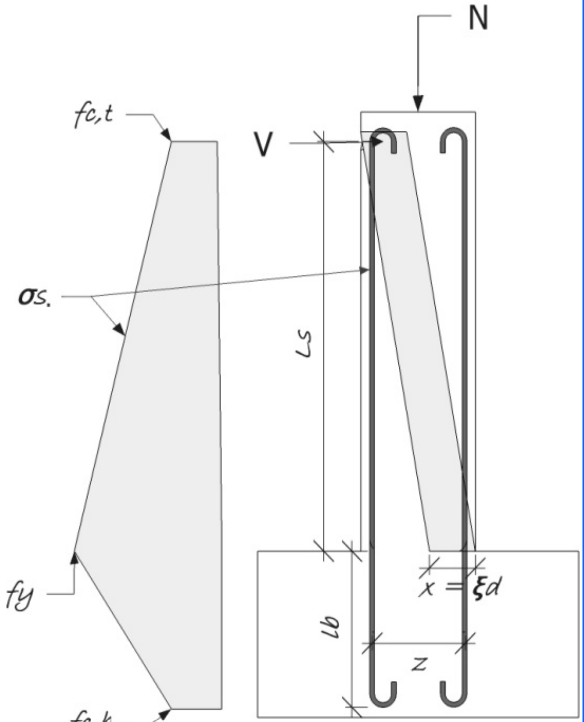

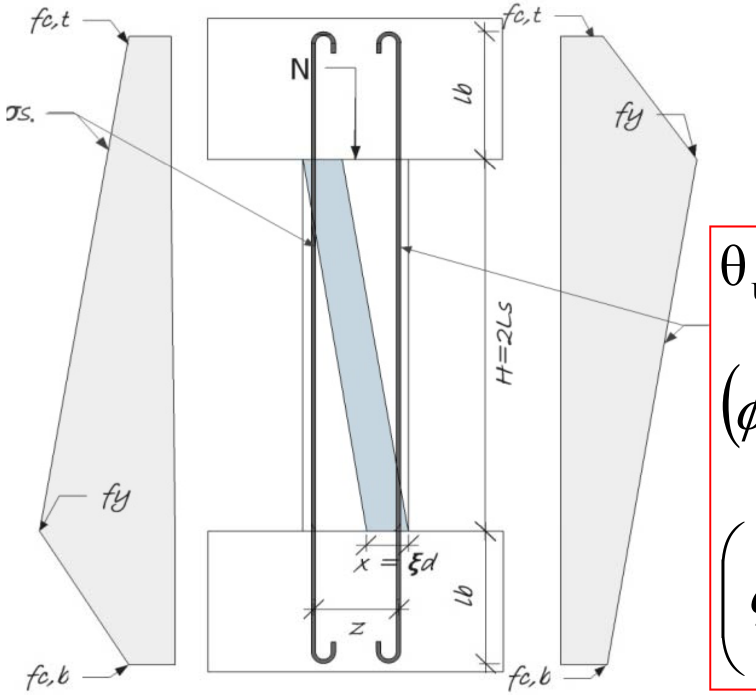

Strut-and-Tie model

$$\theta_{u,\text{continuous, cantilever}} = \theta_{y,\text{continuous, cantilever}} + \left(\phi_u - \phi_y\right)\left(a_{\max}\max(L_s;l_b) + a_{\min}\min(L_s;l_b)\right) + \left(\frac{\phi_u \xi_u d}{2}\left(1 - \frac{L_{FRP}}{L_s}\right) + \frac{\phi_{u,c}\xi_{u,c} d}{2}\frac{L_{FRP}}{L_s}\right)\left(\frac{L_s}{z} + \frac{z}{L_s}\right)$$

$\phi_{u,c}$, $\xi_{u,c}$: ult. curvature & normalised neutral axis depth of section w/ FRP wrapping

$$\theta_{u,\text{continuous,double fixity,FRP}} = \theta_{y,\text{continuous,double fixity}} + \left(\phi_u - \phi_y\right)\left(a_{\max}\max\left(\frac{H}{2};l_b\right) + a_{\min}\min\left(\frac{H}{2};l_b\right)\right) + \left(\phi_u \xi_u d\left(\frac{1}{2} - \frac{L_{FRP}}{H}\right) + \phi_{u,c}\xi_{u,c} d\frac{L_{FRP}}{H}\right)\left(\frac{H}{z} + \frac{z}{H}\right)$$

Ultimate chord rotation of members with lap-spliced smooth bars & FRP wraps

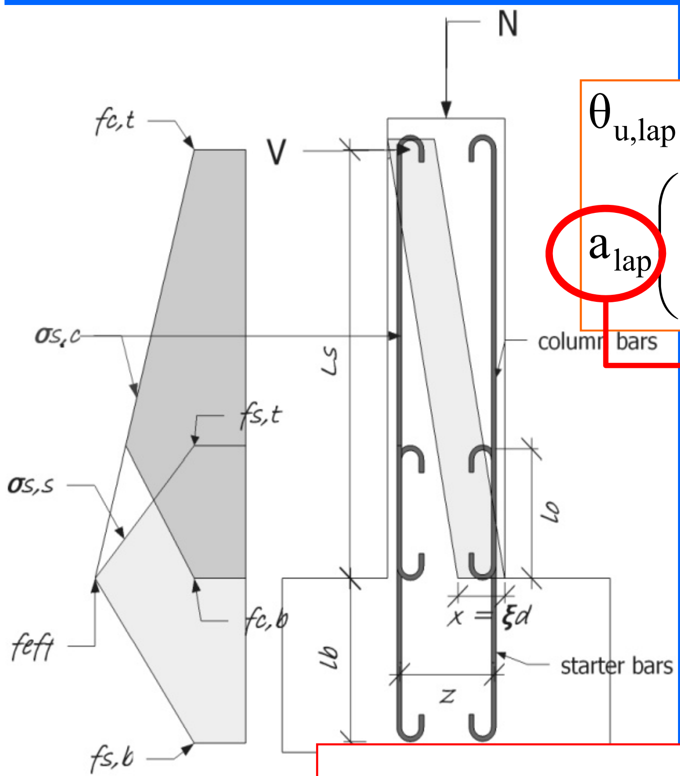

$$\theta_{u,lap} = \theta_{y,lap} + a_{lap}\left(\left(\phi_u - \phi_y\right)\left(a_{max}\max(L_s;l_b) + a_{min}\min(L_s;l_b)\right) + \frac{\phi_u \xi_u d}{2}\left(\frac{L_s}{z} + \frac{z}{L_s}\right)\right)$$

hooked bars: $\mathrm{a}_{lap} = \mathrm{a}_{lap,\ hooked} = \min\left(1;\ \frac{l_o}{50 d_b}\right)$

With FRPs: $$\theta_{u,lap,FRP} = \theta_{y,lap} + \mathrm{a}_{lap,FRP}\left(\begin{array}{l}\left(\phi_u - \phi_y\right)\left(a_{max}\max(L_s;l_b) + a_{min}\min(L_s;l_b)\right) + \\ \frac{1}{2}\left(\phi_u \xi_u d\left(1 - \frac{L_f}{L_s}\right) + \phi_{u,c}\xi_{u,c} d\frac{L_f}{L_s}\right)\left(\frac{L_s}{z} + \frac{z}{L_s}\right)\end{array}\right)$$

hooked bars: $$a_{lap,FRP} = a_{hooked\ lap,FRP} =$$
$$\min\left(1;\ \frac{l_o}{50 d_b}\left(1 + 300\min(0.05;\ \rho_f E_f / E_c)\left(0.1 - \min(0.05;\ \rho_f E_f / E_c)\right)\right)\right)$$

Empirical model for ultimate chord rotation

$$\theta_{u,\text{continuous smooth bars}} = \theta_{y,\text{cont. smooth bars}} + 0.72\,\theta_u^{pl}{}_{\text{empirical, cont. ribbed bars}}$$

$$\theta_{u,\text{cont. smooth bars \& FRP}} = \theta_{y,\text{cont. smooth bars}} + 0.9\,\theta_u^{pl}{}_{\text{empirical, cont. ribbed bars \& FRP}}$$

$$\theta_{u,\text{lapped hooked bars}} = \theta_{y,\text{lap}} + 0.8\,a^{pl}{}_{\text{lap hooked}}\,\theta_u^{pl}{}_{\text{empirical, cont. ribbed bars}}$$

hooked bars:

$$a^{pl}_{lap\ hooked} = \min\left(1;\ \frac{l_o}{50d_b}\left(1+400\min(0.05;\ \rho_f E_f / E_c)\right)\left(0.1-\min(0.05;\ \rho_f E_f / E_c)\right)\right)$$

Test-to-predicted ult. chord-rotation - members w/ smooth bars

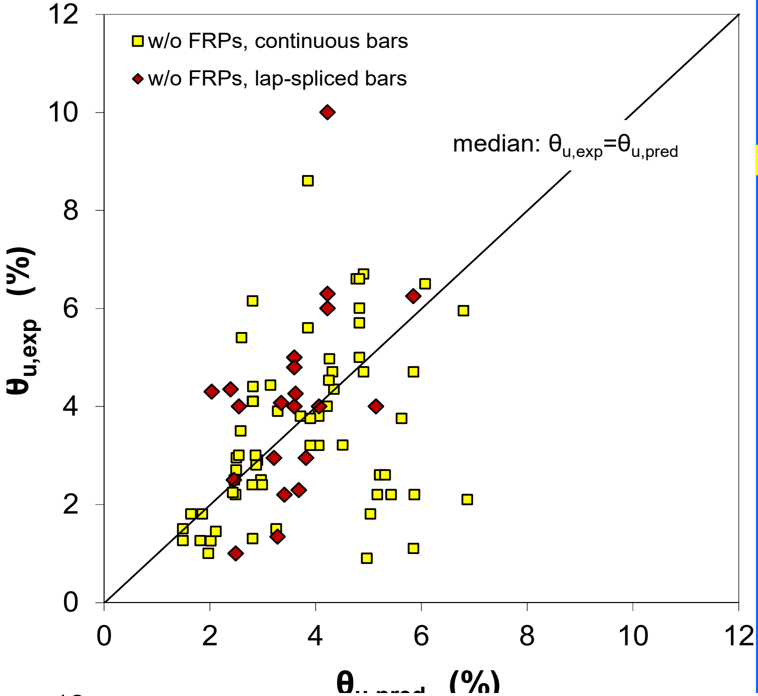

~85 tests
no FRP wraps

Physical model
←CoV 44.5%

Empirical model
CoV 39%→

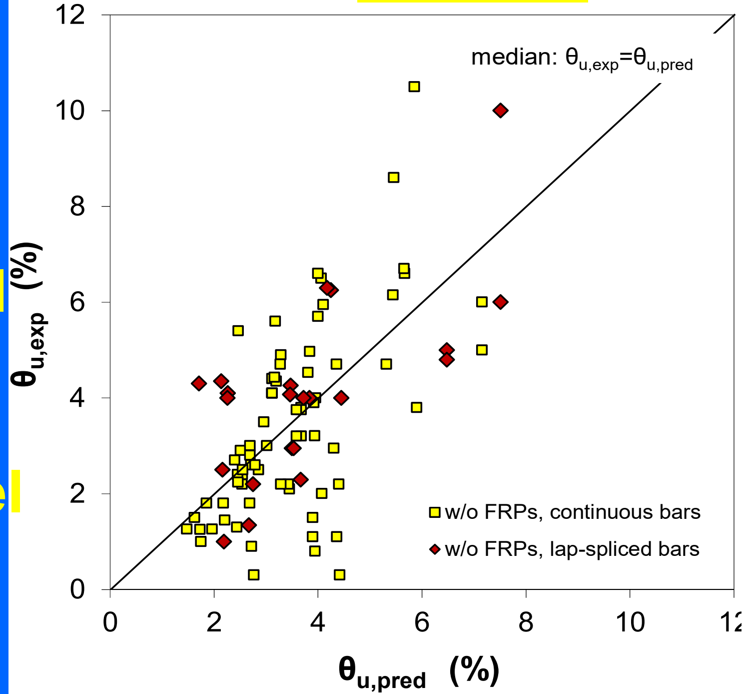

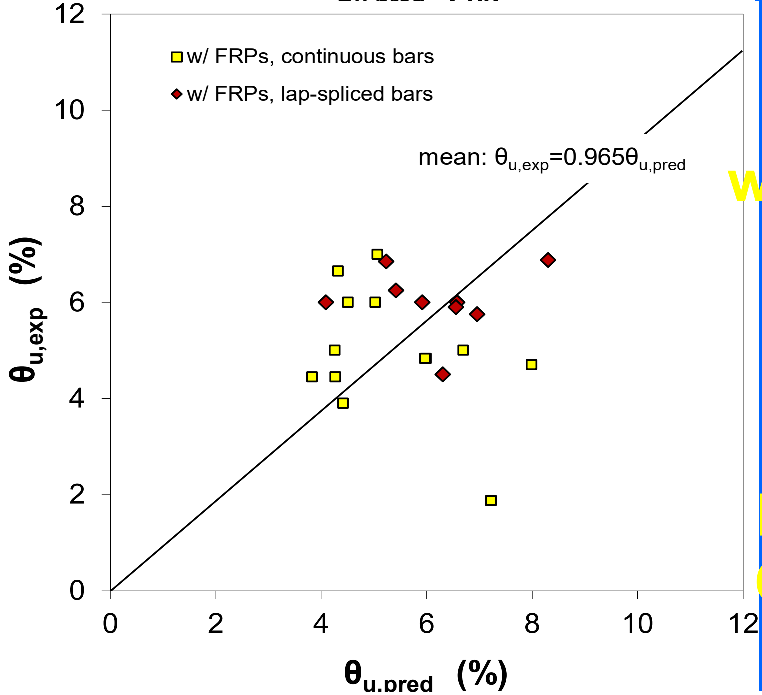

~25 tests
with FRP wraps

Physical model
←CoV 36.5%

Empirical model
CoV 35%→